ORIGIN AND CHEMICAL EVOLUTION OF THE SAN ISABEL BATHOLITH, WET MOUNTAINS, COLORADO

by

Thomas J. Griffin

B.S. Kansas State University, 1982

A MASTER'S THESIS

submitted in partial fulfillment of the

requirements for the degree

MASTER OF SCIENCE

Department of Geology

KANSAS STATE UNIVERSITY
Manhattan, Kansas

1987

Approved by:

Robert Cullers

Major Professor

CONTENTS

TABLES

ILLUSTRATIONS

Figure

I N T R O D U C T I O N

STATEMENT OF THE PROBLEM

Much of the Precambrian basement of the midcontinent region of the United States consists of an extensive terrane of rhyolite and epizonal granite emplaced upon and within an older crust 1.35 to 1.4 b.y. ago (Thomas et al., in press). The 1.36 b.y. old San Isabel batholith is exposed in the southern Wet Mountains of Colorado (Figure 1) and may represent a deeper-seated manifestation of this 1.35 - 1.4 b.y. old igneous activity (Thomas et al., in press).

This investigation is focused on the development of petrogenetic models to constrain the chemical formation and evolution of the San Isabel batholith. Major- and trace-element data, field relationships, isotopic data, and petrographic observations are integrated in an attempt to: (1) define possible source rocks for the San Isabel magma, (2) estimate the extent of partial melting including the proportion of phases in melt, and (3) explain the modal and chemical variation in the San Isabel batholith.

In addition, assessment of the tectonic setting during emplacement of the San Isabel batholith will be attempted by the utilization of various discrimination diagrams combined with field relationships, chemical characteristics, and petrographic data.

Figure 1: Index map of south-central Colorado.

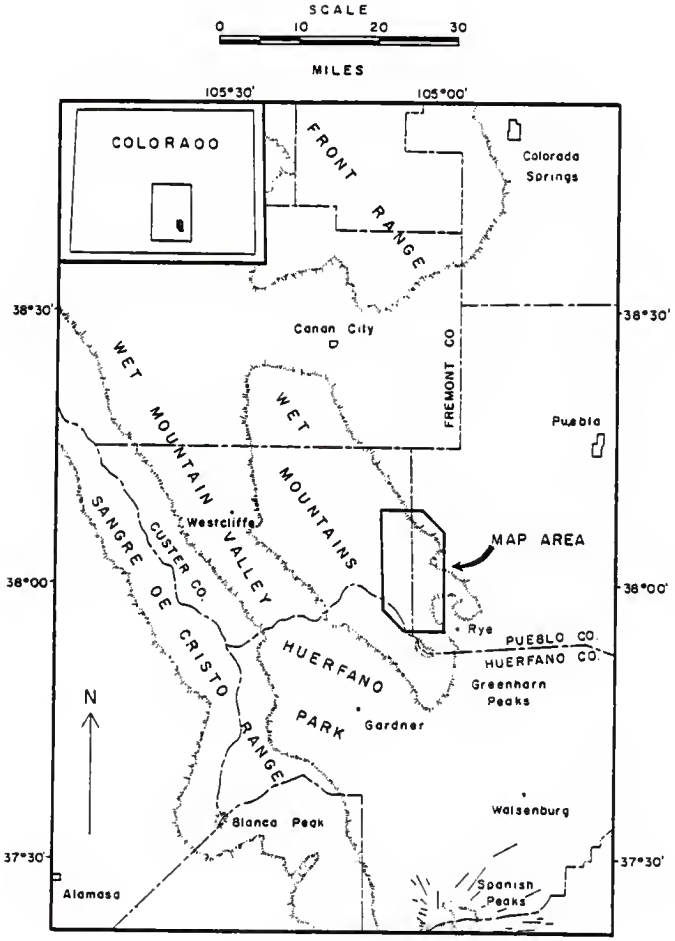

ACKNOWLEDGMENTS

I would like to thank my major professor Robert L. Cullers for his guidance and encouragement throughout my academic career. Without his help this research project would not have been possible. I would also like to thank George R. Clark II, Joseph L. Graf, Jr., and William G. Fateley for serving on my supervisory committee and for their assistance in this study. The remaining members of the faculty of the Department of Geology at Kansas State University have all contributed valuable advice regarding this thesis and it is greatly appreciated.

I would also like to thank the staff of the Department of Nuclear Engineering at Kansas State University for their assistance in this study - Professor Gale Simons and Jack Higginbotham were especially helpful.

The assistance of Jim Stone in generating computer variation diagrams is also greatly appreciated. I would also like to thank Lex D. Shaw for his help in producing the geologic map of the San Isabel batholith - the northern half of the map is the result of his efforts. In addition, I would like to thank Mark Patzkowsky for his help in separating minerals. The courtesy and generosity of Mr. and Mrs. George Best of San Isabel, Colorado will always be remembered. I reserve a special thanks for my wife Gara and my mother Jeanette for their support and inspiration.

This research project was funded by a grant (#EAR-8208564) awarded to Professor Robert L. Cullers, Kansas State University from the National Science Foundation.

PREVIOUS INVESTIGATIONS

The earliest geologic study of the southern Wet Mountain area was done by Gilbert (1897) and Hills (1900) who described the structural geology of the Pueblo, Colorado and Walsenburg, Colorado quadrangles. Metamorphic rocks and part of the San Isabel batholith and smaller associated intrusive rocks in the southern Wet Mountains have been mapped in detail by Boyer (1962) and Whitten and Boyer (1964). Singewald (1966) described and reevaluated the Ilse Fault zone which transects the San Isabel batholith. The petrology and structure of the San Isabel batholith was characterized by Boyer (1962). Additional studies of the petrology and structure of the batholith were done by Murray (1970) with emphasis on the petrogenesis and origin of the monzogranite magma. Murray and Rogers (1973) evaluated the distribution of Rb and Sr in the potassium feldspars of the San Isabel batholith. Isotopic studies of the San Isabel batholith have been conducted by Shuster (1984) and Thomas et al. (in press) in which the initial $^{87}Sr/^{86}Sr$ ratio and

the U/Pb age from zircons were determined.

METHODS

FIELD TECHNIQUES

The initial phase of this study consisted of a reconnaissance and field check of the geologic map of Murray (1970) in which representative samples from each major facies of the southern half of the batholith were collected (Figure 5). The least weathered samples were chosen for petrographic study and major- and trace-element analysis. Collection of samples from the northern half of the batholith was accomplished by Lex D. Shaw of Kansas State University; several of these samples were analyzed and considered in this study.

PETROGRAPHIC TECHNIQUES

Fifty-one of the freshest, least altered samples were chosen for thin section preparation. Standard thin sections (27 X 46 mm) were prepared from medium-grained samples while enlarged thin sections (38 X 76 mm) were cut from coarse-grained porphyritic samples. Chayes (1949) point-count method was utilized in determining mineral percentages. The composition of plagioclase was estimated by the Michel-Lèvy method (1877).

MINERAL SEPARATION TECHNIQUES

One of the freshest, least altered hornblende-rich samples (TG-16) was selected for analyses of mineral separates. Separation of minerals was accomplished with the use of a heavy liquid (methylene iodide; density = 3.325) and the Frantz Isodynamic (Magnetic) Separator. Homogeneity of each mineral fraction was determined with the petrographic microscope.

CHEMICAL TECHNIQUES

Fifty-one samples representing the compositional range of the San Isabel batholith were chosen for chemical analysis. Major-element contents were determined for all samples by atomic absorption and emission spectrophotometry using methods adopted from Medlin et al. (1969) and Shapiro (1978). Details of the procedure for major-element analyses are in Appendix B.

Sixteen of the above samples were selected for instrumental neutron activation analysis (INAA) to determine trace-element contents. Again, these samples represent the range of composition within the suite. Methods adopted from Gordon et al. (1968) and Jacobs et al. (1977) were used in this study. Details of the procedure for instrumental neutron activation analysis are in Appendix C.

Loss on ignition (LOI) or total volatile content was determined gravimetrically. Details of the gravimetric procedure are in Appendix D.

U.S. Geological Survey standard rock samples and a Canadian soil sample were utilized as primary standards in this study. Major- and trace-element contents of standard samples are presented in Tables 1 and 2.

TRACE-ELEMENT MODELING

Development of a quantitative model that predicts trace-element concentrations in a rock suite is based on the selection of chemical processes that distribute the elements among the rock-forming minerals. In this study, the non-modal aggregate melt formulation defined by Shaw (1970) is used to model partial melting of source rocks. Fractional crystallization processes are modeled using the equation of Haskin et al. (1970). The simple mixing equation discussed by Allegre and Minster (1978) and Cox et al. (1980) is used to model mixing phenomena. Details regarding these equations are given in Appendix A.

Table 1: Major-element contents of U.S.G.S. standards QLO-1 and RGM-1 (after Abbey, 1982), and Canadian soil sample SO-4 (after Bowman et al., 1978).

	QLO-1		RGM-1		SO-4	
	This study	Abbey, 1982	This study	Abbey, 1982	This study	Bowman et al., 1978
SiO_2	65.99	65.93	73.69	73.47	68.23	68.45
Al_2O_3	16.67	16.37	13.95	13.80	10.20	10.32
TiO_2	0.65	0.62	0.28	0.27	0.59	0.57
Fe_2O_3	4.35	4.29	1.84	1.89	3.33	3.39
MgO	0.99	1.04	0.23	0.28	1.01	0.93
CaO	3.26	3.24	1.10	1.15	1.53	1.55
Na_2O	4.18	4.23	4.08	4.12	1.29	1.31
K_2O	3.66	3.63	4.39	4.35	1.95	2.08
MnO	0.09	0.09	0.04	0.04	0.08	0.08
Rb	79	74	149	155	70	75
Sr	346	350	106	100	167	170

Table 2: Trace-element contents of standardized Canadian soil sample SO-4 (after Bowman et al., 1978 and Gladney et al., 1984).

	This study	Bowman et al., 1978	Gladney et al., 1984
La	26.7	31	28.6
Ce	50.6	54	53.2
Sm	4.62	4.9	4.7
Eu	0.92	1.0	0.99
Tb	0.58	0.6	0.6
Yb	2.26	2.3	2.3
Lu	0.35	0.4	0.39
Ba	697	780	730
Th	9.14	8.7	8.5
Hf	7.53	8.0	8.1
Ta	0.92	0.5	0.62
Sc	7.86	10	8.5

G E O L O G Y

WET MOUNTAINS

The Wet Mountains of Colorado are part of the southern Rocky Mountain physiographic province and are bounded on the north by the Arkansas River and Canon City Embayment (Figures 2 and 3). This northern boundary separates the Wet Mountains from the Front Range. The Sangre de Cristo Range lies to the west of the Wet Mountains and is separated from them by the Wet Mountain Valley and Huerfano Park (Figures 1 and 2).

"The southern Wet Mountains form a southeast-plunging anticline outlined by the upturned sedimentary units that bound the range" (Boyer, 1962, p. 1061). The southwestern flank of the range is bounded by high-angle normal and reverse faults. The southeastern end of the Wet Mountains is characterized by a structural bifurcation - the southern spur of the split forms the Greenhorn anticline (Figure 2), while the main branch plunges southeastward and forms the Apishapa uplift (McGinnis, 1956). The Wet Mountains are bounded on the east by upturned sedimentary rock units of Paleozoic and Mesozoic age and by the Wet Mountain Fault zone (Figure 2).

The oldest rocks in the Wet Mountain area are metamorphosed sedimentary and volcanic rocks (approximately

Figure 2: Generalized tectonic map of the area around the Wet Mountains, modified from Boyer (1962).

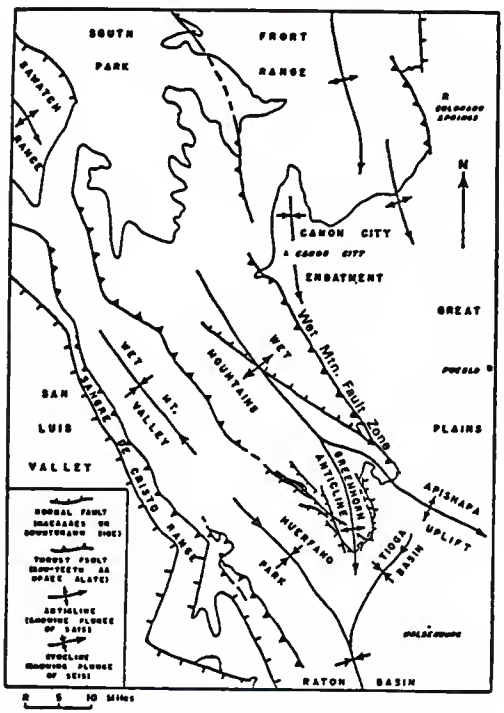

1.8 b.y. old) consisting mostly of schists and gneisses concordantly foliated with granite gneiss, lit-par-lit gneiss, and migmatite (Figure 3).

The metamorphic rocks form the country rock into which a variety of granitic plutons intrude. The oldest granitic intrusives in the Wet Mountains are foliated granodiorites that are 1.7 b.y. in age (Figure 3). These foliated granodiorites are the most abundant granitoids in the northern Wet Mountains but are absent in the central and southern portions of the Wet Mountains.

Relatively unfoliated monzogranites and syenogranites characterize most of the younger plutons in the Wet Mountains. Examples include the 1.47 b.y. old West McCoy Gulch pluton and the 1.36 b.y. old Bear Basin granite (Figure 3). The 1.44 b.y. old Oak Creek pluton differs from most of these younger plutons with respect to foliation. The Oak Creek pluton consists mostly of a foliated, monzogranite to granodiorite porphyry intruded by dikes of leucogranite (Stone, 1984).

The 1.36 b.y. old San Isabel batholith, the focus of this study, forms the center of the southern Wet Mountains. The batholith is cut by two major fault zones that trend north-northwest, the Ilse Fault zone and the Wet Mountain Fault zone (Figure 4). To the southwest of the San Isabel batholith are several other smaller Precambrian silicic plutons. These smaller plutons, namely the leucogranites of

Figure 3: Precambrian and Cambrian rocks of the Wet Mountains area, Colorado (Cullers, 1985; Scott and Taylor, 1978; Boyer, 1962).

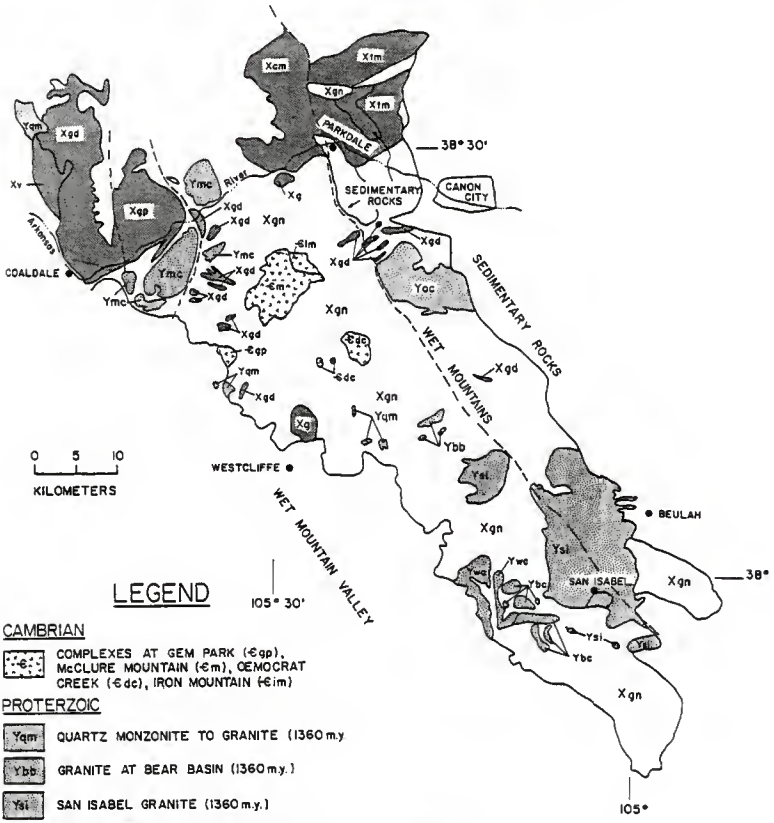

LEGEND

CAMBRIAN

- Є: COMPLEXES AT GEM PARK (Єgp), McCLURE MOUNTAIN (Єm), OEMOCRAT CREEK (Єdc), IRON MOUNTAIN (Єim)

PROTEROZOIC

- Yqm — QUARTZ MONZONITE TO GRANITE (1360 m.y.)
- Ybb — GRANITE AT BEAR BASIN (1360 m.y.)
- Ysi — SAN ISABEL GRANITE (1360 m.y.)
- Y — GRANITE OF WILLIAMS CREEK (Ywc), BEAR CREEK (Ybc), CLIFF CREEK (Ycc)
- Yoc — GRANITE AT OAK CREEK (1440 m.y.)
- Ymc — GRANITE AT WEST McCOY GULCH (1460; 1474 m.y.)
- X — GRANODIORITE TO GRANITE AT GARELL PEAK (Xgp) (1665 and 1670 m.y.)
  GRANODIORITE TO GRANITE AT CRAMPTON MOUNTAIN (Xcm), TWIN MOUNTAIN (Xtm), (1700 m.y.)
  GRANODIORITE TO GRANITE, UNNAMED (Xgd - g, ~1700 m.y.?)
- Xv — METAVOLCANIC (1670 + 1710 m.y.)
- Xg — METAGABBRO
- Xgn — GNEISSES, SCHISTS, MIGMATITES
- ---- MAJOR FAULT ZONES

Figure 4: Geologic map of the San Isabel batholith, Custer and Pueblo Counties, Colorado

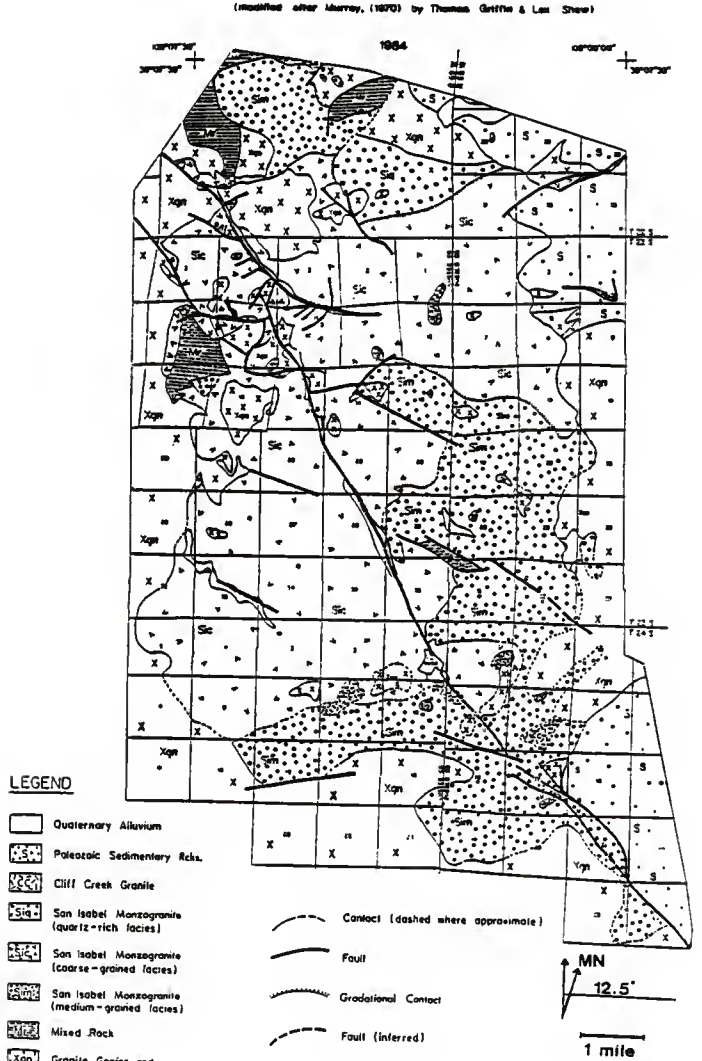

Figure 5: Sample location map of the San Isabel batholith.

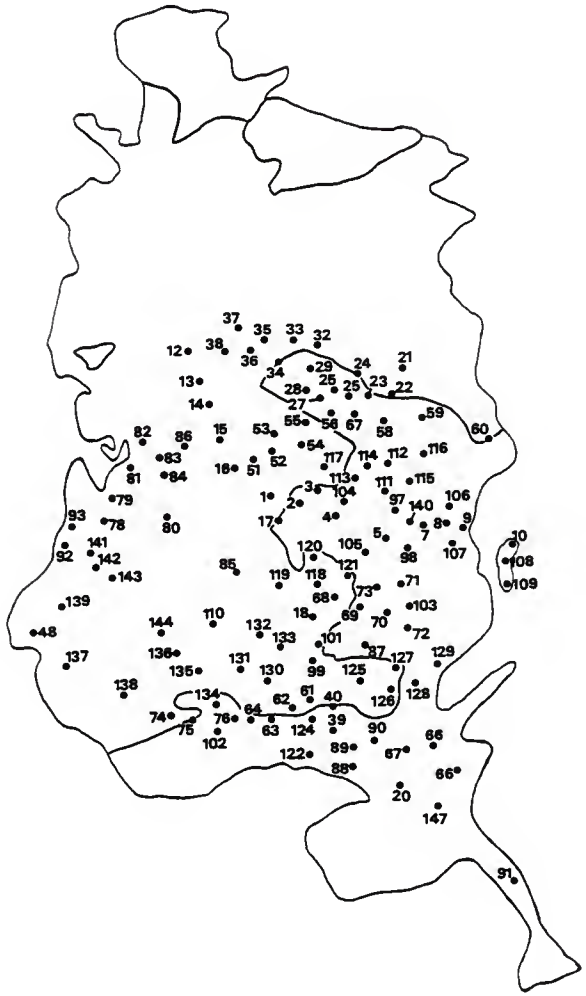

Cliff Creek, Bear Creek, and Williams Creek are similar to the San Isabel monzogranite in plagioclase composition (An_{25}-An_{30}) but differ in appearance and heavy-mineral content (Boyer, 1962). The leucogranites contain trace amounts of biotite and other mafic minerals and contain rounded, sedimentary zircons with euhedral overgrowths (Boyer, 1962). For the most part, these small, silicic plutons are emplaced within the concordantly foliated lit-par-lit gneisses and migmatites that border the San Isabel batholith in most areas.

SAN ISABEL BATHOLITH

Boyer (1962) and Logan (1966) recognized two distinct textural facies of the San Isabel batholith: a coarse-grained porphyritic facies and a medium-grained equigranular facies. In this study, both facies have been mapped as suggested by Boyer (1962) but a third facies recognized by Murray (1970), the quartz medium-grained facies, has been added (Figure 4). The coarse-grained porphyritic facies and the medium-grained facies are indistinguishable with respect to mineral composition while the quartz medium-grained facies is quartz-rich and mafic-poor compared to the other two facies (Murray, 1970).

Megascopically, samples of the San Isabel batholith are characterized by alkali feldspar phenocrysts with abundant

interstitial mafics, feldspar, and quartz (Murray, 1970). Segregations of mafic minerals are locally abundant (Figures 6 and 7) imparting a cumulate appearance to the rock. These mafic clusters may comprise up to 30 percent of the rock in some areas (Murray, 1970).

In addition, xenoliths of hornblende-biotite gneiss and granite gneiss occur throughout the San Isabel batholith. In general, contacts between xenoliths and batholith are sharp regardless of lithology (Murray, 1970). Foliation in xenoliths is usually not parallel to the foliation in the monzogranite or in the metamorphic country rocks (Murray, 1970).

Regional foliation of the metamorphic country rocks wraps around the intrusion and is discordant to the planar flow structure of the batholith (Boyer, 1962). Foliation within the batholith is weakly defined and strikes roughly north-northeast (Murray, 1970).

Pegmatites are abundant and are generally found near the contacts between the batholith and country rock (Murray, 1970). Although many pegmatites occur exclusively within the batholith, some may be traced from batholith to country rock (Murray, 1970). The pegmatites are predominantly composed of microcline and quartz. Aphanitic "Bostonite" dikes of similar composition also occur throughout the batholith and country rocks (Murray, 1970). These dikes are

Figure 6: Isopleth map of total mafic mineral content in the San Isabel batholith, from Murray (1970). Contour interval is 3 percent.

Figure 7: Isopleth map of hornblende content in the San Isabel batholith, from Murray (1970). Contour interval is 0.5 percent.

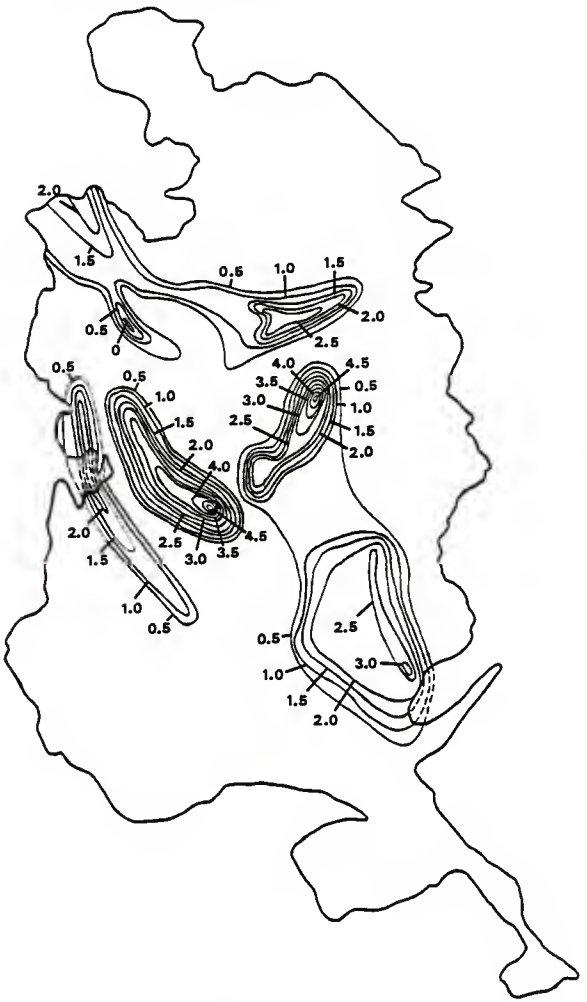

characterized by trachytic alkali feldspar laths with interstitial quartz. Mafic dikes of Tertiary (?) age occur and are commonly veined with calcite. Epidotization is common near the margins of these mafic dikes and is clearly secondary in origin (Murray, 1970).

R E S U L T S

PETROGRAPHY

Fifty-one representative samples from the coarse-grained porphyritic facies and medium-grained facies from the central and southern portions of the batholith were selected for petrographic study. Although the textural facies of the San Isabel monzogranite can be easily distinguished from each other in hand specimen, Murray (1970) has shown that the textural facies of the batholith are indistinguishable from each other on mineral pair plots. This study tested whether or not the textural facies were likewise indistinguishable from each other on elemental variation diagrams.

A compilation of modal analyses of the San Isabel batholith is given in Table 3. Classification of the San Isabel monzogranite based on modal quartz, alkali feldspar, and plagioclase is presented in Figure 8. Generalized descriptions of typical coarse-grained porphyritic, medium-grained, and quartz medium-grained samples are given in Appendix 6.

Table 3: Modal analyses of the San Isabel batholith, coarse-grained porphyritic facies.

COARSE-GRAINED PORPHYRITIC FACIES

HORNBLENDE-RICH

	TG-14	TG-102	TG-18	TG-94	TG-16	TG-136	TG-134	TG-110	TG-135	TG-93	TG-124
Microcline*	28.8	20.5	26.4	29.0	27.8	31.6	29.8	30.1	30.5	30.8	30.0
Plagioclase	28.1	30.7	25.9	26.0	29.0	29.6	28.0	32.4	25.5	22.2	28.5
Quartz	19.0	22.2	28.2	20.9	22.5	19.7	21.3	20.9	22.0	23.7	25.4
Biotite	11.5	11.3	7.1	10.7	7.6	8.6	10.3	8.6	9.4	8.3	6.8
Sphene	3.3	3.4	2.5	4.3	4.6	2.6	3.0	1.1	2.6	4.8	2.1
Hornblende	5.0	4.8	4.7	3.0	4.0	4.0	3.0	3.0	4.2	3.0	3.0
Opaques**	2.9	2.7	2.2	3.2	3.8	1.6	2.4	2.8	3.6	4.2	2.2
Accessories***	1.4	4.4	3.0	2.9	0.7	2.3	2.2	1.1	2.2	3.0	2.0

COARSE-GRAINED PORPHYRITIC FACIES

INTERMEDIATE

	TG-137	TG-12	TG-100	TG-126	TG-129	TG-127
Microcline*	25.0	34.3	32.1	32.0	31.0	31.9
Plagioclase	29.8	33.0	29.4	32.2	32.4	29.7
Quartz	22.0	22.3	26.3	20.1	25.9	23.8
Biotite	11.4	5.8	8.4	9.2	6.9	6.2
Sphene	3.3	1.4	1.6	1.8	1.2	3.0
Hornblende	2.3	1.1	1.0	1.3	1.0	1.3
Opaques**	2.9	1.0	0.8	1.5	0.9	2.3
Accessories***	3.3	1.1	0.4	1.9	0.7	1.8

COARSE-GRAINED PORPHYRITIC FACIES

HORNBLENDE-POOR

	TG-1	TG-142	TG-79	TG-139	TG-125	TG-143	TG-48	TG-95	TG-13	TG-68
Microcline*	28.4	29.6	27.4	27.8	29.2	33.3	25.3	30.6	34.5	37.4
Plagioclase	40.6	27.3	30.5	26.4	29.0	24.8	25.7	27.1	24.6	32.6
Quartz	20.0	20.9	23.4	24.4	22.4	21.9	24.9	27.6	32.0	24.8
Biotite	6.5	10.9	9.8	12.3	11.3	10.5	11.8	11.0	7.3	3.1
Sphene	1.3	3.6	5.0	3.1	2.9	3.1	5.4	2.4	0	1.1
Hornblende	0.5	1.0	0.3	0.9	1.0	1.0	0.7	0.1	0	0
Opaques**	1.3	2.9	1.9	1.4	1.9	2.0	2.3	0.8	1.3	0.6
Accessories***	1.4	3.8	1.7	3.7	2.3	3.4	3.9	0.4	0.3	0.4

* including perthite
** including pyrite
*** including epidote, chlorite, apatite, zircon, allanite, hematite, fluorite, and muscovite

Table 3: Modal analyses of the San Isabel batholith, medium-grained facies.

MEDIUM-GRAINED FACIES

HORNBLENDE-RICH

	TG-28	TG-87	TG-56	TG-23
Microcline*	24.1	24.1	32.9	24.6
Plagioclase	32.0	29.3	24.2	29.2
Quarte	21.8	21.0	25.5	21.5
Biotite	10.0	14.1	7.0	10.9
Sphene	3.4	3.1	3.0	4.1
Hornblende	3.8	3.6	4.6	3.0
Opaques**	1.9	2.5	2.0	3.4
Accessories***	3.0	2.3	0.8	3.3

MEDIUM-GRAINED FACIES

INTERMEDIATE

	TG-32	TG-108	TG-24	TG-3	TG-5	TG-10	TG-26	TG-96	TG-59	TG-4	TG-105	TG-70
Microcline*	31.5	29.5	28.3	29.2	32.7	29.4	23.6	27.1	25.9	29.8	29.8	29.3
Plagioclase	30.1	30.5	28.5	29.8	25.8	32.0	30.0	29.0	28.2	26.5	31.6	26.0
Quarte	21.1	20.0	26.0	22.7	24.4	24.6	19.8	27.5	23.0	25.9	24.7	23.6
Biotite	8.5	9.0	9.3	9.1	8.4	7.8	11.6	7.7	11.5	8.8	7.5	9.0
Sphene	3.1	4.7	3.2	2.9	4.4	1.4	6.1	4.0	3.2	2.6	1.2	3.2
Hornblende	2.5	2.1	1.2	1.2	1.8	1.9	2.1	1.1	3.0	1.9	1.0	1.4
Opaques**	1.4	1.7	1.8	1.9	1.8	1.3	2.7	1.9	2.6	3.0	2.6	3.3
Accessories***	1.8	2.5	1.7	3.2	0.7	1.6	4.1	1.7	2.6	1.5	1.6	4.2

MEDIUM-GRAINED FACIES

HORNBLENDE-POOR

	TG-29	TG-25	TG-17	TG-22	TG-27	TG-109	TG-91	TG-77
Microcline*	25.5	29.3	27.5	27.4	26.4	28.2	34.9	29.1
Plagioclase	27.9	28.3	32.3	28.7	31.0	30.0	25.7	26.0
Quarte	23.4	23.3	20.0	25.4	23.3	22.3	24.1	24.1
Biotite	13.3	11.8	10.2	10.7	10.4	10.4	8.1	14.6
Sphene	3.9	2.4	3.7	2.2	2.9	2.4	3.0	2.8
Hornblende	0.8	0.3	1.0	0.6	1.0	1.0	0	0
Opaques**	2.2	2.6	2.8	2.0	2.6	2.3	2.0	1.3
Accessories***	3.0	2.0	2.5	3.0	2.4	3.4	2.2	2.1

* including perthite
** including pyrite
*** including epidote, chlorite, apatite, zircon, allanite, hematite, fluorite, and muscovite

Figure 8: Classification of the San Isabel batholith based on modal quartz, alkali feldspar, and plagioclase contents, from Streckeisen (1967).

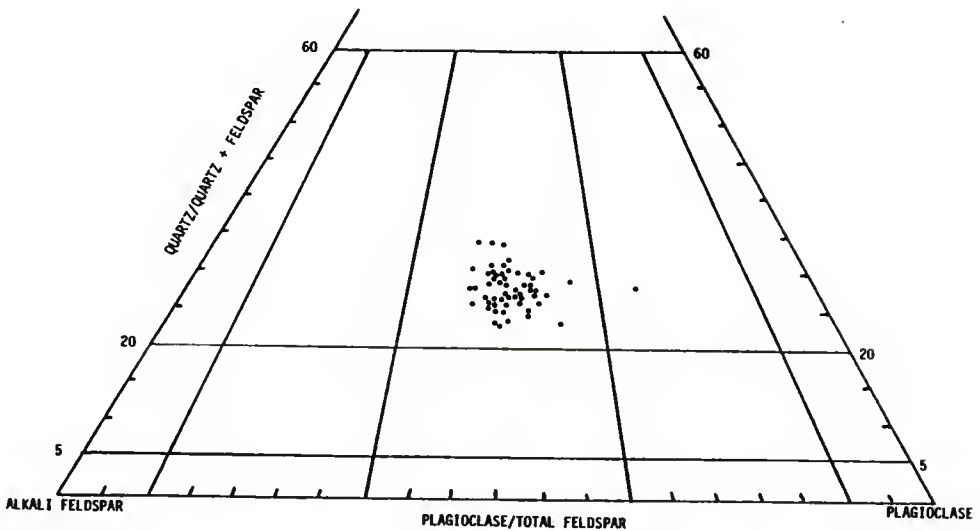

Mineral Descriptions

The following is a brief description of the mineralogy of the San Isabel monzogranite. Mineral descriptions apply to both textural facies.

Microcline: anhedral to euhedral; average phenocryst size in coarse-grained porphyritic facies is 2 to 4 cm, up to 30 cm in some areas; average size in medium-grained facies is 2 to 3 mm; invariably perthitic (string, vein, or minor poorly developed braid perthite); tartan twinned; rapakivi texture rarely developed but present; contains inclusions of plagioclase, quartz, and biotite; occasionally altered to sericite.

Plagioclase: anhedral to euhedral; up to 1 cm in coarse-grained porphyritic facies; average size in medium-grained facies is 2 to 3 mm; faint albite twinning; usually extremely altered and sericitized; An_{25} - An_{35}; contains poikilitic inclusions of opaques, hornblende, biotite, sphene, apatite, and microcline.

Quartz: anhedral; up to 8 mm in coarse-grained porphyritic facies; average size in medium-grained facies is 1.0 to 1.5 mm; exhibits undulatory extinction; always interstitial to feldspars; occasionally myrmekitic when in contact with microcline.

Biotite: anhedral to euhedral; up to 5 mm in coarse-grained porphyritic facies; average size in medium-grained

facies is 1.0 to 1.5 mm; most abundant mafic mineral; light brown to green; occurs in early-formed glomerocrysts with sphene, hornblende, and opaques and as interstitial material with quartz; contains inclusions of sphene, zircon, epidote, apatite, opaques, hornblende, and quartz; sometimes altered to chlorite, epidote, and hematite.

Hornblende: anhedral to euhedral; up to 5 mm in coarse-grained porphyritic facies; average size in medium-grained facies is 1.5 mm; green to blue-green when fresh, brown when altered; poikilitic; usually deeply embayed and resorbed; frequently occurs in early-formed glomerocrysts with biotite, sphene, and opaques; occasionally twinned; contains inclusions of apatite, opaques, zircon, plagioclase, and sphene; alters to epidote.

Sphene: anhedral to euhedral; up to 3 mm in coarse-grained porphyritic facies; average size in medium-grained facies is 1.0 mm; brown; usually fractured; frequently occurs in early-formed glomerocrysts associated with hornblende, biotite, and opaques; occasionally twinned; contains inclusions of apatite, opaques, and plagioclase; sometimes altered to epidote, opaques, and leucoxene.

Opaque minerals: anhedral to subhedral; up to 2 mm in coarse-grained porphyritic facies; up to 1 mm in medium-grained facies; usually associated with other mafic minerals; frequently occur in early-formed glomerocrysts; alter to hematite.

In addition, the San Isabel monzogranite contains the accessory minerals epidote, apatite, chlorite, zircon, allanite, hematite, pyrite, fluorite, and muscovite.

Sequence of crystallization in the San Isabel monzogranite is presented in Figure 9. Early crystallization of zircon, apatite, opaque minerals, and sphene occurred followed by hornblende, biotite, and plagioclase. Alkali feldspar crystallized slightly later than plagioclase and continued to form in the magma. Biotite occurs in early-formed glomerocrysts with hornblende, sphene, and opaque minerals and as late, interstitial material with quartz. Quartz and biotite were the last major phases to crystallize from the magma.

Protoclastic Texture

Protoclastic texture is locally manifested in the San Isabel batholith and occurs almost exclusively in the coarse-grained porphyritic facies. Evidence for the development of protoclastic texture include: (1) undulose extinction in quartz and feldspar, (2) rounded, lenticular phenocrysts of feldspar wrapped by stretched biotite and quartz, and (3) granulation of interstitial quartz and mafics. This texture is exhibited by the following samples: TG-48, TG-94, TG-95, TG-102, TG-110, TG-138, and TG-139.

Figure 9: Crystallization sequence for the San Isabel batholith, modified from Murray (1970).

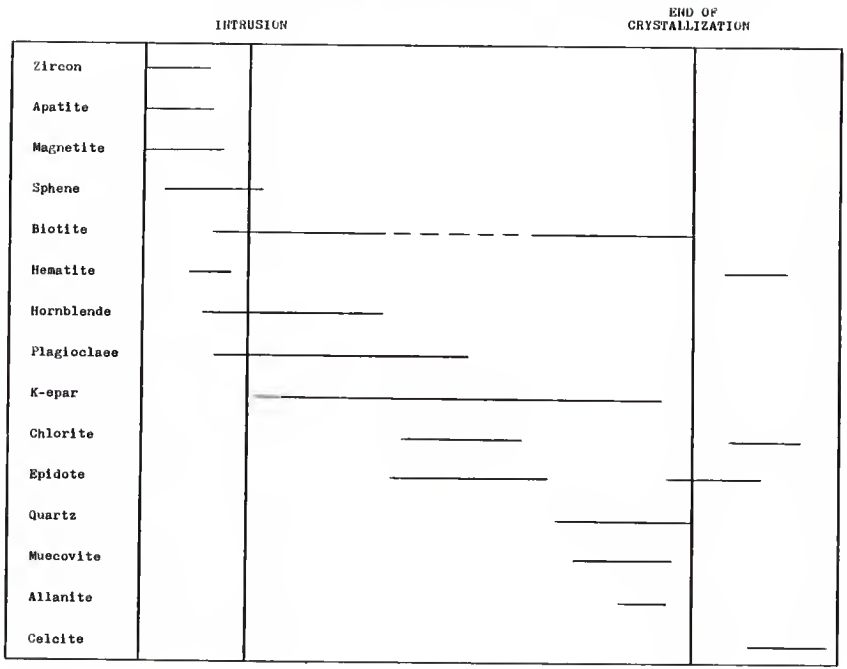

GEOCHEMISTRY

Introduction

Fifty-one samples were selected from both textural facies for major-element analysis. These samples represent the range of composition from hornblende-rich to hornblende-poor. For this study, "hornblende-rich" samples are designated as those having 3-6 percent modal hornblende and hornblende/biotite ratios greater than 0.26. "Intermediate" samples are characterized by 1-3 percent modal hornblende and hornblende/biotite ratios ranging from 0.11 to 0.25. "Hornblende-poor" samples have 0-1 percent modal hornblende and hornblende/biotite ratios ranging from 0 to 0.10.

Major Elements

Major-element data for the San Isabel monzogranite are given in Table 4. Elemental variation diagrams were plotted by texture (coarse-grained porphyritic facies and medium-grained facies) and by mineralogy (hornblende-rich, intermediate, and hornblende-poor). Examples of elemental variation diagrams (MgO vs. SiO_2, Fe_2O_3 vs. SiO_2, CaO vs. SiO_2, and TiO_2 vs. SiO_2) based on texture are shown in

Table 4: Major-element contents of the San Isabel batholith, coarse-grained porphyritic facies, hornblende-rich portion.

	COARSE-GRAINED PORPHYRITIC FACIES										
	HORNBLENDE-RICH										
	TG-14	TG-102	TG-18	TG-94	TG-16	TG-136	TG-134	TG-110	TG-135	TG-93	TG-124
SiO_2	56.05	58.78	58.87	59.09	60.04	60.42	60.66	61.02	61.31	61.39	64.26
Al_2O_3	14.39	14.89	14.15	15.49	14.20	15.33	14.72	14.46	14.24	13.96	14.34
TiO_2	1.83	1.45	1.77	1.45	1.34	1.34	1.51	1.27	1.56	1.39	1.32
Fe_2O_3	11.27	8.24	9.31	8.03	8.09	8.15	8.45	8.25	8.24	7.83	6.63
MgO	2.90	2.33	2.38	1.98	2.00	2.15	2.18	1.88	2.07	1.80	1.33
CaO	6.12	4.86	5.01	3.63	4.37	4.30	5.04	4.75	3.85	4.28	3.35
Na_2O	2.57	3.01	2.88	3.35	4.35	3.26	3.43	3.56	3.54	3.45	3.16
K_2O	4.18	4.99	4.17	6.03	5.08	3.96	3.54	2.86	3.15	4.09	5.31
MnO	0.21	0.16	0.18	0.14	0.16	0.13	0.15	0.13	0.13	0.17	0.12
Rb*	114	136	131	150	112	112	104	89	106	106	147
Sr*	449	555	447	563	570	528	559	580	459	281	371
Rb/Sr	0.25	0.25	0.29	0.27	0.20	0.21	0.19	0.15	0.23	0.38	0.40
LOI	0.81	0.79	1.12	0.89	0.76	0.94	0.81	0.97	1.00	0.72	0.54
Total	100.33	99.50	99.84	100.08	100.39	99.98	100.49	99.15	99.09	99.08	100.36

* ppm

Table 4: Major-element contents of the San Isabel batholith, coarse-grained porphyritic facies, intermediate portion.

	COARSE-GRAINED PORPHYRITIC FACIES					
	INTERMEDIATE					
	TG-137	TG-12	TG-100	TG-126	TG-129	TG-127
SiO_2	57.10	59.69	61.49	61.61	63.72	64.19
Al_2O_3	12.71	13.57	13.92	14.86	14.80	13.90
TiO_2	2.09	1.91	1.65	1.26	0.96	1.28
Fe_2O_3	11.64	8.76	8.94	6.59	6.28	7.17
MgO	3.00	2.14	1.84	1.55	1.54	1.60
CaO	5.75	5.23	4.55	3.69	3.35	3.81
Na_2O	2.82	3.29	2.61	3.11	3.43	3.22
K_2O	3.85	4.11	4.89	5.59	4.78	4.13
MnO	0.21	0.15	0.17	0.13	0.11	0.12
Rb*	134	115	129	165	133	117
Sr*	205	446	353	524	504	485
Rb/Sr	0.65	0.26	0.37	0.32	0.26	0.24
LOI	0.73	0.97	0.70	0.73	0.89	1.05
Total	99.90	99.82	100.76	99.12	99.87	100.47

* ppm

Table 4: Major-element contents of the San Isabel batholith, coarse-grained porphyritic facies, hornblende-poor portion.

	COARSE-GRAINED PORPHYRITIC FACIES									
	HORNBLENDE-POOR									
	TG-1	TG-142	TG-79	TG-139	TG-125	TG-143	TG-48	TG-95	TG-13	TG-68
SiO_2	58.97	60.12	60.54	61.24	63.68	63.71	64.18	64.94	70.70	71.96
Al_2O_3	13.86	13.59	13.86	14.34	14.43	14.92	14.12	13.82	14.45	13.43
TiO_2	1.83	1.44	1.55	1.42	1.29	1.05	1.11	1.12	0.49	0.72
Fe_2O_3	8.81	9.22	8.38	8.29	7.17	6.17	6.18	6.07	2.17	3.52
MgO	1.90	2.35	1.96	1.87	1.78	1.60	1.58	1.30	0.34	0.76
CaO	4.96	4.64	4.64	3.97	3.92	3.75	2.58	3.35	0.53	1.46
Na_2O	2.94	3.15	3.14	3.11	3.68	3.38	3.61	3.20	3.60	2.92
K_2O	4.85	3.69	4.11	4.73	3.02	4.78	5.67	4.21	5.90	5.00
MnO	0.16	0.17	0.16	0.16	0.13	0.12	0.13	0.11	0.02	0.07
Rb*	129	124	107	151	103	125	171	116	134	170
Sr*	580	502	457	403	503	527	358	138	121	302
Rb/Sr	0.22	0.25	0.23	0.38	0.21	0.24	0.48	0.84	1.11	0.56
LOI	0.83	0.76	0.78	0.57	1.12	0.66	0.65	0.90	0.88	0.69
Total	99.11	99.13	99.12	99.70	100.22	100.14	99.81	99.02	99.10	99.01

* ppm

Table 4: Major-element contents of the San Isabel batholith, medium-grained facies, hornblende-rich portion.

	MEDIUM-GRAINED FACIES			
	HORNBLENDE-RICH			
	TG-28	TG-87	TG-56	TG-23
SiO_2	61.91	63.13	63.15	65.24
Al_2O_3	13.44	14.53	14.41	13.34
TiO_2	1.55	1.35	1.26	1.57
Fe_2O_3	7.90	7.25	7.10	6.39
MgO	1.91	1.64	1.84	1.74
CaO	4.53	4.07	3.91	3.76
Na_2O	2.98	3.01	3.07	2.73
K_2O	4.10	3.81	4.10	4.19
MnO	0.14	0.12	0.12	0.15
Rb*	153	102	133	140
Sr*	457	542	528	382
Rb/Sr	0.34	0.19	0.25	0.37
LOI	0.93	1.09	1.14	1.28
Total	99.39	100.00	100.10	100.39

* ppm

Table 4: Major-element contents of the San Isabel batholith, medium-grained facies, intermediate portion.

	MEDIUM-GRAINED FACIES											
	INTERMEDIATE											
	TG-32	TG-108	TG-24	TG-3	TG-5	TG-10	TG-26	TG-96	TG-59	TG-4	TG-105	TG-70
SiO_2	59.43	60.08	60.48	60.96	61.34	61.42	61.74	61.82	62.46	62.55	64.78	65.11
Al_2O_3	13.38	13.28	13.84	14.38	14.13	14.52	12.14	13.81	14.30	13.75	14.30	14.74
TiO_2	1.54	2.05	1.53	1.76	1.69	1.33	1.75	1.34	1.43	1.53	1.10	1.14
Fe_2O_3	8.61	8.94	8.43	7.21	6.98	6.69	8.73	8.68	7.10	7.76	6.24	6.32
MgO	2.28	2.22	2.06	1.67	1.89	1.86	1.94	1.74	1.93	1.87	1.27	1.22
CaO	3.78	5.22	4.56	5.32	4.45	3.93	5.00	3.59	4.17	4.19	3.25	3.27
Na_2O	3.85	2.61	2.65	3.12	3.00	2.89	2.57	2.60	3.06	2.75	3.29	3.03
K_2O	5.68	4.87	5.10	4.91	4.79	5.42	4.05	4.49	4.97	4.85	3.86	4.38
MnO	0.17	0.17	0.16	0.17	0.16	0.15	0.14	0.15	0.16	0.16	0.11	0.12
Rb*	154	140	169	152	150	184	136	138	160	148	120	140
Sr*	418	475	441	474	373	401	525	279	487	513	463	448
Rb/Sr	0.37	0.29	0.38	0.32	0.40	0.46	0.26	0.50	0.33	0.29	0.26	0.31
LOI	0.78	0.88	0.88	0.60	0.88	0.87	0.93	0.88	0.94	0.71	1.03	0.66
Total	99.50	100.32	99.69	100.10	99.31	99.08	98.99	99.10	100.52	100.12	99.23	99.99

* ppm

Table 4: Major-element contents of the San Isabel batholith, medium-grained facies, hornblende-poor portion.

	MEDIUM-GRAINED FACIES							
	HORNBLENDE-POOR							
	TG-29	TG-25	TG-17	TG-22	TG-27	TG-109	TG-91	TG-77
SiO_2	59.50	59.50	60.68	60.75	60.89	62.75	64.61	65.89
Al_2O_3	13.40	13.79	14.46	14.45	13.76	15.10	14.42	14.36
TiO_2	1.63	1.94	1.65	1.54	1.50	1.29	1.30	0.74
Fe_2O_3	9.86	8.98	7.04	8.11	9.23	6.74	5.48	5.81
MgO	2.45	1.94	2.01	2.00	1.91	1.79	1.56	1.11
CaO	5.48	4.89	4.44	4.24	4.29	3.86	2.98	2.04
Na_2O	2.57	2.47	2.67	2.86	2.47	2.96	2.99	3.10
K_2O	4.37	4.88	4.81	4.72	5.04	5.29	5.66	5.19
MnO	0.20	0.16	0.14	0.16	0.14	0.14	0.18	0.10
Rb*	166	167	157	174	175	182	192	142
Sr*	480	489	430	506	426	445	311	154
Rb/Sr	0.35	0.34	0.37	0.34	0.41	0.41	0.62	0.92
LOI	0.92	0.85	1.12	0.75	0.71	0.74	0.96	0.67
Total	100.38	99.40	99.02	99.58	99.94	100.66	100.14	99.01

* ppm

Figure 10: Elemental variation diagrams of the San Isabel batholith based on textural facies; Fe_2O_3 vs. SiO_2 and MgO vs. SiO_2.

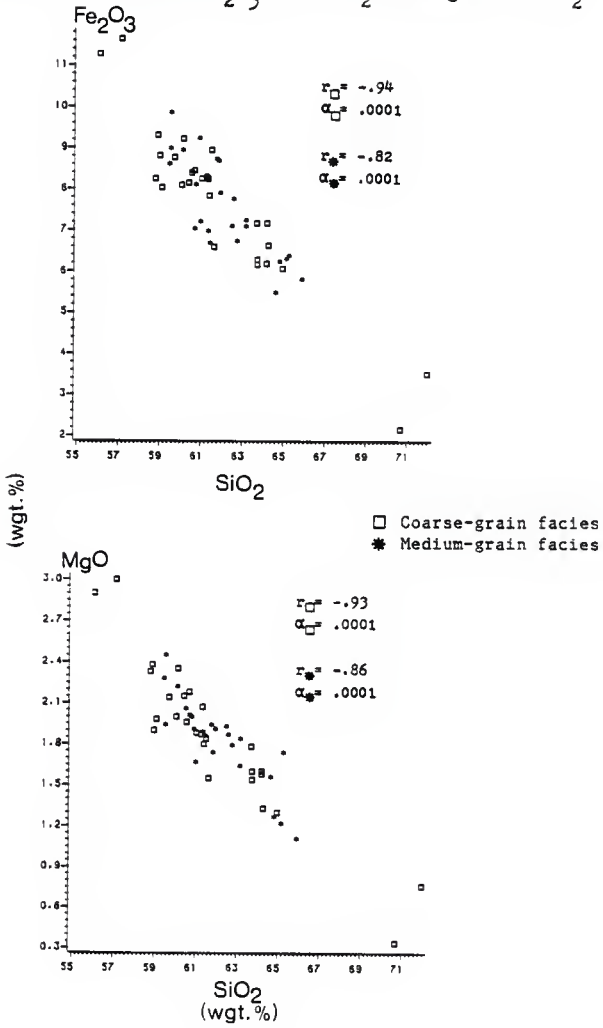

Figure 11: Elemental variation diagrams of the San Isabel batholith based on textural facies; CaO vs. SiO_2 and TiO_2 vs. SiO_2.

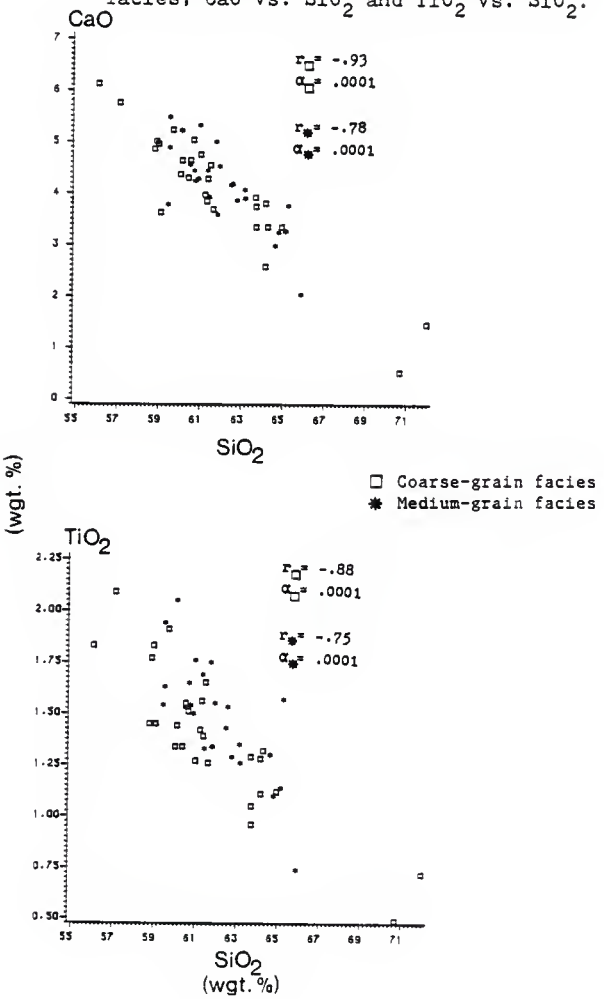

Figure 12: Elemental variation diagrams of the San Isabel batholith based on mineralogy; Fe_2O_3 vs. SiO_2 and MgO vs. SiO_2.

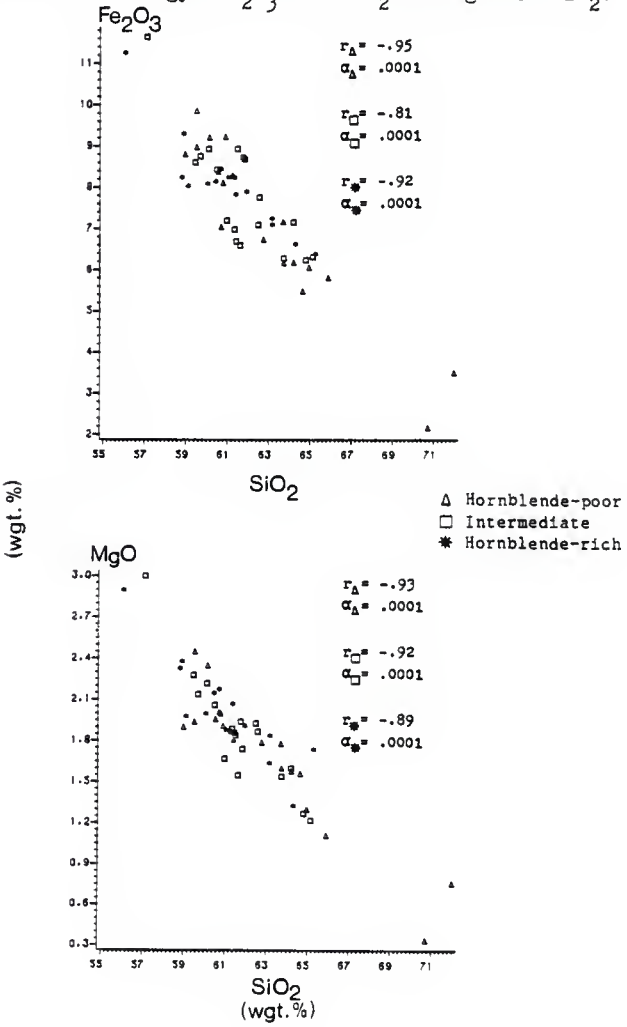

Figure 13: Elemental variation diagrams of the San Isabel batholith based on mineralogy; CaO vs. SiO_2 and TiO_2 vs. SiO_2.

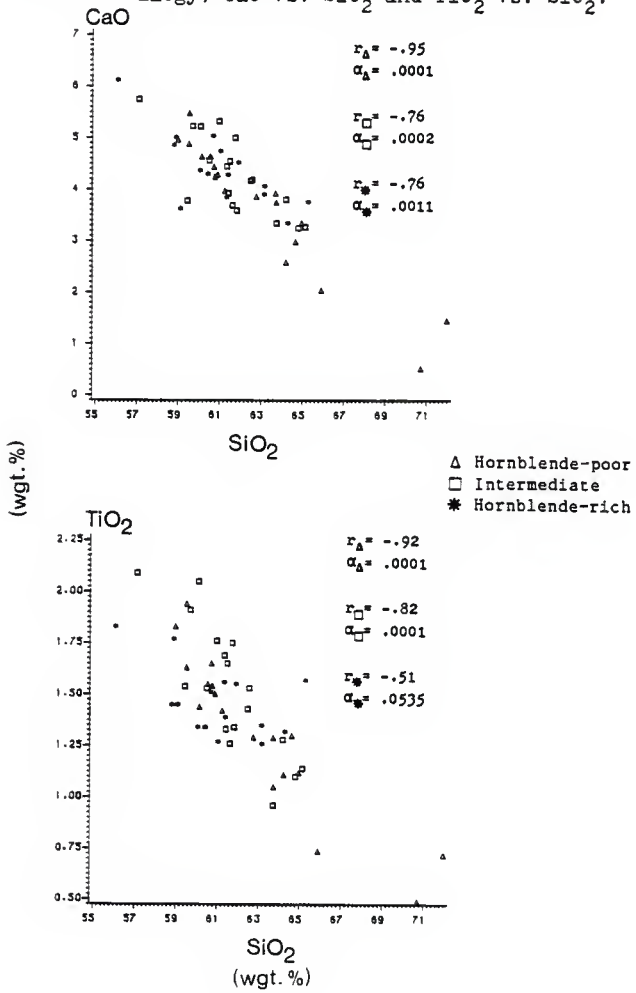

Figures 10 and 11. For comparison, examples of the same elemental variation diagrams based on mineralogy are shown in Figures 12 and 13. Variation diagrams plotted by texture show that the textural facies of the San Isabel batholith are indistinguishable from each other not only on mineral pair plots (Murray, 1970) but also on most elemental variation diagrams. Based on confidence intervals (C.I.) for both textural facies (Table 20), significant overlap between coarse-grained porphyritic samples and medium-grained samples exists for all elements except Na_2O and Rb. The coarse-grained porphyritic facies tends to have higher Na_2O and lower Rb contents than the medium-grained facies (Table 20). Variation diagrams based on mineralogy show significant overlap of hornblende-rich and hornblende-poor samples but minor separation of hornblende-poor samples from all other samples is evident on most plots. The most felsic samples, and presumably the most differentiated, are always hornblende-poor. Therefore, the majority of elemental variation diagrams in this study are plotted by mineralogy rather than texture.

Elemental variation diagrams for Na_2O vs. SiO_2 and K_2O vs. SiO_2 are shown in Figure 14. Enrichment of FeO relative to MgO is demonstrated by the FER vs. K_2O plot (Figure 15) where FER = FeO/(FeO+MgO). The degree of alumina saturation in the San Isabel monzogranite is demonstrated by the SHAND vs. SiO_2 plot (Figure 15) where SHAND = molecular

Figure 14: Elemental variation diagrams of the San Isabel batholith based on mineralogy; Na_2O vs. SiO_2 and K_2O vs. SiO_2.

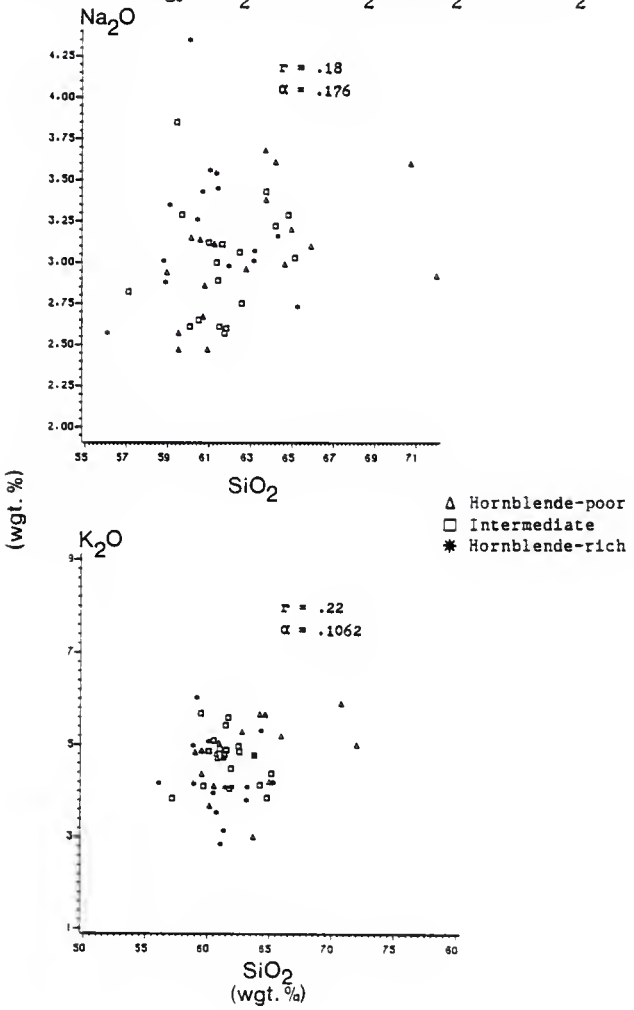

Figure 15: Elemental variation diagrams of the San Isabel batholith based on mineralogy; FER (FeO/FeO + MgO) vs. K_2O and SHAND (mol. Al_2O_3 / Na_2O + K_2O + CaO) vs. SiO_2.

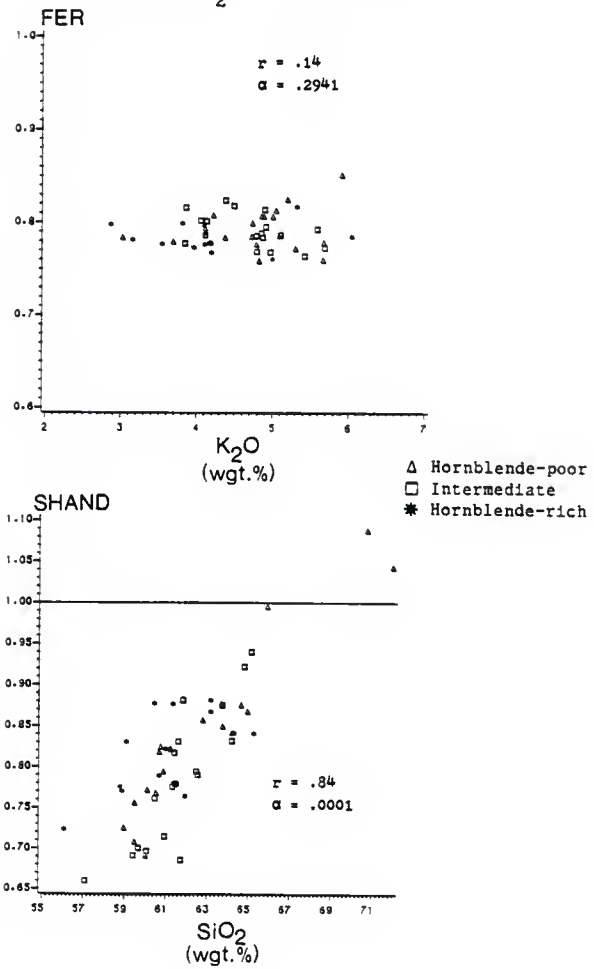

$Al_2O_3/(Na_2O+K_2O+CaO)$. Major-element contents are plotted versus differentiation index (DI) in Figures 40, 41, and 42 in Appendix F. Differentiation index (DI) is calculated as the sum of normative quartz, orthoclase, albite, nepheline, leucite, and potassium metasilicate.

The San Isabel monzogranite is too Fe-rich to be calc-alkaline (average $FeO/(FeO+MgO)$ = 0.79) and is metaluminous to slightly peraluminous. Hornblende-poor samples consistently have the lowest Fe_2O_3, MgO, CaO, and TiO_2, and the highest SiO_2 and DI. In most cases, the reverse is true for hornblende-rich samples although some hornblende-poor samples plot at the undifferentiated end of major-element trends. These hornblende-poor samples contain abundant sphene, biotite, and epidote which may account for the overlap between hornblende-poor and hornblende-rich samples on most variation diagrams. Fifteen out of eighteen hornblende-poor samples have high accessory minerals with epidote being the most abundant accessory. Complete alteration of hornblende to epidote may have occurred in these rocks producing "hornblende-poor" samples that plot in the undifferentiated, hornblende-rich portion of major-element trends.

Percentages of SiO_2, K_2O, and Na_2O increase with increasing DI while percentages of Fe_2O_3, MgO, CaO, TiO_2, and MnO decrease. Rb/Sr, $FeO/(FeO+MgO)$, Na_2O+K_2O, $(Na_2O+K_2O)/CaO$, and molecular $Al_2O_3/(Na_2O+K_2O+CaO)$ all

increase with increasing DI.

Variation diagrams involving ferromagnesian elements invariably show linear trends with high correlation coefficients (greater than 0.80) while those involving Na_2O, K_2O, and Al_2O_3 have correlation coefficients approaching zero and tend to be non-linear in comparison.

Trace Elements

Sixteen of the samples discussed above were selected from both textural facies for trace-element analysis. These samples represent the range of composition from hornblende-rich to hornblende-poor. Trace-element contents of the San Isabel monzogranite, except for Rb and Sr, are given in Table 5. Rb and Sr concentrations are given in Table 4. Elemental variation diagrams are presented in Figures 16, 17, 18, and 23. Chondrite-normalized rare-earth element (REE) patterns for the San Isabel batholith are plotted in Figure 19. In addition, chondrite-normalized REE patterns of mineral separates from a hornblende-rich sample (TG-16) are given in Figure 20. Trace-element contents of the mineral separates from TG-16 are presented in Table 6.

Hornblende-poor samples consistently plot at the most differentiated end of trends in elemental variation diagrams. Hornblende-poor samples tend to have the largest

negative Eu anomalies, the highest Rb/Sr ratios, and the highest concentrations of Th and REE. Eu/Sm ratios decrease slightly from hornblende-rich to hornblende-poor samples.

Table 5: Trace-element contents of the San Isabel batholith, coarse-grained porphyritic facies.

	COARSE-GRAINED PORPHYRITIC FACIES					
	HORNBLENDE-RICH				INTERMEDIATE	HORNBLENDE-POOR
	TG-14	TG-16	TG-136	TG-135	TG-127	TG-48
Ba	2286	2384	2110	1477	1540	1793
La	160	138	104	91	144	205
Ce	318	247	212	228	309	385
Sm	32	23	20	27	24	26
Eu	6	5	4	4	4	5
Tb	3	3	3	3	3	3
Yb	10	9	8	10	10	12
Lu	2	1	1	2	1	2
Th	9	8	8	9	13	23
Hf	34	19	13	17	15	30
Sc	34	27	16	19	15	14
Ta	2	2	2	3	4	4

*** Ba values not available

Table 5: Trace-element contents of the San Isabel batholith, medium-grained facies.

	MEDIUM-GRAINED FACIES									
	HORNBLENDE-RICH			INTERMEDIATE				HORNBLENDE-POOR		
	TG-28	TG-87	TG-56	TG-32	TG-5	TG-26	TG-59	TG-29	TG-22	TG-91
Ba	1675	1707	1420	1972	1732	1677	***	1493	1854	***
La	142	94	86	150	153	146	173	204	143	236
Ce	242	194	180	285	280	254	287	321	281	450
Sm	22	20	18	26	28	23	22	24	26	40
Eu	4	3	3	5	5	4	4	4	4	6
Tb	3	2	2	4	4	2	2	3	3	5
Yb	9	7	6	13	12	8	7	10	8	15
Lu	1	1	1	2	2	1	1	2	1	2
Th	22	10	10	18	19	23	22	34	20	27
Hf	20	12	12	36	24	21	12	28	16	18
Sc	24	19	14	26	28	16	24	25	20	24
Ta	3	2	3	3	3	2	2	3	3	5

*** Ba values not available

Figure 16: Elemental variation diagrams of the San Isabel batholith based on mineralogy; Rb/Sr vs. SiO_2 and Rb vs. Ba.

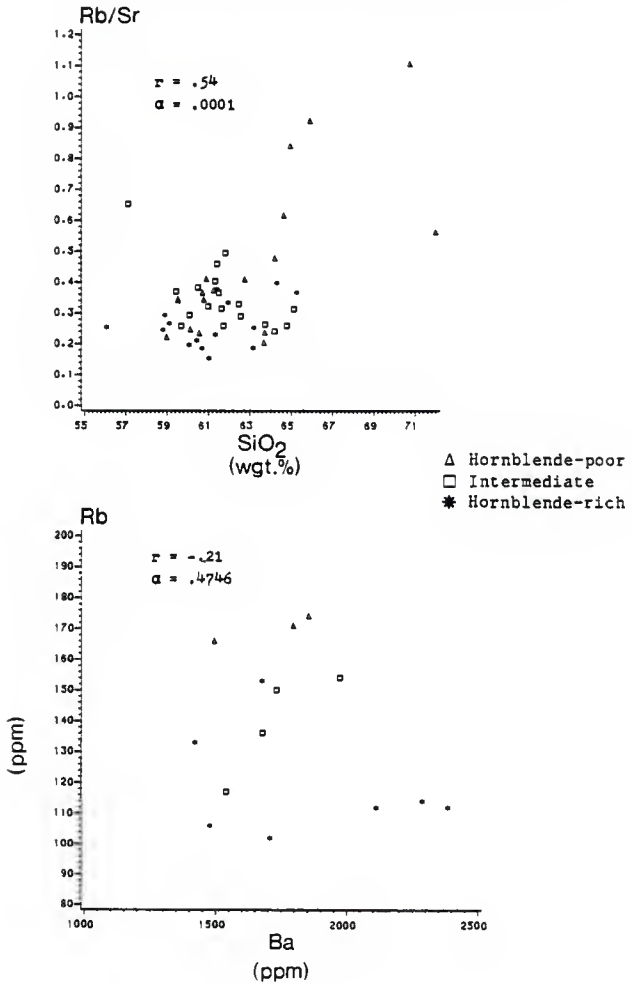

Figure 17: Elemental variation diagrams of the San Isabel batholith based on mineralogy; Ba vs. Eu/Sm and Th vs. Rb/Sr.

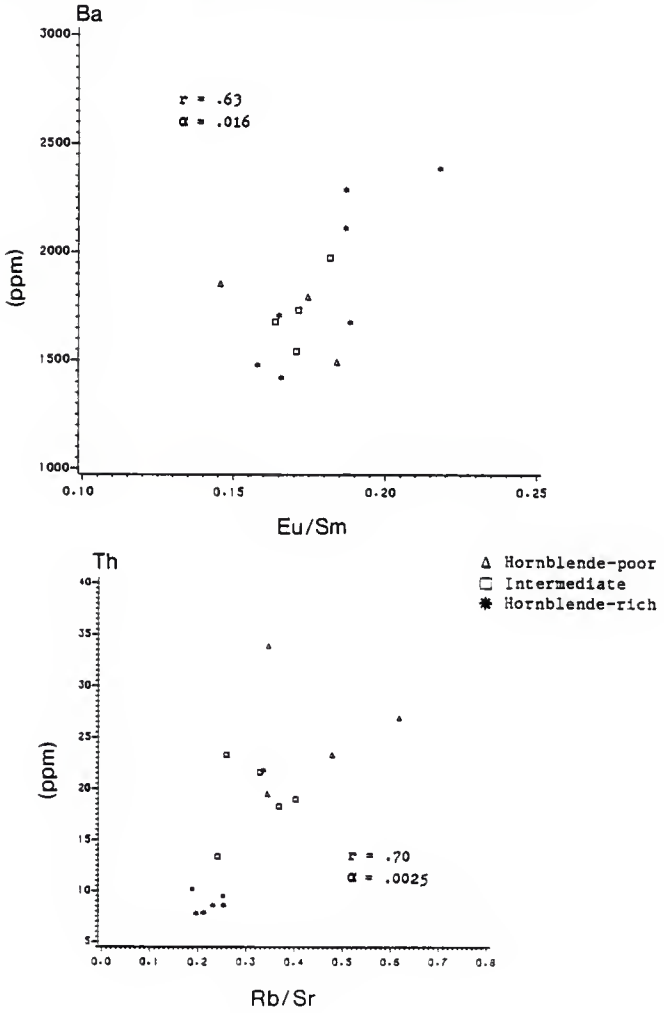

Figure 18: Elemental variation diagrams of the San Isabel batholith based on mineralogy; Rb vs. Th and Yb vs. Th.

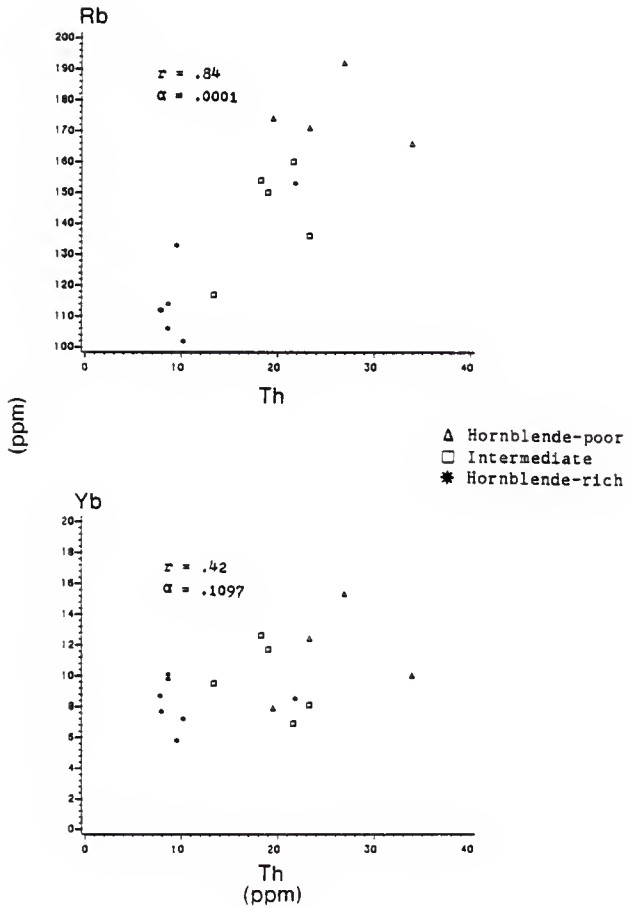

Figure 12: Chondrite normalized rare-earth element (REE) patterns for the San Isabel batholith.

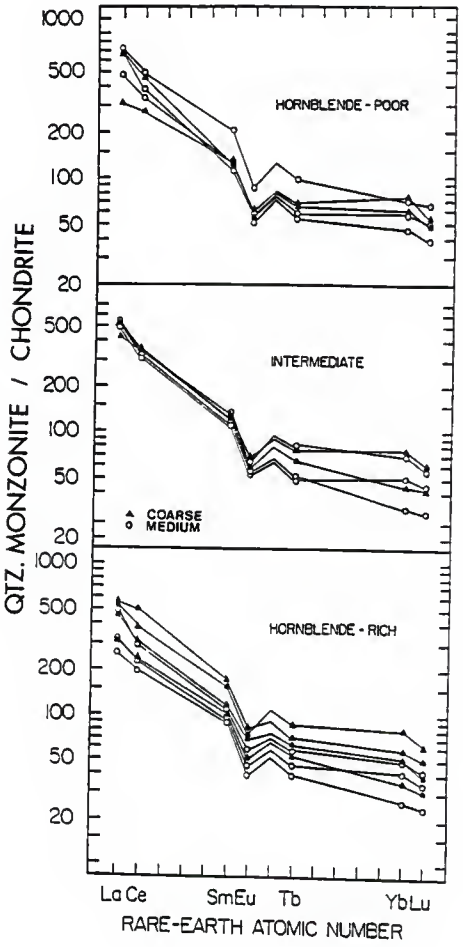

Figure 20: Rare-earth element (REE) ranges of mineral separates from the San Isabel monzogranite.

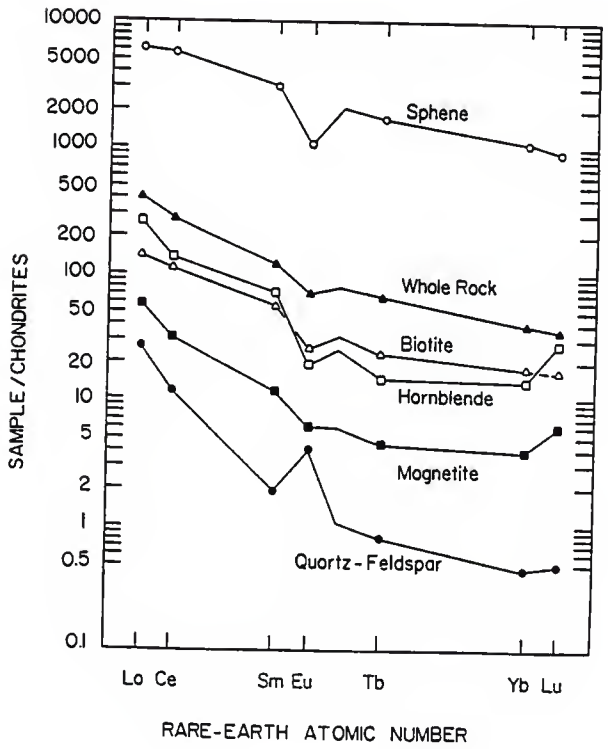

Table 6: Trace-element contents of mineral separates from TG-16, hornblende-rich sample, San Isabel batholith.

	QUARTZ+FELDSPAR	BIOTITE	HORNBLENDE	SPHENE
Ba	2320	2260	106	167
Rb	50	581	18	49
Ce	10	109	119	5203
Sm	0.37	10.9	13.8	101
Eu	0.30	1.86	1.37	77
Yb	0.10	3.8	2.94	241
Lu	0.02	0.56	0.95	31
Sc	0.25	30	259	35

D I S C U S S I O N

COMPARISON OF SAN ISABEL BATHOLITH WITH OTHER GRANITIC ROCKS

Compared to other granitic rocks (Tables 7 and 8), the San Isabel monzogranite is characterized by low SiO_2, moderate Sr, high Fe_2O_3, TiO_2, K_2O, Ba, Sc, and REE, and small, negative Eu anomalies (Eu/Sm = 0.146 to 0.218).

A comparison of elemental variation in selected Wet Mountain granitoids is presented in Figures 30 through 39 in Appendix E. Granitoid plutons considered in this comparison include:

(1) 1.36 b.y. old San Isabel monzogranite

(2) 1.44 b.y. old Oak Creek monzogranite to granodiorite; data provided by Stone (1984)

(3) 1.46-1.47 b.y. old West McCoy Gulch monzogranite to syenogranite; data provided by Sassarini (1984)

(4) 1.67 b.y. old Garell Peak granodiorite; data provided by McCabe (1984)

Other Wet Mountain plutons selected for this comparison are: Blue Ridge, Bear Creek, Grape Creek, Buckskin Joe, Baker Gulch, north of Gem Park, Parkdale Gneiss, Royal Gorge, Twin Mountain, and Temple Canyon. Chemical data for these rocks were provided by Cullers (1985). For plotting purposes, most of these samples were assigned names based on location.

Table 7: Comparison of average major-element contents of selected acid plutonic rocks.

	ALKALI FELOSPAR GRANITE[1]	QUARTZ MONZONITE (AOAMELLITE)[1]	GRANODIORITE[1]	TONALITE[1]	SAN ISABEL MONZOGRANITE
SiO_2	72.04	69.51	66.80	63.04	62.06
Al_2O_3	14.42	14.76	15.99	16.68	14.12
TiO_2	0.30	0.51	0.54	0.73	1.44
Fe_2O_3	3.09	3.65	4.71	6.16	7.59
MgO	0.71	1.11	1.80	2.78	1.83
CaO	1.82	2.55	3.92	5.42	4.05
Na_2O	3.69	3.51	3.77	3.64	3.06
K_2O	4.12	4.14	2.79	1.99	4.64
MnO	0.05	0.08	0.08	0.08	0.14

[1] from Hyndman, 1985

Table 8: Comparison of average trace-element contents of selected acid plutonic rocks.

	ACID ROCKS (HIGH Ca)[1]	ACID ROCKS (LOW Ca)[1]	GRANITOID ROCKS[1]	SAN ISABEL MONZOGRANITE
Rb	110	170	200	143
Sr	440	100	300	429
Ba	420	840	830	1794
La	45	55	60	148
Ce	81	92	100	279
Eu	1.4	1.6	1.5	4.4
Sm	8.8	10	9	25
Yb	3.5	4	4	9.5
Lu	1.1	1.2	1	1.4
Th	8.5	17	18	17
Sc	14	7	3	22
Ta	3.6	4.2	3.5	3

[1] from Rösler and Lange, 1972

For the most part, these samples represent the foliated 1.7 b.y. old granodiorites (Xgd) which are abundant in the northern Wet Mountains.

In addition, the major- and trace-element concentrations of selected Wet Mountain granitic rocks is presented in Table 19 in Appendix H. Chemical data from the 1.36 b.y. old Bear Basin granite and the 1.7 b.y. old Crampton Mountain granodiorites are included in this compilation.

Conclusions based on examination of elemental ranges (Table 19) and comparison plots of selected Wet Mountain granitoid plutons (Figures 30 to 39) include the following:

(1) Compared to the San Isabel monzogranite, the most similar granitoid pluton in the Wet Mountains, based on chemistry, is the porphyritic facies of the Oak Creek monzogranite to granodiorite. The only major differences between the two are:
    (a) Oak Creek has higher Th and Ba (Figure 39).
    (b) Oak Creek samples occasionally plot in the calc-alkaline field defined by the SiO_2 vs. FeO/(FeO+MgO) plot (Figure 33).
    (c) Oak Creek is more peraluminous (Figure 32).
(2) The least differentiated tonalites and granodiorites from the Crampton Mountain/Twin Mountain area are also chemically similar to the San Isabel batholith (Table 19). These metaluminous granitoids have similar SiO_2,

Ba, and ferromagnesian element contents to the San Isabel batholith.

(3) Compared to most of the Wet Mountain granitoids other than Oak Creek, the San Isabel monzogranite is characterized by:

(a) lower Rb/Sr ratios (Figure 30)

(b) higher Sr contents (Figure 31)

(c) lower molecular $Al_2O_3/(Na_2O+K_2O+CaO)$; The San Isabel batholith is predominantly metaluminous while all other granitoids tend to be peraluminous (Figure 32).

(d) higher TiO_2 and MgO contents (Figure 36)

(e) higher CaO, FeO, and Ba contents; The San Isabel monzogranite, the Crampton Mountain tonalites and granodiorites, and the porphyritic facies of the Oak Creek pluton have the highest CaO, FeO, and Ba concentrations of all Wet Mountain granitoids (Figures 37 and 39 and Table 19).

(4) Almost all Wet Mountain granitoids are too Fe-rich to be calc-alkaline (Figure 33 and Table 19) and are subalkalic to alkalic in nature (Figure 34).

(5) All Wet Mountain plutons show similar trends on the $(Na_2O+K_2O)/CaO$ vs. SiO_2 variation diagram (Figure 35) except the West McCoy Gulch monzogranite to syenogranite which lacks any discernable trend.

ASSIMILATION OF XENOLITHS

Xenoliths of hornblende-biotite gneiss and granite gneiss are common in some parts of the San Isabel batholith. Evidence for contamination of the San Isabel magma by assimilated xenoliths includes the following:

(1) Some mafic mineral schlieren up to 30 cm in length have gradational boundaries with the batholith (Murray, 1970).

(2) The San Isabel monzogranite has high K and Ba contents - melting of felsic portions of xenoliths could produce melts with high K and Ba.

Assimilation of xenoliths by the San Isabel magma appears to be minimal though, based on the following observations:

(1) Xenoliths usually exhibit sharp contacts with the batholith (Murray, 1970).

(2) The low initial $^{87}Sr/^{86}Sr$ ratio of the San Isabel monzogranite suggests that negligible contamination by 1.8 b.y. old metasedimentary and metavolcanic rocks occurred.

(3) Whole rock samples of the San Isabel batholith define a straight line when plotted on Concordia diagrams regardless of location or proximity to xenoliths (Thomas et al., in press).

METASOMATISM AND ALTERATION

Deuteric alteration of the San Isabel batholith was recognized by Murray (1970) and is largely responsible for alteration of biotite to chlorite, sphene to leucoxene, hornblende to epidote, and feldspar to sericite. Plagioclase, in particular, is usually extremely altered and sericitized. Elemental variation diagrams involving Na, K, Sr, and Ba are characterized by low correlation coefficients (r) and may be further evidence of deuteric alteration. In addition, metasomatism involving fluids rich in alkalis may also be responsible for non-linear variation diagrams involving Na, K, and Ba. Trace-elements that tend to become mobile during weathering processes, deuteric alteration, or metasomatism include Na, K, Rb, Sr, Cs, Ba, and P (Tarney et al., 1977; Cox et al., 1980). Therefore, a mechanism for altering certain elemental concentrations (Na, K, Sr, and Ba) in the San Isabel batholith exists.

Ba contents in the San Isabel batholith are especially variable (Table 5 and Figure 16). Due to the extreme variability of Ba in the batholith, use of the element in trace-element modeling of fractional crystallization processes will be avoided. Rb and Sr contents in the San Isabel batholith also show some variation (Figure 31) but the linear nature of the Rb-Sr whole rock isochron (Shuster, 1984) and the general agreement between Rb-Sr and U-Pb ages

(Shuster, 1984; Thomas et al., in press) argue against significant mobilization of Rb or Sr. Therefore, Rb and Sr will be utilized in trace-element modeling of the San Isabel batholith.

INTENSIVE PARAMETERS

The San Isabel batholith is considered to be a mesozonal-catazonal pluton (Murray, 1970) based on the following criteria as defined by Buddington (1959):

(1) no evidence of contact metamorphism of country rock

(2) no evidence of chill zones in the batholith

(3) abundant migmatites and lit-par-lit gneisses

(4) abundant pegmatites

(5) foliation of country rock wraps around the margins of the batholith

(6) the batholith is generally coarse-grained

Mesozonal-catazonal intrusions are presumably emplaced at depths of 10-15 km and a pressure of 3-5 Kb.

The normative composition of the San Isabel batholith in terms of quartz, albite, and orthoclase at various Ab/An ratios is presented in Figure 21. Pressures in excess of 7-10 Kb are suggested by the normative Q-Ab-Or diagram, but conclusions based on this diagram must be made with care for the following reasons:

Figure 21: Normative composition of the San Isabel batholith in terms of quartz, orthoclase, and albite at various Ab/An ratios. These are compared to the experimental system at H_2O-saturated conditions.

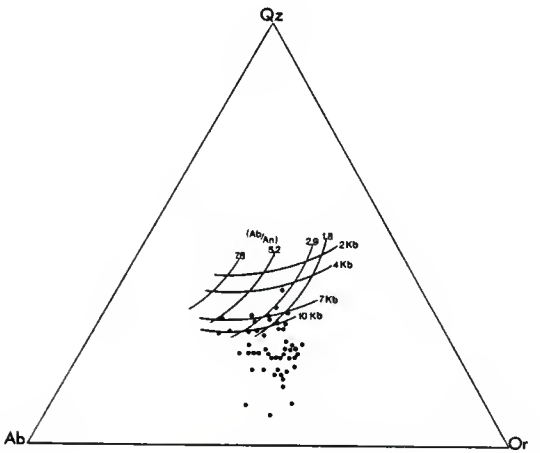

(1) Samples plotted on the normative Q-Ab-Or diagram are compared to the experimental system at H_2O-saturated conditions - samples from anhydrous melts may give anomalous pressures (Steiner et al., 1975).

(2) Samples may not represent minimum melt compositions (Anderson and Cullers, 1978).

The presence of euhedral, magmatic epidote as inclusions in the biotite suggests that crystallization of the San Isabel magma did indeed occur at very high pressures (Holdaway, 1972; Liou, 1973; Naney, 1983; Zen, 1985) as indicated by the normative Q-Ab-Or diagram.

Murray (1970) estimated the temperature of the San Isabel magma at the time of emplacement by a number of procedures involving quartz, feldspar, and muscovite:

(1) Coexistence of microcline containing 25-35% perthite and plagioclase (An_{30}) implies a temperature of 600-700° C (Barth, 1951).

(2) Exsolution of albite from alkali feldspar (Ab_{30}) occurs at about 675° C (Barth, 1969).

(3) Concurrent growth of plagioclase (An_{30}) and alkali feldspar (Ab_{25}-Ab_{35}) takes place at about 725° C (Deer et al., 1966).

(4) Minimum melt conditions of a granite with quartz, plagioclase (An_{34}), and alkali feldspar (Ab_{25}-Ab_{35}) are 670° C and 5 Kb (Winkler, 1967).

(5) Muscovite is unstable at temperatures greater than 725°C at about 5 Kb pressure (Barth, 1969).

The anhydrous nature of the San Isabel batholith during initial crystallization is suggested by the presence of late, interstitial biotite and occasional fluorite (Chappell, 1966; White and Chappell, 1977; Collins et al., 1982), although some early biotite does occur in the mafic glomerocrysts. The occurrence of abundant pegmatites throughout the batholith indicates hydrous conditions during later stages of crystallization in the San Isabel magma. Simultaneous crystallization of late biotite and quartz is characteristic of the San Isabel batholith and suggests an H_2O content of 1.2-1.5% in the magma (Maaløe and Wyllie, 1975; Wyllie et al., 1976).

Based on the preceding discussions, the temperature of the San Isabel magma at the time of emplacement was approximately 725°C (Murray, 1970). A pressure of 5-7 Kb during emplacement is indicated by the normative Q-Ab-Or diagram, the presence of magmatic epidote, and criteria defined by Buddington (1959). H_2O content of the San Isabel magma was 1.2-1.5% based on sequence of crystallization.

PETROGENESIS

Introduction

Models for the origin and chemical evolution of the San Isabel batholith must be consistent with major- and trace-element data, petrography, field relationships, results of experimental petrography, and isotopic data. In this study, assessment of possible source rocks that could melt to form the least differentiated portions of the San Isabel batholith is based on compatibility with the above data.

Isotopic Constraints

Isotopic data place constraints on the type of source rock that can melt to form an igneous rock, the age of crystallization, the residence time of an igneous rock in the crust, and the time of crustal-derivation from the mantle.

Nelson and DePaolo (1985) have shown that the "crust-formation age" or time of differentiation of the crust from the mantle for a large portion of the central United States, based on Nd isotopic data, is 1.7 to 1.9 b.y. ago (Figure 22). Thomas et al. (in press) demonstrated that most of the Precambrian basement of the central United States is underlain by a great terrane of rhyolitic ash flow tuff and

Figure 22: Generalized maps showing crystallization ages of basement rocks in North America and crust-formation ages for North and Central American petrographic provinces.

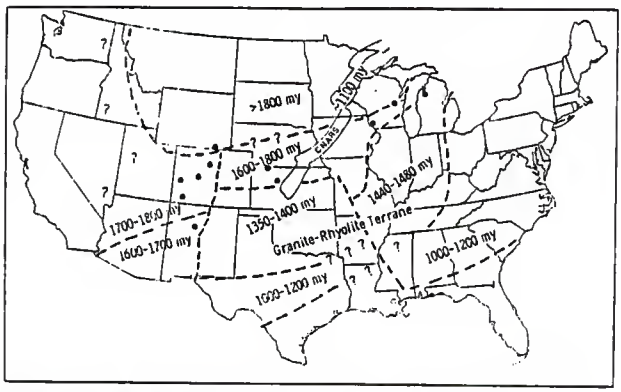

Generalized map showing U/Pb ages from zircons of basement rocks. Age range for each terrane indicates the oldest rocks known from that region; younger rocks may also be present. Dots indicate locations of known 1420-1480 m.y. old anorogenic plutons within older terranes. (from Thomas, J., Shuster, R., and Bickford, M., in press).

Schematic outline of crust-formation age provinces for North and Central America based on Nd/Sm data. Boundaries are queried where highly speculative. (from Nelson, B. and DePaolo, D., 1985).

epizonal granite plutons dated at 1.35-1.4 b.y. (Figure 22). Thomas et al. (in press) also provided a U/Pb age from zircons of 1.36 b.y. for the San Isabel batholith. The calculated initial $^{87}Sr/^{86}Sr$ ratio for the San Isabel batholith is 0.7031 (Shuster, 1984).

The age of crustal-derivation from the mantle for selected samples from the central United States is 1.7 to 1.9 b.y. (Nelson and DePaolo, 1985). The assumption that rocks in the Wet Mountains have similar crustal-derived ages may be unfounded because only one Wet Mountain sample was analyzed in the above study, although Nelson and DePaolo (1985) analyzed many samples from the Rocky Mountains of Colorado and these were shown to have crust-formation ages of 1.7 to 1.9 b.y..

The San Isabel batholith is contemporaneous with the 1.35 to 1.4 b.y. old terrane of rhyolite and unfoliated, epizonal granite that occurs in the Precambrian basement of the central United States and may represent a deeper-seated (mesozonal-catazonal) manifestation of this anorogenic tectonic activity (Thomas et al., in press).

The low initial $^{87}Sr/^{86}Sr$ ratio of the 1.36 b.y. old San Isabel batholith suggests that the source rock that melted to form the batholith was (1) mantle-derived or (2) characterized by a short residence time in the lower crust. In addition, the low initial $^{87}Sr/^{86}Sr$ ratio of the

batholith places constraints on the maximum Rb/Sr ratio that a given source rock may have. Assuming that the source rocks have initial $^{87}Sr/^{86}Sr$ ratios ranging from 0.700 to 0.703, and assuming that no pre-San Isabel melting events have occurred, the highest Rb/Sr ratio the source rocks can have and still be compatible with the low initial $^{87}Sr/^{86}Sr$ ratio of the San Isabel batholith, is 0.22.

Additional Constraints

Trace-element modeling of the processes responsible for the range of composition in the San Isabel batholith can be a valuable aid in placing constraints on (1) the type of source rock that can melt to form the batholith, (2) the degree of partial melting, and (3) the proportion of phases in the melt.

Petrographic data and trace-element contents of the San Isabel batholith suggest that the hornblende-rich portion of the batholith is the least differentiated, most primitive rock in the suite. Hornblende-poor samples consistently plot at the differentiated end of trends in elemental variation diagrams (Figures 16, 17, and 18). Therefore, the origin of the hornblende-rich portion of the batholith will be considered first followed by models for the formation of the hornblende-poor portions.

Any model for the origin of the least differentiated,

hornblende-rich portion of the batholith must account for the following characteristics:

(1) small, negative Eu anomalies

(2) high concentrations of REE

(3) moderate concentrations of Sr

(4) high concentrations of large-ion-lithophile elements (LILE) such as K, Ba, and LREE

(5) high, but extremely variable Ba contents

(6) low to moderate LREE/HREE

(7) high concentrations of Fe, Mg, Ca, and Ti

(8) metaluminous nature

(9) low initial $^{87}Sr/^{86}Sr$ ratio

(10) abundant mafic minerals

(11) abundant modal quartz

(12) presence of mafic glomerocrysts and cumulate mafic material throughout the batholith

(13) presence of partially assimilated hornblende-biotite gneiss and granite gneiss xenoliths

Production of a granitic rock with the above characteristics by partial melting processes requires a source with little or no Eu anomaly and no garnet (Cullers and Graf, 1984). In addition, the small, negative Eu anomaly, moderate Sr, and high Ba and K contents of the batholith require that residual plagioclase and no alkali feldspar be present in the source (Cullers and Graf, 1984).

Potential Source Rock Types

The following rock types will be tested as source rocks for the San Isabel magma:

(1) Metamorphic rocks similar in composition to the 1.8 b.y. old hornblende-biotite gneiss and granite gneiss country rocks,

(2) Quartz-normative tholeiitic gabbro,

(3) Granitic rocks similar in composition to the 1.7 b.y. old foliated plutons at Garell Peak, Royal Gorge, and Twin Mountain, and

(4) Tonalites and granodiorites similar in composition to other 1.7 b.y. old tonalites and granodiorites in the mid-continent and having negligable Eu anomalies (Anderson and Cullers, 1978; Cullers and Graf, 1984).

Melting of 1.8 b.y. old Metamorphic Country Rock

Metamorphic country rocks in the Wet Mountains of Colorado consist of biotite gneiss, granite gneiss, amphibolite, and biotite schist but granite gneiss is the most abundant rock type with the lowest melting point. Partial melting of 1.8 b.y. old granite gneiss country rock

to form the San Isabel magma is an attractive model because large volumes of metamorphic country rock are available for generation of granitic melts. In addition, melting of granite gneiss could produce K-spar-rich melts and could explain high K and Ba in the San Isabel batholith. But the low initial $^{87}Sr/^{86}Sr$ ratio of the batholith (0.7031) precludes radiogenic 1.8 b.y. old metamorphic country rock as source material. Rb/Sr ratios in the granite gneiss range from 0.63 to 1.30 (Cullers, 1985) and are too high to be compatible with the low initial $^{87}Sr/^{86}Sr$ ratio of the San Isabel batholith.

Partial melting of biotite gneisses and schists to form the San Isabel magma is unlikely because melting of metapelitic schists and gneisses tends to produce peraluminous granites (Collins et al., 1982; Didier et al., 1982). In addition, granitic rocks formed from partial melting of metapelitic source rocks (S-type granites) have initial $^{87}Sr/^{86}Sr$ ratios greater than 0.708 (Collins et al., 1982; Didier et al., 1982). The San Isabel monzogranite is distinctly metaluminous and contains abundant modal hornblende and sphene. These characteristics are indicative of an igneous source rather than a metasedimentary one (Collins et al., 1982; Didier et al., 1982). Therefore, the 1.8 b.y. old metamorphic country rock must be rejected as the source rock for the San Isabel magma.

Melting of Quartz-Normative Tholeiitic Gabbro

Partial melting of basaltic source rocks to produce granitic magmas has been recognized as a viable mechanism in a number of previous studies (Barker et al., 1975; Thorpe et al., 1977; Perfit et al., 1980; Snoke et al., 1981; Cullers and Graf, 1984). Therefore, a quartz-normative tholeiitic gabbro was tested as a source rock for the San Isabel monzogranite. Trace-element contents for the tholeiitic gabbro source are taken from data on altered tholeiites (Wood et al., 1976; Hellman et al., 1979; Luden and Thompson, 1979; Apted, 1981; Cullers and Graf, 1984; Anderson and Cullers, 1985) and are given in Table 9.

Five to ten percent partial melting of quartz-normative tholeiitic gabbro (mode: plagioclase/clinopyroxene/orthopyroxene/hornblende/biotite/sphene = .50/.30/.10/.05/.02/.03; melting ratio = .30/.25/.04/.30/.10/.01) can produce melts characterized by:

(1) small, negative Eu anomalies

(2) moderate to high REE

(3) low initial $^{87}Sr/^{86}Sr$ ratios

(4) high Fe/Mg ratios

The San Isabel batholith possesses all of the above characteristics. In addition, Eu, Sm, Yb, and Lu concentrations in the San Isabel batholith are well within

Table 9: Trace-element ranges of rocks used in partial melting and crystallization models.

	Tonalite / Granodiorite (1)	Tholeiitic Gabbro (2)	Tonalitic Hornbl.-Biotite Gneise (3)	San Isabel Batholith Hornblende-rich (4)	San Ieabel Batholith Hornblende-poor (4)
Rb	50 - 200	1 - 20	86 - 218	89 - 153	103 - 192
Sr	300 - 940	65 - 300	337 - 345	281 - 580	121 - 580
Ba	900 - 2000	40 - 190	1860 - 1970	1420 - 2384	1493 - 1854
Ce	42 - 76	4 - 41	47 - 240	180 - 318	281 - 450
Sm	3 - 8	2 - 7	3 - 20	18 - 32	24 - 40
Eu	1 - 2.7	1 - 2	1 - 3	3 - 6	4 - 6
Yb	1.1 - 3.4	1 - 6	1.4 - 7.4	6 - 10	8 - 15
Lu	0.2 - 0.6	0.2 - 1.0	0.2 - 1.2	1 - 2	1 - 2
Sc	1 - 43	20 - 50	3 - 6	14 - 34	14 - 25

1- Trace-element ranges are for trondhjemites, tonalites, and granodiorites having little or no Eu anomalies. Data are from Anderson and Cullers (1978) and Cullers and Graf (1984).

2- Trace-element ranges for tholeiitic gabbro include both fresh oceanic basalts and enriched, altered tholeiites. Data are from papers summarized in Wood et al. (1976), Hellman et al. (1979), Luden and Thompson (1979), Apted (1981), Cullers and Graf (1984), and Anderson and Cullers, unpublished data of Proterozoic orogenic tonalites and their source rocks.

3- Trace-element ranges are based on analyses of metamorphic country rocks and xenoliths associated with the San Isabel batholith, (from Cullers, unpublished data of Wet Mountain Proterozoic rocks).

4- Trace-element ranges of San Isabel monzogranite. Data compiled from this study.

Table 10: Distribution coefficients used in melting and crystallization models.

	SILICIC MELTS						BASIC MELTS					
Element	Plag	K-spar	Qtz	Biot	Hornbl	Sphene	Plag	Cpx	Opx	Sphene	Biot	Hornbl
Rb	.041	.37	.001	2.2	.014	--	.07	.03	.02	.01	3.1	.40
Sr	4.4	3.87	.001	.12	.022	--	1.83	.12	.017	.01	.08	.46
Ba	.31	6.1	.001	9.7	.044	--	2.2	.02	.013	.01	1.1	.50
Ce	.27	.044	.001	.32	1.52	139	.12	.15	.024	.08	.034	.20
Sm	.13	.018	.001	.26	7.77	70	.067	.50	.054	.05	.031	.52
Eu	2.2	1.13	.001	.24	8.9	61	.34	.51	.054	.03	.03	.59
Yb	.049	.012	.001	.44	8.4	--	.067	.62	.34	.02	.042	.49
Lu	.046	.006	.001	.33	5.5	21	.06	.56	.42	.02	.046	.43
Sc	.02	.06	.001	11.0	15.0	--	.035	3.0	1.2	--	11.0	10.0

Table 10 is based on a compilation of data from the following sources: Berlin and Henderson (1969), Ewart and Taylor (1969), Griffin and Murthy (1969), Higuichi and Nagasawa (1969), Schnetzler and Philpotts (1970), Tanaka and Nishizawa (1975), Arth and Barker (1976), Condie and Hunter (1976), and Cullers and Graf (1984).

the range predicted by trace-element modeling of partial melting of tholeiitic gabbro (Table 11).

But, the model is inconsistent with respect to Rb, Sr, and Ce contents as they are predicted by the partial melting model to be too low (Table 11). The model cannot account for Rb contents greater than 138 ppm, Sr contents greater than 306 ppm, or Ce concentrations greater than 126 ppm in the hornblende-rich portion of the batholith. Fractional crystallization of the tholeiitic liquid can produce higher Ce and Rb values but results in further depletion of Sr in the melt. In addition, partial melting of tholeiitic gabbro cannot account for Ba concentrations greater than 165 ppm in the predicted melt. Obviously, Ba concentrations in the San Isabel batholith (1420-2384 ppm) are much too high to be compatible with such a melting model. Partial melting of mantle-derived tholeiitic gabbro is a reasonable mechanism for the production of small amounts of granitic rock but is untenable with respect to the formation of large, granite batholiths (Hyndman, 1985). Presumably, assimilation of large amounts of felsic country rock by the evolved tholeiitic liquid is required to form granitic intrusions of batholithic proportions (Hyndman, 1985).

The abundance of partially assimilated gneissic xenoliths in some parts of the batholith suggests that limited assimilation of gneissic country rock could have

Table 11: Trace-element contents in quartz-normative tholeiitic gabbro source rock, in hypothetical liquid that is produced by 5-10 percent partial melting of source, and in hornblende-rich portion of San Isabel batholith (data in ppm).

	Quartz-normative tholeiitic gabbro	Predicted valuee in hypothetical melt	Obeerved values in hornblende-rich portion of the batholith
Rb	1 - 20	6 - 138	89 - 153
Sr	65 - 300	65 - 306	281 - 580
Ce	4 - 41	6 - 126	180 - 318
Sm	2 - 7	8 - 30	18 - 32
Eu	1 - 2	2.6 - 5.3	3 - 6
Yb	1 - 6	3.2 - 20	6 - 10
Lu	0.2 - 1	0.7 - 3.6	1 - 2

Table 12: Trace-element contents in tonalitic hornblende-biotite gneiss and granite gneiss country rock, in hypothetical liquid that is produced by 20 percent partial melting of gneissic country rock, in hypothetical liquid produced by 30 percent assimilation of gneissic melt by tholeiitic liquid, and in hornblende-rich portion of San Isabel batholith (data in ppm).

	Tonalitic hornblende-biotite gneiss and granite gneiss	Predicted values in hypothetical melt	Predicted values for 30% assimilation of gneissic melt by tholeiitic liquid	Observed values in hornblende-rich portion of the batholith
Rb	86 - 218	392 - 994	122 - 395	89 - 153
Sr	337 - 345	148 - 152	90 - 260	281 - 580
Ce	47 - 240	102 - 518	35 - 244	180 - 318
Sm	3 - 20	2 - 15	6 - 26	18 - 32
Eu	1 - 3	0.4 - 1.2	2 - 4	3 - 6
Yb	1.4 - 7.4	1 - 5.3	2.5 - 16	6 - 10
Lu	0.2 - 1.2	0.2 - 1.25	0.6 - 2.9	1 - 2

produced high K, Sr, and Ba contents in the San Isabel batholith. But the low initial $^{87}Sr/^{86}Sr$ ratio of the San Isabel batholith (0.7031) argues against significant mixing of radiogenic metamorphic country rock with the San Isabel magma; therefore, only limited "reaction-melting" and mixing of gneissic country rock is proposed. Trace-element contents for the gneissic country rock are taken from analyses of xenoliths in the San Isabel batholith and are given in Table 9.

Twenty percent partial melting of hornblende-biotite gneiss and granite gneiss (average mode: plagioclase/K-spar/quartz/biotite/hornblende = .45/.10/.25/.05/.15; melting ratio = .19/.35/.20/.25/.01) produces melts with high Rb and Ce but low Sr and Eu (Table 12). Predicted trace-element values for thirty percent assimilation of this gneissic melt by the tholeiitic liquid are presented in Table 12. Rb, Sm, Yb, and Lu concentrations in the San Isabel batholith are well within the range predicted by 30% assimilation of gneissic country rock by tholeiitic liquid (Table 12). But the model cannot account for Sr contents greater than 260 ppm, Ce contents greater than 244 ppm, or Eu concentrations greater than 4 ppm in the hornblende-rich portion of the San Isabel batholith. Fractional crystallization of the liquid can produce higher Ce values but results in further depletion of Sr and Eu in the melt. In addition, the low initial $^{87}Sr/^{86}Sr$ ratio of the San Isabel batholith and the

highly linear nature of the Rb-Sr whole rock isochron (Shuster, 1984) argue against significant mixing of mantle-derived tholeiite with 1.8 b.y. old crustal rock. Mixing of two such isotopically diverse magmas would tend to produce scatter along the mixing line (Scambos et al., 1986). Therefore, partial melting and fractionation of quartz-normative tholeiite coupled with "reaction-melting" and mixing of gneissic country rock to form the San Isabel magma must be tentatively rejected on these grounds.

Melting of 1.7 b.y. old Garell Peak, Royal Gorge, Blue Ridge, and Twin Mountain Granodiorites

Partial melting of rocks similar to the 1.7 b.y. old Garell Peak, Royal Gorge, Blue Ridge, and Twin Mountain granodiorites to form the San Isabel batholith is treated in this section. The 1.7 b.y. old granodiorites are the oldest and most abundant granitoids in the Wet Mountains. Large volumes of 1.7 b.y. old granodiorites could also exist at greater depth (Thomas et al., in press). Partial melting of these granodiorites to produce the younger plutons in the Wet Mountains may have occurred during late Proterozoic times.

Partial melting models involving plagioclase/melt or K-spar/melt equilibria result in depletion of Eu and Sr in evolving magmas (Hanson, 1978; Cullers and Graf, 1984).

Formation of granitic rocks with small, negative Eu anomalies and moderate Sr contents requires a source with minor residual feldspar, high Sr contents, and little or no Eu anomaly (Cullers and Graf, 1984).

Most of the 1.7 b.y. old granodiorites in the Wet Mountains have small to large, negative Eu anomalies (Table 19). Royal Gorge, Blue Ridge, Crampton Mountain, and Twin Mountain samples have Eu/Sm ratios ranging from 0.06 to 0.27 and an average Eu/Sm ratio of 0.17 (Cullers, 1985). Garell Peak samples have Eu/Sm ratios ranging from 0.02 to 0.14 and an average Eu/Sm ratio of 0.10 (McCabe, 1984). There is at least one rock in the Crampton Mountain/Twin Mountain pluton with little or no Eu anomaly (Eu/Sm = 0.27; Cullers, 1985). In addition, charnockites containing abundant modal plagioclase and hornblende, minor K-spar, low SiO_2 (57.1 to 57.8 wgt.%), high ferromagnesian elements, and positive Eu anomalies (Eu/Sm = 0.48 to 0.51) occur in the Mt. Tyndell area (Cullers, 1985). These charnockites are characterized by moderate Sr (535 ppm) and low Rb (1.1 ppm) and K_2O (0.86 to 0.93 wgt.%) concentrations (Cullers, 1985). Modal biotite is generally absent in these rocks.

Sr contents in the 1.7 b.y. old granodiorites tend to be low to moderate and range from 66 to 339 ppm, although at least one sample from the small, foliated granodiorite stocks that occur in the Wet Mountains has high Sr contents

(Table 19). Sr concentrations in these smaller stocks range from 94 to 981 ppm.

Royal Gorge and Blue Ridge samples have Rb/Sr ratios ranging from 0.33 to 5.42 and an average Rb/Sr ratio of 2.15 (Cullers, 1985). Garell Peak samples have Rb/Sr ratios ranging from 0.52 to 6.11 with an average Rb/Sr ratio of 1.87 (McCabe, 1984) while samples from Crampton Mountain have Rb/Sr ratios ranging from 0.46 to 2.48 and an average Rb/Sr ratio of 1.27 (Cullers, 1985).

Initial $^{87}Sr/^{86}Sr$ ratios for granitic rocks range from 0.700 to 0.740 (Cox et al., 1980). Assuming that the 1.7 b.y. old foliated granodiorites have initial $^{87}Sr/^{86}Sr$ ratios ranging from 0.700 to 0.703, and assuming that no pre-San Isabel melting event involving these granodiorites occurred, the highest Rb/Sr ratio these 1.7 b.y. old granitoids can have and still be compatible with the low initial $^{87}Sr/^{86}Sr$ ratio of the 1.36 b.y. old San Isabel batholith, is 0.22. Clearly, the 1.7 b.y. old granodiorites have Rb/Sr ratios that are too high to be compatible with the low initial $^{87}Sr/^{86}Sr$ ratio of the batholith. Therefore, generation of the hornblende-rich San Isabel magma by partial melting of rocks similar to the Garell Peak, Royal Gorge, Blue Ridge, and Twin Mountain granodiorites is unlikely although rocks with little or no Eu anomalies and high Sr contents do exist in the Wet Mountains.

Melting of Tonalite/Granodiorite With Little or no Eu Anomaly

Partial melting of tonalites and granodiorites having little or no Eu anomalies to form the least differentiated, hornblende-rich portion of the San Isabel batholith is treated in this section. Trace-element contents for the hypothetical tonalite/granodiorite source rock are taken from Anderson and Cullers (1978) and Cullers and Graf (1984) and are given in Table 9. Compared to the 1.7 b.y. old granodiorites in the Wet Mountains, the tonalite/granodiorite source rock has higher Sr and Sc contents, little or no Eu anomaly, and lower Rb and REE contents (Tables 13 and 19).

Twenty to thirty percent partial melting of a tonalite/granodiorite with little or no Eu anomaly (mode: plagioclase/K-spar/quartz/biotite/hornblende/sphene = .48/.11/.15/.244/.015/.001; melting ratio = .25/.35/.20/.15/.047/.003) can produce melts chemically similar to the hornblende-rich portion of the San Isabel batholith with respect to all of the trace-elements considered except Ce, Eu, Sr, and Sc (Table 13). Predicted Ce, Eu, Sr, and Sc concentrations in the hypothetical melt are too low when compared to the hornblende-rich portion of the batholith (Table 13). The high Ce contents in the San Isabel batholith may be explained by the presence of sphene as a cumulate or restite

Table 13: Trace-element contents in tonalite/granodiorite source rock having little or no Eu anomaly, in hypothetical liquid that is produced by 20-30 percent partial melting of source, and in hornblende-rich portion of San Isabel batholith (data in ppm).

	Hypothetical source rock: Tonalite/granodiorite with little or no Eu anomaly	Predicted values in hypothetical liquid derived by 20-30% melting of source	Observed values in hornblende-rich portion of the batholith
Rb	50 - 200	73 - 304	89 - 153
Sr	300 - 940	123 - 404	281 - 580
Ce	42 - 76	95 - 184	180 - 318
Sm	3 - 8	8 - 23	18 - 32
Eu	1 - 2.7	0.7 - 2.0	3 - 6
Yb	1.1 - 3.4	2.9 - 9.9	6 - 10
Lu	0.2 - 0.6	0.6 - 2.2	1 - 2
Sc	1 - 43	0.4 - 16	14 - 34

phase. Sphene frequently occurs in early-formed glomerocrysts associated with hornblende, biotite, and opaque minerals. Hellman and Green (1979) have shown that sphene retains its refractory nature with up to 60% partial melting at high pressures, therefore, it would be reasonable to assume that some unmelted, residual sphene was brought up with the San Isabel magma.

The high Eu contents in the San Isabel batholith may be explained by the presence of cumulate or residual plagioclase, although petrographic evidence for cumulate or residual plagioclase is lacking. Alternatively, the distribution coefficient for Eu partitioning between plagioclase and a mafic-rich granitic melt may be lower than that given in Table 10. A smaller distribution coefficient for Eu partitioning between plagioclase and coexisting liquid would result in a more positive Eu anomaly size in succeeding melts (Hanson, 1978).

Predicted values for Sc in the hypothetical tonalite/granodiorite melt show fairly good agreement with the hornblende-rich portion of the batholith (Table 13). Partial melting of a tonalite/granodiorite source with slightly higher Sc contents may account for the observed values in the hornblende-rich portion of the San Isabel batholith. Alternatively, accumulations of residual hornblende, biotite, and opaque minerals in the San Isabel magma could also account for high Sc contents in the batholith.

Partial melting of tonalites and granodiorites with unusually high Sr contents (up to 1500 ppm) could account for the moderate Sr concentrations in the San Isabel batholith. In addition, the distribution coefficient for Sr partitioning between plagioclase and a mafic-rich monzogranite magma may be lower than that given in Table 10. A smaller distribution coefficient for Sr partitioning between plagioclase and coexisting liquid would result in a decrease in depletion of Sr in succeeding melts (Hanson, 1978). The variability of Sr in elemental variation diagrams suggests that mobilization of Sr may have taken place as a result of deuteric alteration, assimilation, metasomatism, or weathering of the San Isabel batholith although the linear nature of the Rb-Sr whole rock isochron (Shuster, 1984) and the general agreement between Rb-Sr and U-Pb ages (Shuster, 1984; Thomas et al., in press) argues against significant movement of Sr. Slight mobilization of Sr could have produced higher Sr concentrations in the batholith. The presence of cumulate or residual plagioclase in the San Isabel magma could also account for samples with high Sr contents, but accumulations of plagioclase tend to be uncommon in the San Isabel batholith.

Alternatively, a pre-San Isabel melting event involving the tonalite/granodiorite source rocks could produce a residuum enriched in Sr. This pre-San Isabel melting event

would also produce a positive Eu anomaly in the residuum and would give higher Sc concentrations. Indeed, the charnockites from the Mt. Tyndell area may represent unmelted residuum left over from such a melting event. Subsequent partial melting of this residuum could produce liquids with moderate Sr and Sc contents and small, negative Eu anomalies.

Thirty percent partial melting of a tonalite/granodiorite with little or no Eu anomaly (mode: plagioclase/K-spar/quartz/biotite/hornblende/sphene = .43/.17/.189/.20/.0103/.0007; melting ratio = .30/.30/.30/.10/0/0) can produce a residuum enriched in Sr and Sc with a positive Eu anomaly (Table 14). Twenty to thirty percent partial melting of this residuum (mode: plagioclase/K-spar/quartz/biotite/hornblende/sphene = .48/.11/.15/.244/.015/.001; melting ratio = .25/.35/.20/.15/.047/.003) can produce melts chemically similar to the hornblende-rich portion of the San Isabel batholith with respect to all of the trace-elements considered except the REE (Table 14). The high REE contents in the San Isabel batholith may be explained by the presence of sphene as a cumulate or residual phase. The occurrence of sphene as residual, unmelted material or as early-formed cumulate in the San Isabel magma is supported by petrographic evidence and experimental results (Hellman and Green, 1979). Mixing of 4 percent residual sphene with the liquid derived from partial melting of the residuum can

Table 14: Trace-element contents in tonalite/granodiorite source rock having little or no Eu anomaly, in hypothetical residuum that is produced by 30 percent partial melting of source, in hypothetical liquid that is produced by 20-30 percent partial melting of residuum, in hypothetical liquid that is produced by mixing 4 percent residual sphene with liquid derived from melting of the residuum, and in hornblende-rich portion of San Isabel batholith (data in ppm).

	Hypothetical source: Tonalite/grenodiorite with little or no Eu anomaly	Predicted values in residuum left from 30% melting of source	Predicted values in hypothetical liquid derived by 20-30% melting of residuum	Predicted values for hypothetical liquid (from column 3) mixed with 4% residual sphene	Observed values in hornblende-rich portion of the batholith
Rb	50 - 200	38 - 150	55 - 228	55 - 221	89 - 153
Sr	300 - 940	372 - 1166	153 - 501	*	281 - 580
Ce	42 - 76	21 - 39	48 - 94	254 - 298	180 - 318
Sm	3 - 8	1 - 3	3 - 9	7 - 13	18 - 32
Eu	1 - 2.7	1.1 - 3.0	0.8 - 2.3	3.9 - 5.3	3 - 6
Yb	1.1 - 3.4	0.4 - 1.2	1.0 - 3.5	11 - 13	6 - 10
Lu	0.2 - 0.6	0.04 - 0.12	0.1 - 0.4	1.3 - 1.6	1 - 2
Sc	1 - 43	1.3 - 54	0.5 - 20	2 - 21	14 - 34

* Sr values not available for mineral separates

produce melts chemically similar to the hornblende-rich portion of the batholith with respect to all of the trace-elements considered (Table 14).

Thomas et al. (in press) suggested that most of the mid-continent of the United States may consist of older (possibly 1.7 b.y. old) crust beneath the veneer of 1.35 to 1.4 b.y. old silicic volcanic and plutonic rocks. The 1.7 b.y. old Garell Peak, Royal Gorge, Blue Ridge, and Twin Mountain granodiorites may represent an exposed portion of this older crust. It would not be unreasonable to assume that tonalites and granodiorites similar to these in age, but having little or no Eu anomalies, higher Sr and Sc, and lower Rb, exist at greater depth. Therefore, a tentative age of 1.7 b.y. for these rocks is proposed.

Magmas derived from sources characterized by low Rb/Sr ratios have correspondingly low initial $^{87}Sr/^{86}Sr$ ratios, therefore, the low initial $^{87}Sr/^{86}Sr$ ratio of the 1.36 b.y. old San Isabel batholith suggests that the source rock that melted to form the batholith was (1) mantle-derived or (2) characterized by a short residence time in the lower crust. Initial $^{87}Sr/^{86}Sr$ ratios for granitic rocks range from 0.700 to 0.740 (Cox et al., 1980). Assuming that the 1.7 b.y. old tonalite/granodiorite source rocks have initial $^{87}Sr/^{86}Sr$ ratios ranging from 0.700 to 0.703, and assuming that no pre-San Isabel melting event occurred, the highest Rb/Sr ratio these 1.7 b.y. old granitoids can have and still be

compatible with the low initial $^{87}Sr/^{86}Sr$ ratio of the San Isabel batholith, is 0.22. The extremely low, assumed initial $^{87}Sr/^{86}Sr$ ratio for the tonalite/granodiorite source rock (0.700 to 0.703) is consistent with a deep-seated, mantle-derived tonalite or granodiorite formed during the 1.7 to 1.9 b.y. old crust-forming event described by Nelson and DePaolo (1985), but a pre-San Isabel melting event involving these tonalites and granodiorites allows for higher, more reasonable initial $^{87}Sr/^{86}Sr$ ratios for the source rocks. A pre-San Isabel melting event in which selective melting of K-rich phases occurs, would produce a lower initial $^{87}Sr/^{86}Sr$ ratio in the residuum (Cox et al., 1980). Subsequent partial melting of the residuum may result in lower initial $^{87}Sr/^{86}Sr$ ratios in the melt than would be produced if no previous melting event had occurred. Therefore, a pre-San Isabel melting event allows for initial $^{87}Sr/^{86}Sr$ ratios greater than 0.700 to 0.703 for the 1.7 b.y. old tonalites and granodiorite source rocks.

Formation of tonalites or granodiorites with little or no Eu anomaly may result from partial melting of a mafic granulite (Condie and Harrison, 1976; Glickson, 1976; Simmons and Hedge, 1978; Barker and Millard, 1979; Cullers and Graf, 1984). Therefore, the following model for the formation of the hornblende-rich portion of the San Isabel batholith is proposed:

(1) Continental crust is formed from the mantle 1.7 to 1.9 b.y. ago during a relatively short period of time (Nelson and DePaolo, 1985). Formation of a tonalite/granodiorite with little or no Eu anomaly, high Sr and Sc, and low Rb contents by partial melting of a mafic granulite occurs approximately 1.7 b.y. ago.

(2) The tonalite/granodiorite undergoes a pre-San Isabel melting event in which preferential melting of K-rich phases occurs leaving a residuum with a positive Eu anomaly that is depleted in Rb and enriched in Sr and Sc.

(3) Twenty to thirty percent partial melting of this tonalite/granodiorite residuum coupled with progressive separation of minor residual sphene occurs 1.36 b.y. ago to form the least differentiated, hornblende-rich portion of the San Isabel batholith.

Formation of the Hornblende-Poor Facies of the San Isabel Batholith

Fractional crystallization processes are important mechanisms for producing compositional changes in magmas (e.g. Presnall and Bateman, 1973; Bateman and Nockleberg,

1978; Cox et al., 1980; Cullers and Graf, 1984). Formation of the hornblende-poor portion of the San Isabel batholith by fractional crystallization of hornblende-rich magma is suggested by the following observations:

(1) Hornblende-poor samples consistently plot at the differentiated end of trends in elemental variation diagrams.

(2) Hornblende-poor samples tend to have the largest negative Eu anomalies, the highest Rb/Sr ratios, and the highest Th and REE contents.

In a simple 2-stage fractionation model, five to thirty percent fractional crystallization of the hornblende-rich portion of the San Isabel magma (proportion of phases crystallized: plagioclase/K-spar/quartz/biotite/hornblende = .25/.30/.25/.14/.06) followed by five to twenty percent crystallization of plagioclase/K-spar/quartz/biotite in the ratio .25/.35/.25/.15 can account for all trace-element ranges in the hornblende-poor portion of the batholith with the possible exception of Sr (Table 15). The model fails to account for hornblende-poor samples with Sr contents greater than 507 ppm. Alteration of hornblende-rich samples in which hornblende completely alters to epidote may account for these "hornblende-poor" samples with high Sr contents, although the isotopic data argue against significant mobilization of Sr in the San Isabel batholith.

Simple fractionation of hornblende-rich magma to form

Table 15: Trace-element contents in hornblende-rich portion of San Isabel batholith, in hypothetical liquid 1 produced by 5-30 percent fractional crystallization of plagioclase/K-spar/quartz/biotite/hornblende in the ratio .25/.30/.25/.14/.06, in hypothetical liquid 2 produced by 5-20 percent fractional crystallization of plagioclase/K-spar/quartz/biotite in the ratio .25/.35/.25/.15, and in hornblende-poor portion of the batholith (data in ppm).

	Observed values in the hornblende-rich portion of the batholith	Predicted values in liquid 1	Predicted values in liquid 2	Observed values in the hornblende-poor portion of the batholith
Rb	89 - 153	92 - 188	95 - 212	103 - 192
Sr	281 - 580	177 - 545	127 - 507	121 - 580
Ce	180 - 318	187 - 423	196 - 512	281 - 450
Sm	18 - 32	18 - 37	19 - 46	24 - 40
Eu	3 - 6	2.6 - 5.9	2.6 - 5.9	4 - 6
Yb	6 - 10	6.1 - 12	6.4 - 14.8	8 - 15
Lu	1 - 2	1.0 - 2.5	1.1 - 3.1	1 - 2
Sc	14 - 34	8.3 - 32	7.1 - 31	14 - 25

the hornblende-poor portion of the batholith is thus consistent with the observed trace-element changes in the suite (Table 15) but fails to explain the uneven distribution of mafic minerals in the batholith (Figures 6 and 7). Segregations of mafic minerals in the form of glomerocrysts occur throughout the San Isabel batholith. These mafic accumulations may represent unmelted residual source material or crystallized segregations brought up with the magma. In addition, linear variation diagrams (Figures 12, 13, 17, 18, 23, 24, and 25) suggest that fractional crystallization played a minor role in the evolution of hornblende-poor magma. For example, a fractionation model involving plagioclase/melt equilibria cannot readily explain linear trends on a CaO vs. FeO diagram (Figure 25) because the CaO content of plagioclase systematically decreases as fractionation proceeds and a curved trend is produced (Presnall and Bateman, 1973; Price, 1983). Linear variation diagrams have been attributed to a variety of processes involving magma mixing (McBirney, 1980; Reid et al., 1983; Eichelberger, 1975), mixing of cumulate plus remaining liquid (McCarthy and Robb, 1978), and restite/melt separation (Chappell, 1966; White and Chappell, 1977; Price, 1983; Scambos et al., 1986). Segregations of mafic glomerocrysts and clots throughout the batholith suggest that the compositional range of the San Isabel batholith could result from mixing variable amounts of cumulate mafic

Figure 23: Elemental variation diagram of the San Isabel batholith based on mineralogy; Ce vs. Yb.

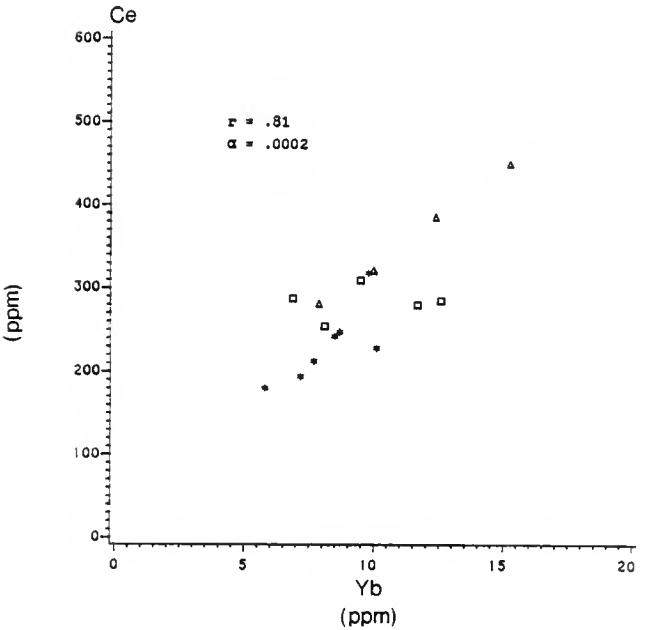

Figure 24: Elemental variation diagrams of the San Isabel batholith based on mineralogy; TiO_2 vs. Fe_2O_3 and TiO_2 vs. CaO.

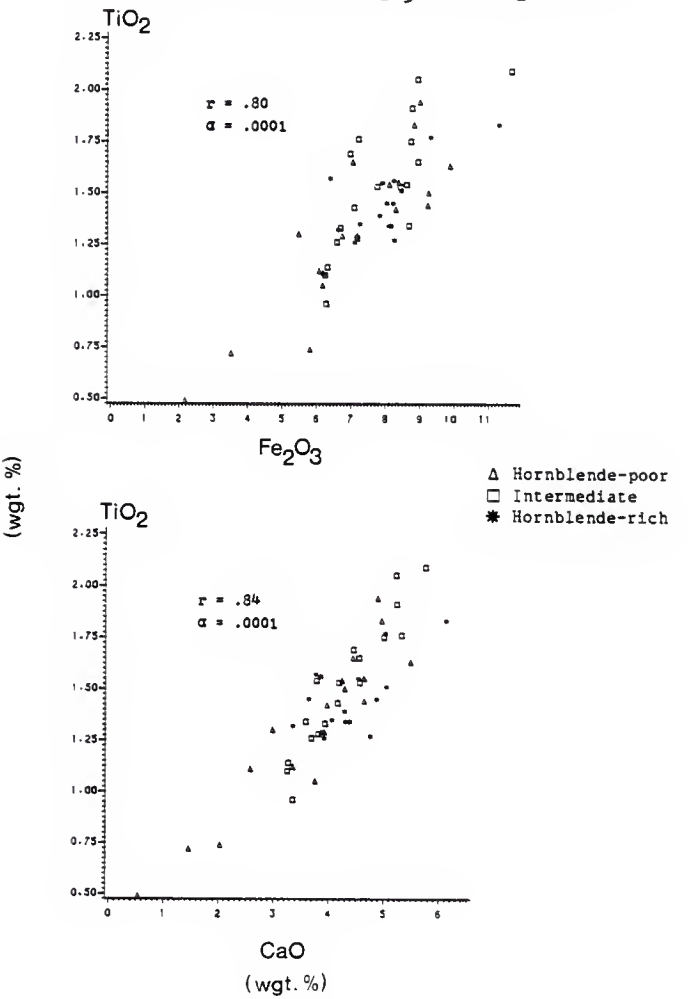

Figure 25: Elemental variation diagrams of the San Isabel batholith based on mineralogy; CaO vs. FeO and MgO vs. Fe_2O_3.

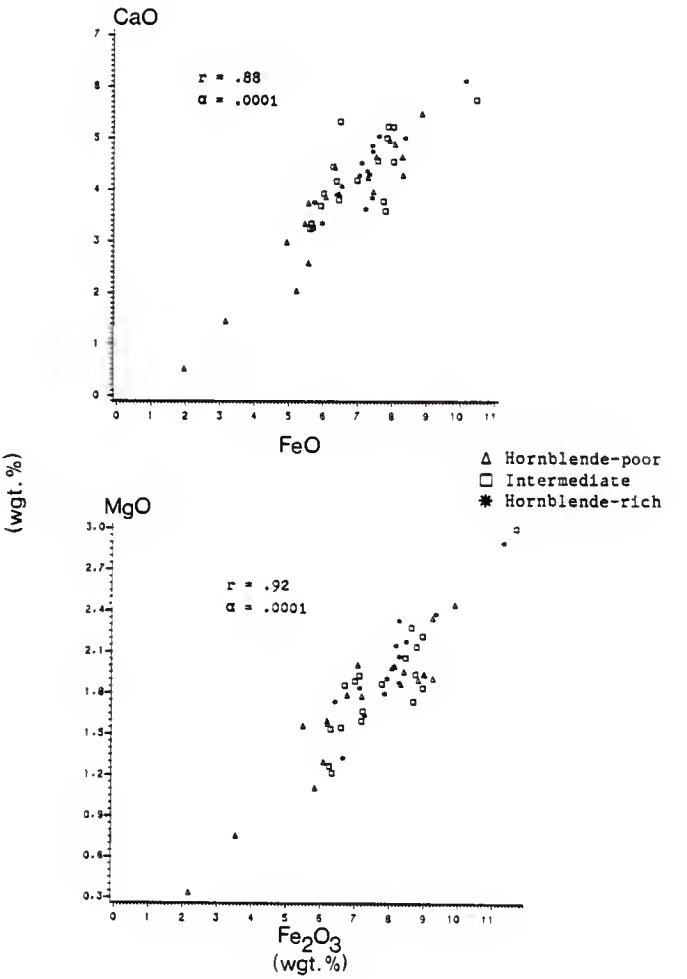

material with remaining liquid. And yet, the importance of crystal-liquid fractionation processes in magma evolution suggests that minor fractionation of hornblende-rich magma must have occurred to help form the hornblende-poor portion of the San Isabel batholith.

Trace-element contents and modal mineralogy of the hornblende-rich portion of the San Isabel monzogranite can be approximated by mixing ten to twenty percent cumulate mafic minerals (composed of 60-64% biotite, 30-35% hornblende, and 1-10% sphene) with a slightly fractionated (up to 5%) liquid (Table 16). One to five percent cumulate mafic minerals plus 10-25% fractional crystallization of plagioclase/K-spar/quartz/biotite in the ratio .25/.35/.25/.15 from the remaining liquid can account for all trace-element concentrations in the hornblende-poor portion of the batholith (Table 16). Cumulate mineralogy is based on petrographic analyses of mafic glomerocrysts in the San Isabel monzogranite. Trace-element contents of minerals used in the cumulate/melt mixing model are determined from analyses of mineral separates from a hornblende-rich sample (Table 6).

Therefore, mixing of cumulate mafic material with remaining liquid combined with fractionation of the liquid appears to be responsible for the range of composition of the San Isabel monzogranite. The overlap in major-element contents between hornblende-poor and hornblende-rich samples

Table 16: Trace-element contents in hornblende-rich portion of San Isabel batholith compared to predicted values for 10-20 percent cumulate mafic minerals plus up to 5 percent fractional crystallization of remaining liquid, and in hornblende-poor portion of San Isabel batholith compared to predicted values for 1-5 percent cumulate mafic minerals plus 10-25 percent fractionation of remaining liquid (data in ppm).

	Obeerved valuea 1n hornblende-rich portion of the batholith	Predicted valuee for 10-20% cumulate mafic minerala + up to 5% fractionation of the remaining liquid	Predictad valuea for 1-5% cumulate mafic minerale + 10-25% fractionation of the remelning liquid	Obearved valuea 1n hornblende-poor portion of the batholith
Rb	89 - 153	49 - 197	78 - 192	103 - 192
Ce	180 - 318	75 - 441	164 - 442	281 - 450
Sm	18 - 32	16 - 37	19 - 43	24 - 40
Eu	3 - 6	1.3 - 7.7	2.5 - 6.4	4 - 6
Yb	6 - 10	1.1 - 15.4	5.2 - 14.4	8 - 15
Lu	1 - 2	0.36 - 2.75	0.9 - 2.8	1 - 2
Sc	14 - 34	9.9 - 45	8 - 36.5	14 - 25

may be a result of alteration of hornblende to epidote, producing "hornblende-poor" samples that plot in the undifferentiated, hornblende-rich portion of major-element trends. The hornblende-rich facies represents the more primitive liquid in which 10-20% cumulate mafic minerals are present as glomerocrysts and mafic clots. Mixing of 10-20% cumulate mafic minerals with the remaining, slightly fractionated liquid is consistent with trace-element contents (Table 16) and modal mineralogy of the hornblende-rich portion of the batholith. The hornblende-poor facies represents a slightly more evolved liquid in which denser cumulate material has sunk into lower parts of the chamber leaving 1-5% cumulate minerals plus a fractionated liquid. Mixing of 1-5% cumulate mafic minerals with the remaining fractionated liquid (10-25% fractional crystallization of plagioclase/K-spar/quartz/biotite in the ratio .25/.35/.25/.15) is consistent with trace-element contents (Table 16) and modal mineralogy of the hornblende-poor portion of the San Isabel batholith.

Figure 26: Preferred model for the formation of the San Isabel batholith.

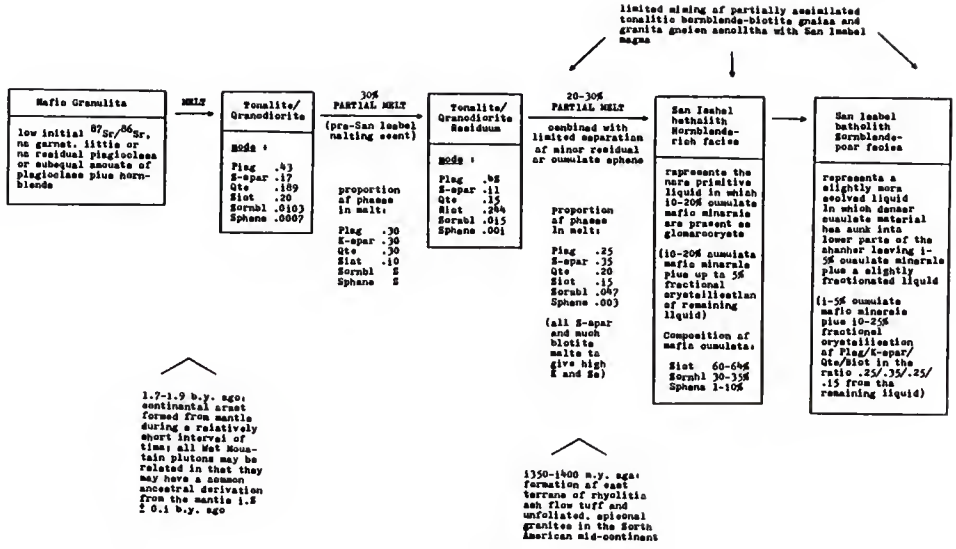

TECTONIC SETTING

Classification of granitoid rocks into S-type, I-type, and A-type granites is based on source rock and tectonic setting (Ishahara, 1977; White and Chappell, 1977; Hine et al., 1978; Taylor, 1980; Collins et al., 1982; Didier et al., 1982; White and Chappell, 1983). A comparison of I-type, S-type, and A-type granites is given in Table 17. I-type granites are derived from a metaigneous source while S-type granites form from melting of a metapelitic source. I-type granites are formed in orogenic settings while A-type granites are anorogenic in origin and are associated with tensional tectonic environments.

The San Isabel batholith possesses several features that are characteristic of both A- and I-type granites (Table 18). I-type characteristics include low SiO_2, high CaO, MgO, and TiO_2, and metaluminous nature. In addition, the San Isabel batholith contains modal hornblende, sphene, and pyrite and abundant mafic-rich xenoliths. Although anhydrous magmatic conditions are suggested by the presence of late, interstitial biotite and occasional fluorite, the abundance of pegmatites throughout the batholith is evidence for an H_2O-saturated magma.

A-type granites are alkaline, anorogenic, and anhydrous in nature. The average SiO_2 content of Proterozoic A-type granites based on analyses compiled by Anderson (1983) is

Table 17: Comparison of A, I, and S-type granites*

A-type	I-type	S-type
abundant K-spar, K-spar megacrystic, K-sper usually perthitic, interstitial mafics, hiotite crystallizes late and occasionally contains thin stripe of fluorite, microscopic intergrowths between feldspars are very common, accessory apatite	oligoclase-andesine, hiotite and sphene common, hornblende common in more mafic rocks, may have pyroxene, epidote, and allanite, opeques: magnatite ± ilmenite ± pyrite, muscovite rare, accessory apatite in minute inclusions	cordierite, garnet, hiotite common; muscovite in felsic varieties, sillimanite inclu- sions may be present, accessory monazite, feldspar is commonly white, opeques: ilmenite ± pyrrhotite ± graphite, no hornblende, apatite in sparse grains
$Na_2O + K_2O$ high (higher than I-type), metaluminous-peraluminous- some peralkaline, high FeO/FeO+MgO, high Ga/Al, high Nb,Ta,Zr,Y, and REE's, high F in metaluminous- peraluminous variaties, high Cl in peralkaline rocks, SiO_2: generally high (commonly near 77%), low CaO and MgO, low Co,Sc,Cr, and Ni, Zr: 300-340 ppm, hiotite has high Fe/Mg	Na_2O greater than 3.2%, weakly peraluminous-metalum- inous (Shand Index less than 1.1), low FeO/FeO+MgO, high TiO_2, high MgO and CaO, (CaO greater than 3.7% at 66% SiO_2), SiO_2: low (53-76%), high Co,Sc,Cr, and Ni, Zr: less than 150 ppm, hiotite has low Fe/Mg, normative corundum less than 1%	Na_2O less than 3.2%, paraluminous (Shand Index greater than 1.5), CaO less than 3.7% at 66% SiO_2, SiO_2: 65-76%, Zr: greater than 150 ppm, alumina oversaturated, normative corundum greater than 1%
anorogenic	orogenic	orogenic or anorogenic
anhydrous melt, few pegmatites, xenoliths uncommon, usually not associated in space and time with inter- mediate rocks	hydrous melt, pegmatites common, xenoliths are hornblende and mafic rich, usually associated in space and time with intermediate rocks	hydrous melt, pegmatites common, xenoliths of shale and sandstone common, association with intermediate rocks varies depending on tectonic setting
initial $^{87}Sr/^{86}Sr$: .703- .712, low-moderate O_2 fugacity	initial $^{87}Sr/^{86}Sr$ less than .706, higher O_2 fugacity than S-type	initial $^{87}Sr/^{86}Sr$ greater than .708, low O_2 fugacity due to interaction with C- bearing pelitic rocks

* Compiled from the following sources: Ishahara (1977), White and Chappell (1977), Hine et al. (1978), Taylor (1980), Collins et al. (1982), and White and Chappell (1983).

Table 18: Compilation of A-type and I-type characteristics of the San Isabel monzogranite.

A-type characteristics	I-type characteristics
$Na_2O + K_2O$ high	weakly peraluminous-metaluminous
high FeO/FeO + MgO	high CaO and MgO
high REE's	high TiO_2
abundant K-spar, K-spar megacrystic	low SiO_2
K-spar perthitic	sphene and hornblende common
interstitial mafics, late-stage biotite	allanite present as an accessory
occasional fluorite, F enriched melt	high mafics
contemporaneous emplacement with other anorogenic intrusives	pyrite present
	xenoliths are hornbl. and mafic-rich
	pegmatites locally abundant

71.67 weight percent. Average TiO_2, FeO, MgO, CaO, and K_2O contents are 0.41, 2.84, 0.54, 1.40, and 4.92 percent by weight, respectively. Average Ba, Rb, and Sr concentrations in these Proterozoic anorogenic granites are 842, 197, and 135 ppm, respectively. The average FeO/(FeO+MgO) ratio is 0.85.

Compared to average analyses of Proterozoic anorogenic granites compiled by Anderson (1983), the San Isabel monzogranite contains lower SiO_2 and higher TiO_2, FeO, MgO, CaO, Ba, and Sr contents (Tables 7 and 8). The San Isabel batholith is similar to these anorogenic granites with respect to K_2O contents (Table 7) and FeO/(FeO+MgO) ratios (Figures 15 and 33). In addition, the San Isabel batholith has high REE contents similar to recognized Proterozoic anorogenic granites (Figure 27).

Classification of granitoid rocks into S-type, I-type, and A-type granites does not always result in a clear-cut interpretation of tectonic setting (Pearce et al., 1984). Pearce et al. (1984) subdivided granites according to their tectonic settings into four main groups: (1) ocean ridge granites (ORG), (2) volcanic arc granites (VAG), (3) within-plate granites (WPG), and (4) collision granites (syn-COLG). The Rb vs. Yb+Ta discrimination diagram for these tectonic settings is presented in Figure 28. Samples from the San Isabel batholith consistently plot in the WPG field.

Figure 27: Comparison of rare-earth element (REE) ranges of San Isabel batholith and selected Proterozoic anorogenic granitoids.

Rare-earth element ranges for the San Isabel Batholith.

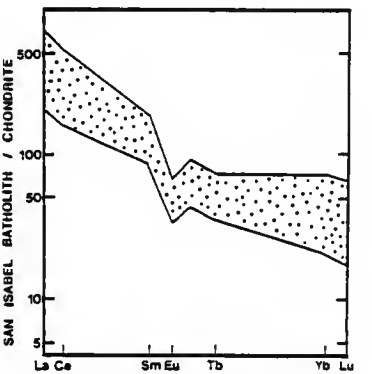

Rare-earth element ranges for selected Proterozoic anorogenic granitoids: (Pikes Peak Biotite Granite, Wolf River Batholith, Red Willow Batholith, Montello Biotite Granite, St. Francois Butler Hill Caldera, Montello 2-mica Granite).

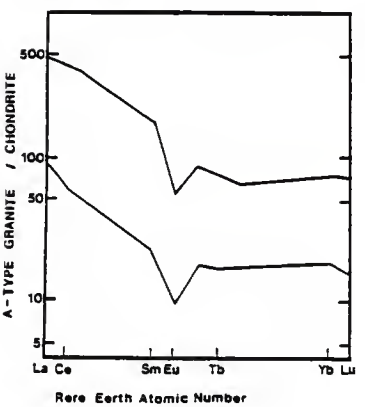

Rare-earth element ranges of San Isabel batholith superimposed over that of selected Proterozoic anorogenic granitoids.

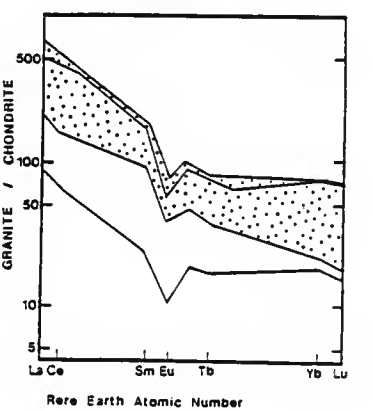

Figure 28: Rb vs. Yb + Ta discriminant diagram for syn-collision (syn-COLG), volcanic arc (VAG), within-plate (WPG), and normal and anomalous ocean ridge (ORG) granites.

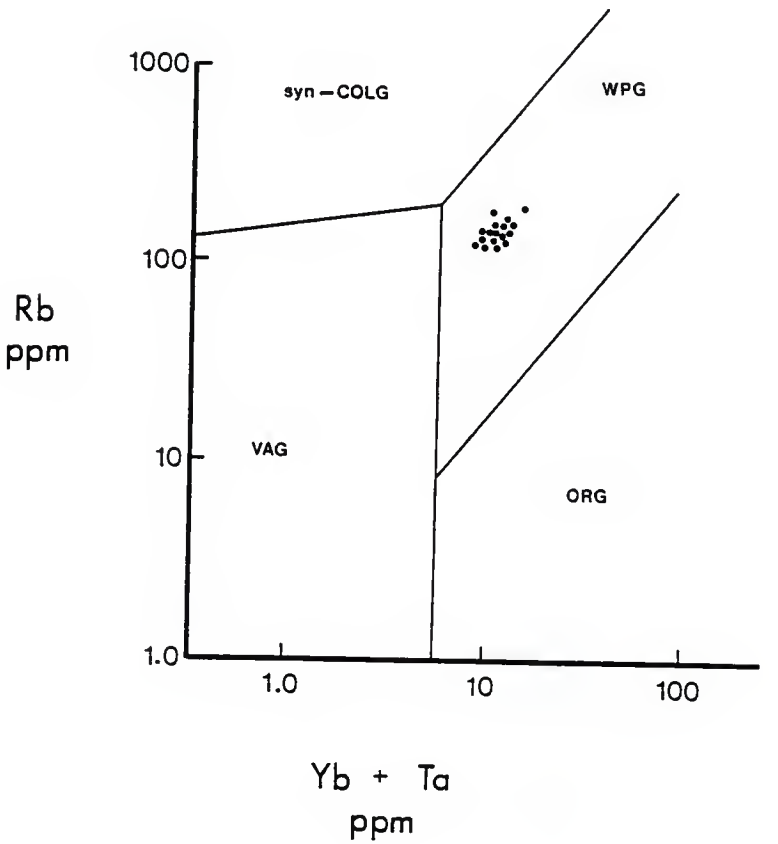

Within-plate granites (WPG) are analagous to A-type granites in most respects.

Harris et al. (in press) recognized four groups of intrusions associated with various stages of collision magmatism. Pre-collision calc-alkaline volcanic arc intrusions (VA) are characterized by selective LILE enrichment. Syn-collision peraluminous leucogranites (Group II) have S-type affinities and are generally enriched in Rb and Ta. Late or post-collision calc-alkaline intrusions (Group III) are distinguished from volcanic arc intrusions by higher Ta contents. Post-collision alkaline intrusions (WP) are analagous to A-type granites and are characterized by high LILE and Zr contents. The Rb/30 - Hf - Ta x 3 ternary diagram for discrimination of these tectonic settings is presented in Figure 29. Samples from the San Isabel batholith plot in two fields - the WP and VA fields. With respect to tectonic setting during emplacement, it seems that the San Isabel batholith possesses both orogenic and anorogenic characteristics.

The late Proterozoic of North America is characterized by "abundant anorogenic magmatic activity" resulting in the emplacement of a variety of rock types including anorthosites, layered gabbros, charnockites, rapakivi granites, and bimodal basalt-rhyolite suites (Anderson, 1983). This generation of magma under anorogenic conditions has been considered a result of tensional forces due to

Figure 29: Rb/30 - Hf - Ta x 3 triangular plot for Group II, Group III, volcanic arc, and within-plate granitic rocks.

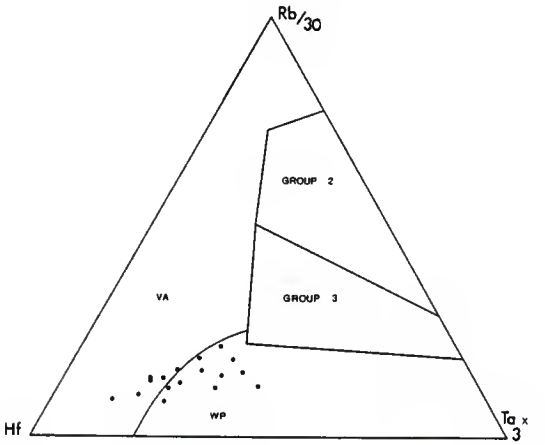

GROUP II : syncollision peraluminous
GROUP III : late or post-collision (calc-alkaline)
WP : within-plate
VA : volcanic arc

incipient rifting of the continent (Silver et al., 1977; Emslie, 1978; Loiselle and Wones, 1979; Anderson, 1983). Anorogenic magmatic activity during the period 1.35-1.4 b.y. ago may be responsible for the production of large volumes of rhyolitic ash flow tuff and unfoliated, epizonal granitic intrusions that comprise the basement rocks of the mid-continent of the United States. The San Isabel batholith is coeval with this silicic terrane (Thomas et al., in press) and probably represents a deeper-seated manifestation of this anorogenic magmatic activity. Partial melting of an igneous rock (tonalite/granodiorite residuum with little or no Eu anomaly) as a result of this anorogenic magmatic activity 1.35-1.4 b.y. ago may be responsible for formation of the San Isabel batholith. Therefore, the San Isabel monzogranite appears to be an A-type granite with I-type affinities.

S U M M A R Y

The 1.36 b.y. old San Isabel batholith is a weakly foliated monzogranite that intrudes the metamorphic rocks of the southern Wet Mountain massif. Other intrusions in the northern Wet Mountains consist of older 1.67-1.7 b.y. old foliated granodiorites and 1.44 and 1.47 b.y. old unfoliated monzogranites. Wet Mountain plutons may be ancestrally related if they have a common mantle-derivation age of 1.8 ± 0.1 b.y. similar to other plutons in the Rocky Mountains (Nelson and DePaolo, 1985). In addition, most granitic plutons in the Wet Mountains are too Fe-rich to be calc-alkaline and are subalkalic to alkalic. The San Isabel batholith differs from most of these plutons since it possesses high FeO, CaO, MgO, TiO_2, and Sr contents compared to most Wet Mountain granitoids. In addition, the San Isabel monzogranite is the most metaluminous granitic pluton in the Wet Mountains. The porphyritic facies of the 1.44 b.y. old Oak Creek monzogranite to granodiorite is the most similar pluton in the Wet Mountains to the San Isabel batholith.

The San Isabel batholith is characterized by low SiO_2, moderate Sr, high FeO, TiO_2, K_2O, MnO, Ba, Sc, REE, FeO/(FeO+MgO), and Na_2O+K_2O, and small, negative Eu anomalies.

Melting of mafic granulite 1.7 to 1.9 b.y. ago during the "crust-formation event" described by Nelson and DePaolo

(1985) may have produced tonalites and granodiorites with little or no Eu anomalies, low Rb, and high Sr, Sc, and REE contents that were emplaced approximately 1.7 b.y. ago. Assuming that these 1.7 b.y. old, mantle-derived tonalites and granodiorites have initial $^{87}Sr/^{86}Sr$ ratios ranging from 0.700 to 0.703, and assuming that no pre-San Isabel melting event involving these rocks occurred, the highest Rb/Sr ratio these 1.7 b.y. old granitoids can have and still be compatible with the initial $^{87}Sr/^{86}Sr$ ratio of the San Isabel batholith, is 0.22. A pre-San Isabel melting event allows for higher, more reasonable initial $^{87}Sr/^{86}Sr$ ratios and Rb/Sr ratios in the tonalite/granodiorite source rocks. In addition, the residuum remaining from a pre-San Isabel melting event will be enriched in Sr and Sc and have positive Eu anomalies. Subsequent partial melting of the residuum may have occurred concurrently with formation of the vast 1.35-1.4 b.y. old rhyolitic ash flow tuff and epizonal granite terrane described by Thomas et al. (in press) and resulted in formation of the 1.36 b.y. old San Isabel batholith.

Twenty to thirty percent partial melting of a tonalite/granodiorite residuum with positive Eu anomalies, high Sr and Sc, and low Rb contents can produce melts chemically similar to the hornblende-rich portion of the San Isabel batholith with respect to Rb, Sr, and Sc. Partial melting

of this residuum combined with limited separation of minor residual sphene could also account for the high REE contents in the San Isabel batholith. Limited mixing of partially assimilated hornblende-biotite gneiss and granite gneiss xenoliths with the San Isabel magma may have also occurred. The temperature of the magma during emplacement was approximately 725°C (Murray, 1970) and the pressure 5-7 Kb. H_2O content of the San Isabel magma, deduced from crystallization sequences, was 1.2-1.5 percent.

The principal factors affecting the range of composition in the San Isabel monzogranite are: (1) the presence or absence of hornblende and (2) the relative abundance of cumulate mafic material in the form of clusters, clots, and glomerocrysts. Mixing of cumulate mafic material with slightly fractionated liquid to form the compositional range in the San Isabel monzogranite is consistent with trace-element contents, field relations, and petrography. The hornblende-rich facies of the batholith represents the more primitive liquid in which 10-20% cumulate mafic minerals are mixed with slightly fractionated liquid. The hornblende-poor facies represents a slightly more evolved liquid in which denser cumulate material has sunk into lower parts of the chamber leaving 1-5% cumulate mafic minerals plus a fractionated liquid. One to five percent mafic cumulate plus 10-25% fractional crystallization of plagioclase/K-spar/quartz/biotite in the

ratio .25/.35/.25/.15 from the remaining liquid can produce the hornblende-poor facies of the San Isabel batholith.

Tectonic setting at the time of emplacement of the San Isabel batholith is ambiguous but appears to have been anorogenic (Silver et al., 1977; Anderson, 1983). The San Isabel batholith is coeval with the vast silicic volcanic and epizonal granite terrane described by Thomas et al. (in press). The abundance of rhyolitic ash flow tuff and unfoliated, epizonal granites and the lack of intermediate rocks (i.e. andesites) suggests that this magmatic event was anorogenic. Therefore, the San Isabel batholith appears to be an A-type granite with I-type affinities. Partial melting of tonalites or granodiorites under anorogenic conditions could produce such a rock.

REFERENCES

Abbey, S., 1982, An evaluation of U.S.G.S. III: Geostandards Newsletter, v. 6, no. 1, p. 47.

Allegre, C. J., and Minster, J. F., 1978, Quantitative models of trace-element behavior in magmatic processes: Earth and Planetary Science Letters, v. 38, pp. 1-25.

Anderson, J. L., 1983, Proterozoic anorogenic granite plutonism of North America: Geological Society of America, Memoir 161, pp. 133-154.

Anderson, J. L., and Cullers, R. L., 1978, Geochemistry and evolution of the Wolf River batholith, a late Precambrian rapakivi massif in N. Wisconsin, U.S.A.: Precambrian Research, v. 7, pp. 287-324.

Anderson, J. L., and Cullers, R. L., 1985, Proterozoic orogenic tonalites: A crust-enriched, mantle-derived fractionation series in the Penokean plutonic complex of central Wisconsin: unpublished.

Apted, M. J., 1981, Rare-earth element systematics of hydrous liquids from partial melting of basaltic eclogite: A re-evaluation: Earth and Planetary Science Letters, v. 52, pp. 172-182.

Arth, J. G., and Barker, F., 1976, Rare-earth partitioning between hornblende and dacitic liquid and implications for the genesis of trondhjemitic-tonalitic magmas: Geology, v. 4, pp. 534-536.

Barker, F., and Millard, H. T., Jr., 1979, Geochemistry of the type trondhjemite and three associated rocks, Norway. In: F. Barker, ed., Trondhjemites, Dacites, and Related Rocks. Elsevier, Amsterdam, pp. 517-529.

Barker, F., Wones, D. R., Sharp, W. N., and Desborough, G. A., 1975, The Pikes Peak Batholith, Colorado Front Range, and a model for the origin of the gabbro-anorthosite-syenite-potassic granite suite: Precambrian Research, v. 2, pp. 97-160.

Barth, T. F. W., 1951, The feldspar geologic thermometers: Neues Jahrbuch Fuer Mineralogie Abhandlungen, v. 82, pp. 143-154.

Barth, T. F. W., 1969, Feldspars: J. Wiley and Sons, New York, p. 261.

Bateman, P. C., and Nockleberg, W. J., 1978, Solidification of the Mount Givens granodiorite, Sierra Nevada, California: Journal of Geology, v. 86, pp. 563-579.

Berlin, R., and Henderson, C. M. B., 1969, The distribution of Sr and Ba between the alkali feldspar, plagioclase, and groundmass phases of porphyritic trachytes and phonolites: Geochimica et Cosmochimica Acta, v. 33, pp. 247-255.

Bowman, W. S., Faye, G. H., Sutarno, R., McKeague, J. A., and Kodama, H., 1978, Soil samples SO-1, SO-2, SO-3, and SO-4 - Certified Reference Materials, CANMET Report 79-3.

Boyer, R., 1962, Petrology and structure of the southern Wet Mountains, Colorado: Geological Society of America Bulletin, v. 73, pp. 1047-1069.

Buddington, A. F., 1959, Granite emplacement with special reference to North America: Geological Society of America, v. 70, pp. 671-747.

Chappell, B. W., 1966, Petrogenesis of the granites at Moonbi, New South Wales, Ph.D. thesis, Australia National University, Canberra.

Chayes, F., 1949, Simple point counter for thin section analysis: American Mineralogist, v. 34, pp. 1-11.

Collins, W. J., Beams, S. D., White, A. J. R., and Chappell, B. W., 1982, Nature and origin of A-type granites with particular reference to southeastern Australia: Contributions to Mineralogy and Petrology, v. 80, pp. 189-200.

Condie, K. C., and Harrison, N. M., 1976, Geochemistry of the Archean Bulawayan Group, Midlands greenstone belt, Rhodesia: Precambrian Research, v. 3, pp. 253-271.

Condie, K. C., and Hunter, D. R., 1976, Trace-element geochemistry of Archean granitic rocks from the Barberton Region, South Africa: Earth and Planetary Science Letters, v. 29, pp. 389-400.

Cox, K. G., Bell, J. D., and Pankhurst, R. J., 1980, The Interpretation of Igneous Rocks, London, George Allen and Unwin, Ltd.

Cullers, R. L., 1985, personal communication.

Cullers, R. L., and Graf, J. L., 1984, Rare-earth elements in igneous rocks of the continental crust: Intermediate and silicic rocks - ore petrogenesis. In: Henderson, P., ed., Rare Earth Geochemistry, Elsevier, Amsterdam, pp. 275-316.

Cullers, R. L., and Wobus, R. A., 1986, Proterozoic framework of the southern Front Range and northern Wet Mountains, Colorado: unpublished.

Cullers, R. L., Medaris, L. G., and Haskin, L. A., 1973, Experimental studies of the distribution of rare-earths as trace-elements among silicate minerals and liquids and water: Geochimica et Cosmochimica Acta, v. 37, pp. 1499-1512.

Cullers, R. L., Koch, R., and Bickford, M. E., 1981, Chemical evolution of magmas in the igneous terrane of the St. Francois Mountains, Missouri: II. Trace element evidence: Journal of Geophysical Research, v. 86, pp. 10365-10387.

Deer, W. A., Howie, R. A., and Zussman, J., 1966, Introduction to the rock-forming minerals, J. Wiley and Sons, New York, 528 p.

Didier, J., Duthou, J. L., and Lameyre, J., 1982, Mantle and crustal granites: Genetic classification of orogenic granites and the nature of their enclaves: Journal of Volcanology and Geothermal Research, v. 14, pp. 125-132.

Eichelberger, J. C., 1975, Origin of andesite and dacite: Evidence of mixing at Glass Mountain in California and at other circum-Pacific volcanoes: Geological Society of America Bulletin, v. 86, pp. 1381-1391.

Emslie, R. F., 1978, Anorthosite massifs, rapakivi granites, and late Proterozoic rifting of North America: Precambrian Research, v. 7, pp. 61-98.

Ewart, A., and Taylor, S. R., 1969, Trace-element geochemistry of the rhyolitic volcanic rocks, central North Island, New Zealand, Phenocryst Data: Contributions to Mineralogy and Petrology, v. 22, pp. 127-146.

Gilbert, G. K., 1897, Description of the Pueblo quadrangle: U.S. Geological Survey, Geologic Atlas 36.

Gladney, E. S., Burns, C. E., and Roelandts, I., 1984, Compilation of elemental concentration data for CCRMP reference soil samples SO-1 to SO-4 (submitted for publication).

Glickson, A. Y., 1976, Trace-element geochemistry and origin of early Precambrian acid igneous series, Barberton Mountain Land, Transvaal: Geochimica et Cosmochimica Acta, v. 40, pp. 1261-1280.

Gordon, G. E., Randle, K., Goles, G., Corliss, J., Beeson, M. H., and Olsey, S. S., 1968, Instrumental neutron activation analysis of standard rocks with high resolution gamma-ray detectors: Geochimica et Cosmochimica Acta, v. 32, pp. 369-396.

Green, T. H., and Pearson, N. J., 1986, Rare-earth element partitioning between sphene and coexisting silicate liquid at high pressure and temperature: Chemical Geology, v. 55, pp. 105-119.

Griffin, W. L., and Murthy, V. R., 1969, Distribution of K, Rb, Sr, and Ba in some minerals relevant to basalt genesis: Geochimica et Cosmochimica Acta, v. 33, pp. 1389-1414.

Hanson, G. N., 1978, The application of trace-elements to the petrogenesis of igneous rocks of granitic composition: Earth and Planetary Science Letters, v. 38, pp. 26-43.

Harris, N. B. W., Pearce, J. A., and Tindle, A. G., Geochemical characteristics of collision magmatism: Journal of Petrology: (in press).

Haskin, L. A., 1984, Petrogenetic modelling - use of rare-earths. In: Henderson, P., ed., Rare-earth Geochemistry. Elsevier, Amsterdam, pp. 115-152.

Haskin, L. A., Allen, R. O., Helmke, P. A., Pastor, T. R., Anderson, M. R., Korotev, R. S., and Zweifel, K. A., 1970, Rare-earths and other trace-elements in Apollo II lunar samples: Proceedings of the Apollo II Lunar Science Conference, supplement 1, v. 2, pp. 1213-1231.

Higuichi, H., and Nagasawa, H., 1969, Partitioning of trace-elements between rock-forming minerals and host volcanic rocks: Earth and Planetary Science Letters, v. 7, pp. 281-287.

Hills, R. C., 1900, Description of the Walsenburg quadrangle: U.S. Geological Survey, Geologic Atlas 68.

Hine, R., Williams, I. S., Chappell, B. W., and White, A. J. R., 1978, Contrasts between I- and S-type granitoids of the Kosciusko Batholith: Journal of the Geological Society of Australia, v. 25, pp. 219-234.

Hellman, P. L., and Green, T. H., 1979, The role of sphene as an accessory phase in the high-pressure partial melting of hydrous mafic compositions: Earth and Planetary Science Letters, v. 42, pp. 191-201.

Hellman, P. L., Smith, R. E., and Henderson, P., 1979, The mobility of the rare-earth elements: Evidence and implications from selected terranes affected by burial metamorphism: Contributions to Mineralogy and Petrology, v. 71, pp. 23-44.

Holdaway, M. J., 1972, Thermal stability of Al-Fe epidote as a function of oxygen fugacity and Fe content: Contributions to Mineralogy and Petrology, v. 37, no. 4, pp. 307-340.

Hyndman, D. W., 1985, Petrology of igneous and metamorphic rocks: McGraw-Hill, New York, pp. 766.

Ishihara, S., 1977, The magnetite-series and ilmenite-series granitic rocks: Mineralogical Geology, v. 27, pp. 293-305.

Jacobs, J. W., Korstev, R. L., Blanchard, D. P., and Haskin, L. A., 1977, A well-tested procedure for instrumental neutron activation analysis of silicate rocks and minerals: Journal of Radioanalytical Chemistry, v. 40, pp. 93-114.

Liou, J. G., 1973, Synthesis and stability relations of epidote, $Ca_2Al_2FeSi_3O_{12}(OH)$: Journal of Petrology, v. 14, no. 3, pp. 381-413.

Logan, J. M., 1966, Structure and petrology of the eastern margin of the Wet Mountains, Colorado: Ph.D. Dissertation, University of Oklahoma.

Loiselle, M. C., and Wones, D. R., 1979, Characteristics and origin of anorogenic granites: Geological Society of America Abstracts with Programs, v. 11, p. 468.

Ludden, J. N., and Thompson, G., 1979, An evaluation of the behavior of the rare-earth elements during weathering of sea-floor basalt: Earth and Planetary Science Letters, v. 43, pp. 85-92.

Maaløe, S., and Wyllie, P. J., 1975, Water content of a granite magma deduced from the sequence of crystallization determined experimentally with water-saturated conditions: Contributions to Mineralogy and Petrology, v. 52, pp. 175-191.

McBirney, A. B., 1980, Mixing and unmixing of magmas: Journal of Volcanology and Geothermal Research, v. 7, pp. 357-371.

McCabe, M., 1984, personal communication.

McCarthy, T. S., and Robb, L. J., 1978, On the relationship between cumulus mineralogy and trace and alkali element chemistry in an Archean granite from the Barberton region, South Africa: Geochimica et Cosmochimica Acta, v. 42, pp. 21-26.

McGinnis, C. J., 1956, A brief description of the physiography of the Ratone Basin, Colorado: p. 10 in Guide Book to the Geology of the Ratone Basin, Colorado: Denver, Rocky Mountain Association of Geologists.

Medlin, J. H., Suhr, N. H., and Bodkin, J. R., 1969, Atomic absorption analysis of silicates employing $LiBO_2$ fusion: Atomic Absorption News, v. 8, pp. 25-29.

Michel-Lèvy, A., 1877, De l'emploi du microscope polarisant à lumière paralèle (Use of the polarizing microscope with parallel illumination): Annales des Mines, v. 12, pp. 392-471.

Murray, M. M., 1970, Petrology, structure, and origin of the San Isabel batholith, Wet Mountains, Colorado: Ph.D. Dissertation, Rice University.

Murray, M. M., 1975, Petrology and chemistry of a hybridized plutonic intrusion: The San Isabel batholith of the Wet Mountains, Colorado: unpublished.

Murray, M. M., and Rogers, J. J. W., 1973, Distribution of Rb and Sr in the potassium feldspars of two granite batholiths: Geochemical Journal, v. 6, pp. 117-130.

Naney, M. T., 1983, Phase equilibria of rock-forming ferromagnesian silicates in granitic systems: American Journal of Science, v. 283, pp. 993-1033.

Nelson, B. K., and DePaolo, D. J., 1985, Rapid production of continental crust 1.7-1.9 b.y. ago: Nd isotopic evidence from the basement of the North American midcontinent: Geological Society of America Bulletin, v. 96, pp. 746-754.

Pearce, J. A., Harris, N. B. W., and Tindle, A. G., 1984, Trace-element discrimination diagrams for the tectonic interpretation of granitic rocks: Journal of Petrology, v. 25, pp. 956-983.

Perfit, M. R., Bruekner, H., Lawrence, J. R., and Kay, R. W., 1980, Trace-element and isotopic variations in a zoned pluton and associated volcanic rocks, Unalaska Island, Alaska: a model for the fractionation of the Aleutian calc-alkaline suite: Contributions to Mineralogy and Petrology, v. 73, pp. 69-87.

Presnall, D. C., and Bateman, P. C., 1973, Fusion relations in the system $NaAlSi_3O_8$-$CaAl_2Si_2O_8$-$KAlSi_3O_8$-SiO_2-H_2O and generation of granitic magmas in the Sierra Nevada batholith: Geological Society of America Bulletin, v. 84, pp. 3181-3202.

Price, R., 1983, Geochemistry of a peraluminous granitoid suite from north-eastern Victoria, south-eastern Australia: Geochimica et Cosmochimica Acta, v. 47, pp. 31-42.

Reid, J. B., Evans, O. C., and Fates, D. G., 1983, Magma mixing in granitic rocks of the central Sierra Nevada, California: Earth and Planetary Science Letters, v. 66, pp. 243-261.

Rösler, H. J., and Lange, H., 1972, Geochemical Tables: Elsevier, Amsterdam, 468 p.

Sassarini, N., 1984, personal communication.

Scambos, T. A., Loiselle, M. C., and Wones, D. R., 1986, The Center Pond Pluton: The restite of the story (phase separation and melt evolution in granitoid genesis): American Journal of Science, v. 286, pp. 241-280.

Schnetzler, C. C., and Philpotts, J. A., 1970, Partition coefficients of rare-earth elements between igneous matrix material and rock-forming mineral phenocrysts II: Geochimica et Cosmochimica Acta, v. 34, pp. 331-340.

Scott, G. R., and Taylor, R. B., 1978, Geologic map of the Pueblo quadrangle, south-central Colorado: U.S. Geological Survey Miscellaneous Inv. Map I-1022.

Shapiro, L., 1978, Rapid analysis of silicate, carbonate, and phosphate rocks - revised edition: U.S. Geological Survey Bulletin 1401, 76 p.

Shaw, D. M., 1970, Trace-element fractionation during anatexis: Geochimica et Cosmochimica Acta, v. 34, pp. 237-243.

Shaw, L. D., 1984, personal communication.

Shuster, R. D., 1984, Age, origin, and significance of the San Isabel batholith, Wet Mountains, Colorado: Geological Society of America, Rocky Mountain section, Symposium: The Ogden Tweto Memorial Symposium: Precambrian Geology of the Southern Rocky Mountain Region I.

Silver, L. T., Bickford, M. E., Van Schmus, W. R., Anderson, J. L., Anderson, T. H., and Medaris, L. G., Jr., 1977, The 1.4-1.5 b.y. transcontinental anorogenic plutonic perforation of North America: Geological Society of America Abstracts with Programs, v. 9, no. 7, pp. 1176-1177.

Simmons, E. C., and Hedge, C. E., 1978, Minor-element and Sr-isotope geochemistry of Tertiary stocks, Colorado mineral belt: Contributions to Mineralogy and Petrology, v. 67, pp. 379-396.

Singewald, Q. D., 1966, Description and relocation of part of the Ilse fault zone, Wet Mountains, Colorado: U.S. Geological Survey Professional Paper 550C, pp. 21-24.

Snoke, A. W., Quick, J. E., and Bowman, H. R., 1981, Bear Mountain igneous complex, Klamath Mountains, California: an ultrabasic to silicic calc-alkaline suite: Journal of Petrology, v. 22, pp. 501-552.

Steiner, J. C., Jahns, R. H., and Luth, W. C., 1975, Crystallization of alkali feldspar and quartz in the Haplogranite system $NaAlSi_3O_8$-$KAlSi_3O_8$-SiO_2-H_2O at 4 Kb: Geological Society of America Bulletin, v. 86, pp. 83-98.

Stone, J. M., 1984, personal communication.

Streckeisen, A. L., 1967, Classification and nomenclature of igneous rocks (final report of an enquiry): Neues Jahrbuch fur Mineralogie Abhandlungen, v. 107, pp. 144-240.

Tanaka, T., and Nishizawa, O., 1975, Partitioning of rare-earth elements, Ba, and Sr between crystals and liquid phases for a natural silicate system at 20 Kb pressure: Geochemical Journal, v. 9, pp. 161-166.

Tarney, J., and Windley, B. F., 1977, Chemistry, thermal gradients, and evolution of the lower continental crust: Journal of the Geological Society of London, v. 134, pp. 153-172.

Taylor, H. P., Jr., 1980, The effects of assimilation of country rocks by magmas on $^{18}O/^{16}O$ and $^{87}Sr/^{86}Sr$ systematics in igneous rocks: Earth and Planetary Science Letters, v. 47, pp. 243-254.

Thomas, J. J., Shuster, R. D., and Bickford, M. E., A terrane of 1350-1400 m.y. old silicic volcanic and plutonic rocks in the buried Proterozoic of the mid-continent and in the Wet Mountains, Colorado: Geological Society of America, (in press).

Thorpe, R. S., Potts, P. J., and Sarre, M. B., 1977, Rare-earth evidence concerning the origin of granites of the Isle of Skye, northwest Scotland: Earth and Planetary Science Letters, v. 36, pp. 111-120.

White, A. J. R., and Chappell, B. W., 1977, Ultrametamorphism and granitoid genesis: Tectonophysics, v. 43, pp. 7-22.

White, A. J. R., and Chappell, B. W., 1983, Granitoid types and their distribution in the Lachlan Fold Belt, southeastern Australia: Geological Society of America Memoir 159, pp. 21-34.

Whitten, E. H. T., and Boyer, R. E., 1964, Process-response models based on heavy mineral content of the San Isabel granite, Colorado: Geological Society of America Bulletin, v. 75, p. 841.

Winkler, H. G. F., 1967, Petrogenesis of metamorphic rocks: Springer Verlag, New York, 237 p.

Wood, D. A., Gibson, I. L., and Thompson, R. N., 1976, Elemental mobility during zeolite facies metamorphism of the Tertiary basalts of eastern Iceland: Contributions to Mineralogy and Petrology, v. 55, pp. 241-254.

Wyllie, P. J., Huang, W., Stern, C. R., and Maaløe, S., 1976, Granitic magmas: possible and impossible sources, water contents, and crystallization sequences: Canadian Journal of Earth Sciences, v. 13, pp. 1007-1019.

Zen, E-an, 1985, Implications of magmatic epidote-bearing plutons on crustal evolution in the accreted terranes of northwestern North America: Geology, v. 13, pp. 266-269.

APPENDIX A: Trace-element modeling equations

The application of trace-elements to the origin and chemical evolution of the San Isabel batholith is an important part of this study. The development of a quantitative model to explain the range of chemical variation in the batholith must be consistent with major- and trace-element data, isotopic data, petrographic observations, field relationships, and results of experimental petrology (Haskin, 1984). Quantitative models involving the use of trace-elements to help explain the petrogenesis of granitic melts are based on the distribution coefficients of the elements (Shaw, 1970; Hanson, 1978). The distribution coefficient (D.C.) is defined as the ratio of the concentration of a given element in a solid phase relative to its concentration in a coexisting liquid. Distribution coefficients are dependent on many factors and are used with the assumption that solid and melt are in equilibrium (Hanson, 1978). Quantitative trace-element modeling has been used with success in many petrogenetic studies but several constraints and assumptions exist:

(1) Distribution coefficients are approximate and are a function of the following parameters (Shaw, 1970; Hanson, 1978; Haskin, 1984):

a) temperature

b) pressure

c) alkalinity

d) SiO_2 content

e) oxygen fugacity

f) presence of halogens

(2) Source rocks are usually hypothetical, therefore modal mineralogy must be estimated.

(3) Trace-element concentrations in source rocks must be approximated by utilization of published data on compositionally similar rocks.

(4) The proportion of each phase in the melt must be assumed (i.e. modal versus non-modal melting).

(5) The physical processes responsible for the formation of the rock suite must be estimated (i.e. batch melting versus aggregate melting, fractional crystallization, magma mixing, assimilation, and restite/unmixing).

(6) Trace-element modeling equations assume that trace-elements are relatively refractory and resistant to weathering and alteration (Haskin, 1984).

Nevertheless, the application of trace-elements to the petrogenesis of a given rock suite provides important constraints on the source rock and mechanism of melting involved in formation of the suite.

In this study, the non-modal aggregate melt formulation described by Shaw (1970) is used to model partial melting processes:

$$C_L / C_O = 1/F(1-(1-PF/D_O)^{1/P})$$

where C_L = trace-element concentration in derived melt

C_O = trace-element concentration in residual source

F = fraction of source rock that has melted

P = proportionality constant = $P_1K_1 + P_2K_2 + \ldots$

where P_i = proportion of phase i in the melt

K_i = distribution coefficient of a given trace-element for phase i

D_O = bulk distribution coefficient = $X_1K_1 + X_2K_2 + \ldots$

where X_i = abundance of phase i in the source

K_i = distribution coefficient of a given trace-element for phase i

Fractional crystallization processes were modeled using the equation of Haskin et al. (1970):

$$C_L / C_O = (1-X)K-1$$

where C_L = trace-element concentration in the residual liquid

C_O = initial trace-element concentration in the magma

X = fraction of the original magma that has crystallized

K = distribution coefficient of a given trace-element for the crystallizing phase

The simple mixing equation discussed by Allegre and Minster (1978) and Cox et al. (1980) is used to model mixing processes:

$$C_T = C_A F + C_B(1-F)$$

where C_T = trace-element concentration in the mixed or contaminated magma

C_A = trace-element concentration in magma A

C_B = trace-element concentration in magma B

F = weight proportion of magma A

APPENDIX B: Atomic absorption and emission spectrophotometry

Rb, Sr, and major-element contents were determined by atomic absorption and emission techniques outlined by Medlin et al. (1969) and Shapiro (1978). Procedures for the preparation of granitic rocks for analysis are presented below:

(A) Precisely weigh out 0.2000 ± 0.0001 g of powdered rock sample.

(B) Mix sample with 1.0000 ± 0.0001 g of $LiBO_2$ in a graphite crucible.

(C) Place crucibles in furnace at 1000° C for 1 hour.

(D) Allow fused samples to cool.

(E) Place fused sample in 50 ml 1N HCl, 1% La solution (1% La solution = 25.697 g lanthanum chloride in 1 liter of distilled-deionized H_2O).

(F) Place solutions with sample beads on magnetic stirers until beads are completely dissolved (usually 1-3 hours).

(G) When beads are completely dissolved, filter solution with Whatman #2 filter paper to remove graphite particles and rinse 4 times with deionized water.

(H) Blank solutions containing only 1.0000 ± 0.0001 g $LiBO_2$ are prepared exactly as described above.

The dilution scheme used in this study for analysis of granitic rocks is presented below:

(A) Solution A
Initial solution, 50 ml
Analyze for Ti, Sr, and Mn

(B) Solution B
20 ml of Solution A + 20 ml distilled-deionized H_2O
Analyze for Rb

(C) Solution C
6 ml of Solution B + 40 ml distilled-deionized H_2O
Analyze for Al, Si, and Ca

(D) Solution D
10 ml of Solution C + 20 ml distilled-deionized H_2O
Analyze for Na, Fe, and Mg

(E) Solution E
4 ml of Solution D + 20 ml distilled-deionized H_2O
Analyze for K

Samples were analyzed using a Perkin-Elmer model 305B spectrophotometer. Elemental concentrations were determined by linear regression in which a Canadian soil sample and two United States Geological Survey (U.S.G.S.) samples were used as standards for comparison. These standard samples include:

(1) RGM-1; rhyolite

(2) QLO-1; quartz latite

(3) SO-4; Canadian soil sample

APPENDIX C: Instrumental neutron activation analysis

Na, Fe, and trace-element contents were determined by instrumental neutron activation techniques outlined by Gordon et al. (1968) and Jacobs et al. (1977). Procedures used in this study are presented below:

(A) Precisely weigh out 0.3000 ± 0.0001 g of powdered rock sample and place in a plastic vial.

(B) Plastic vials are then sealed and wrapped with 0.1000 ± 0.0001 g of Fe wire (Fe wire serves as a neutron flux monitor).

(C) Standard samples are prepared exactly as described above. In this study, a Canadian soil sample (SO-4) was used as the standard.

(D) Samples are then irradiated for 4 hours in a Triga Mark II reactor.

(E) Approximately two days after irradiation, samples are placed in small plastic bags and mounted on 3 inch by 5 inch cards. Fe wires are coiled and then mounted in a similar manner.

(F) 5, 10, and 40-day counts are performed on all samples using a Canberra Model 8180 multichannel analyzer and a 25 $_{cm}3$ Ge(Li) detector.

Calibration of the Canberra Model 8180 multichannel analyzer was accomplished by using two radioactive sources:

^{152}Eu (0.122 meV and 0.344 meV)

^{60}Co (1.333 meV)

Elemental concentrations were determined by comparing the emission rates of gamma-ray energies for samples and standards and then correcting for (1) variations in neutron flux and (2) interference by elements that emit similar gamma-ray energies. Variations in neutron flux are accounted for in the following equation:

$$C_s = C_{st}(\text{st. wgt./s. wgt.})(\text{st. Fe/s. Fe})(\text{s./st.})$$

where C_s = concentration of element in sample

C_{st} = concentration of element in standard

st. wgt./s. wgt. = ratio of standard weight to sample weight

st. Fe/s. Fe = standard to sample activity ratio with respect to reactor flux

s./st. = activity ratio of sample to standard

Interference by elements that emit similar gamma-ray energies necessitates further corrections in the following isotopes:

(1) ^{233}Th (398.5 keV) interferes with ^{175}Yb (396.1 keV)

(2) ^{59}Fe (142 keV) interferes with ^{141}Ce (145 keV)

(3) ^{233}Th (312 keV) interferes with ^{159}Tb (299 keV)

APPENDIX D: Gravimetric determinations (loss on ignition)

The procedure for determination of total volatile content of samples is presented below:

(A) Precisely weigh out 1.0000 ± 0.0001 g of powdered rock sample and place in a pre-ignited platinum crucible.

(B) Place crucibles in furnace at 1000°C for 1 hour.

(C) Transfer crucibles to a dessicator and allow samples to cool to room temperature.

(D) Weigh samples.

(E) The weight loss for each sample is reported as loss on ignition (LOI).

APPENDIX E: Comparison of San Isabel batholith with other Wet Mountain plutons

Figure 30: Comparison of Rb/Sr vs. SiO_2 variation diagrams of selected Wet Mountain granitoids.

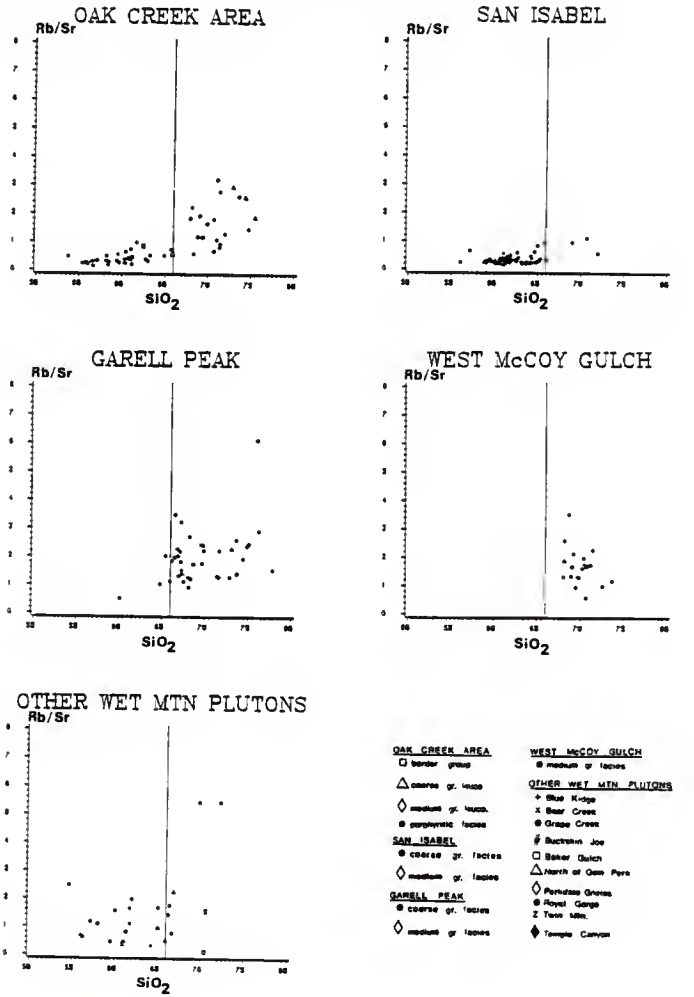

Figure 31: Comparison of Rb vs. Sr variation diagrams of selected Wet Mountain granitoids.

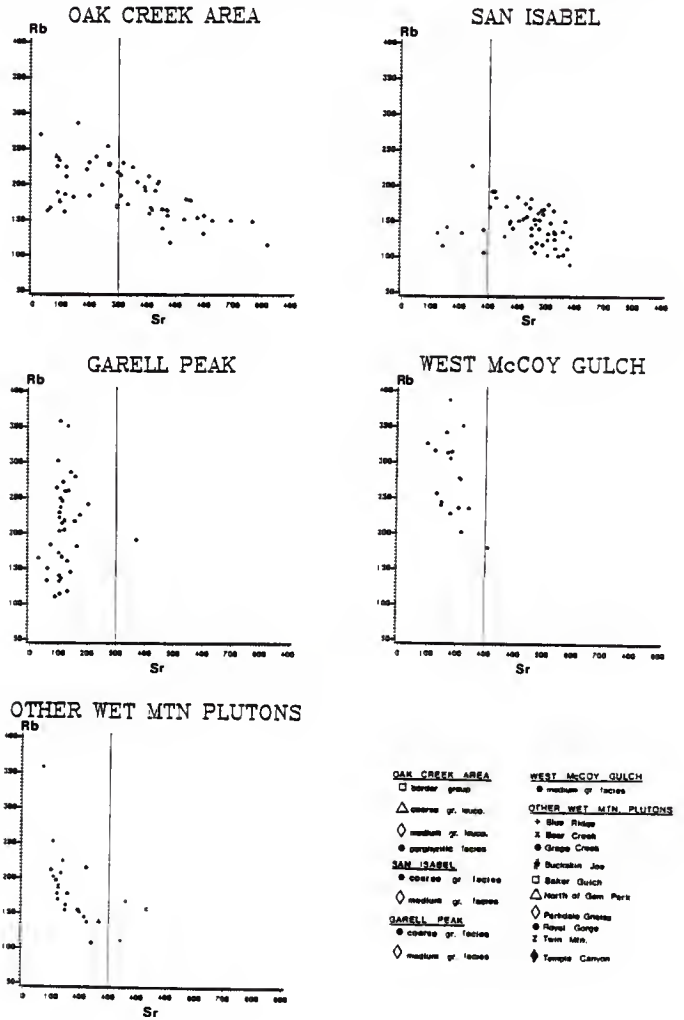

Figure 32: Comparison of SHAND (mol. Al_2O_3/K_2O+Na_2O+CaO) vs. SiO_2 variation diagrams of selected Wet Mountain granitoids.

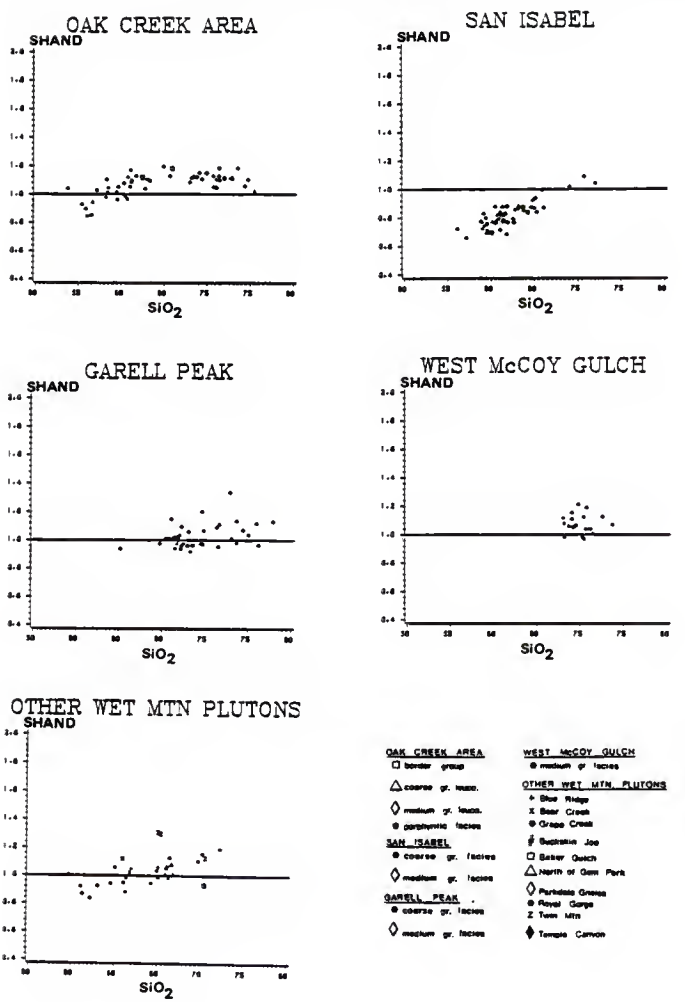

Figure 33: Comparison of SiO_2 vs. FER (FeO/FeO+MgO) variation diagrams of selected Wet Mountain granitoids.

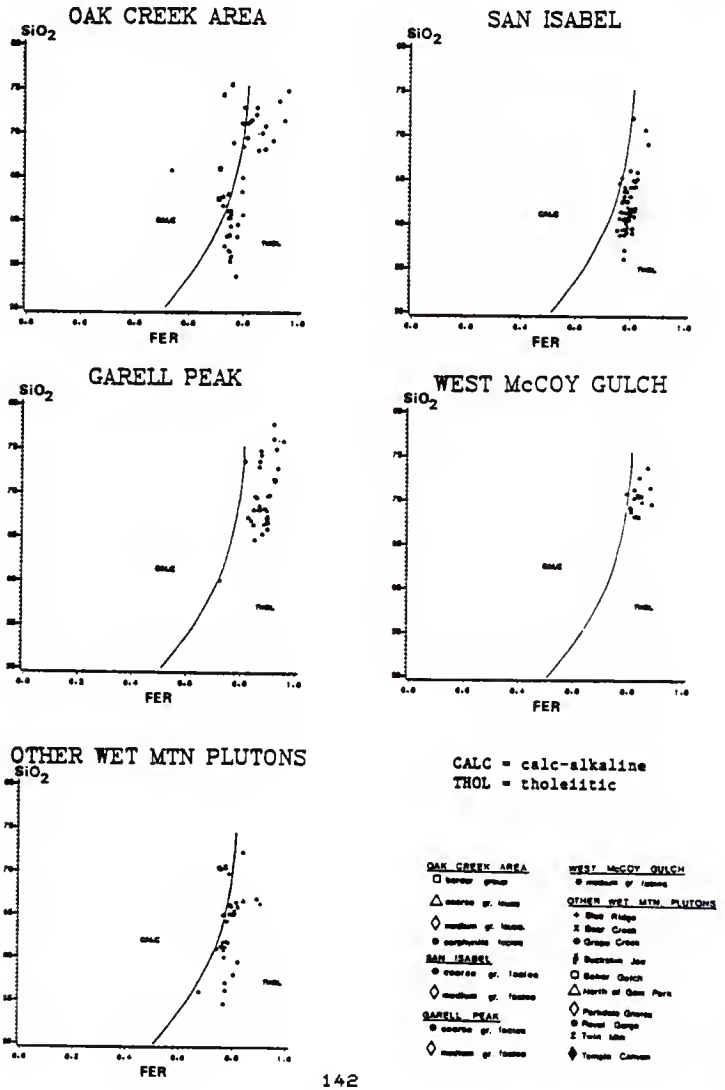

Figure 34: Comparison of NK (Na_2O+K_2O) vs. SiO_2 variation diagrams of selected Wet Mountain granitoids.

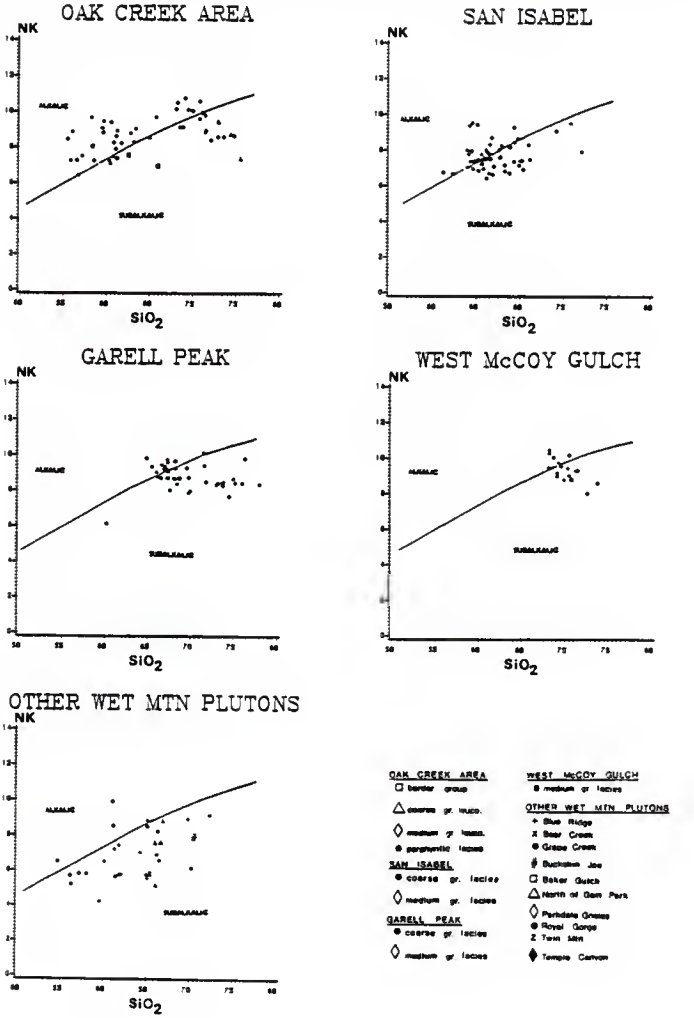

Figure 35: Comparison of NKC (Na_2O+K_2O/CaO) vs. SiO_2 variation diagrams of selected Wet Mountain granitoids.

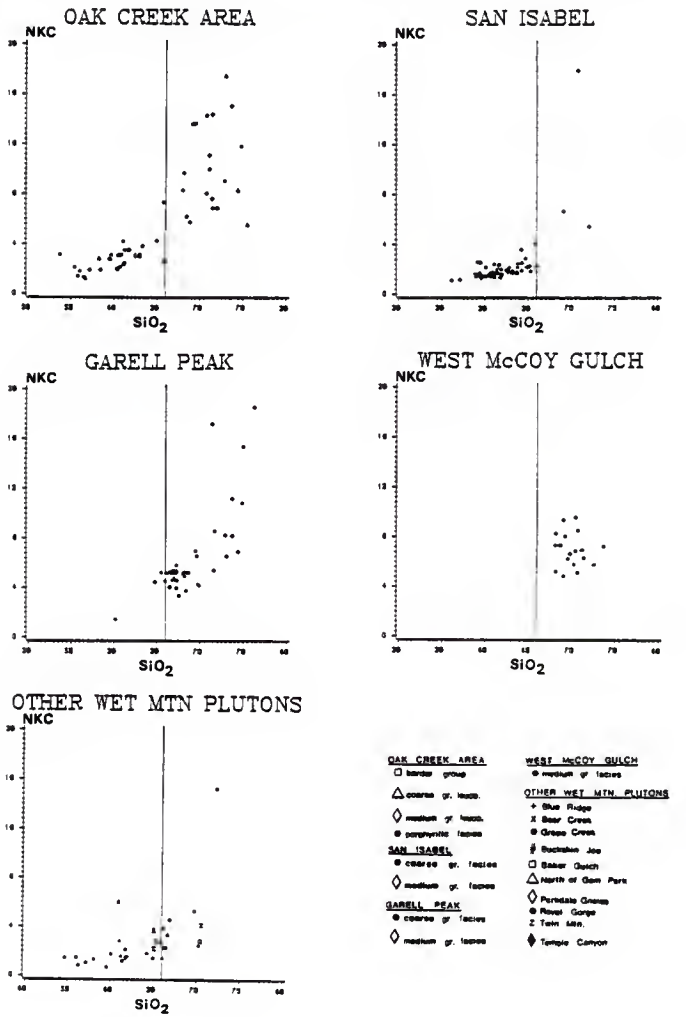

Figure 36: Comparison of TiO_2 vs. MgO variation diagrams of selected Wet Mountain granitoids.

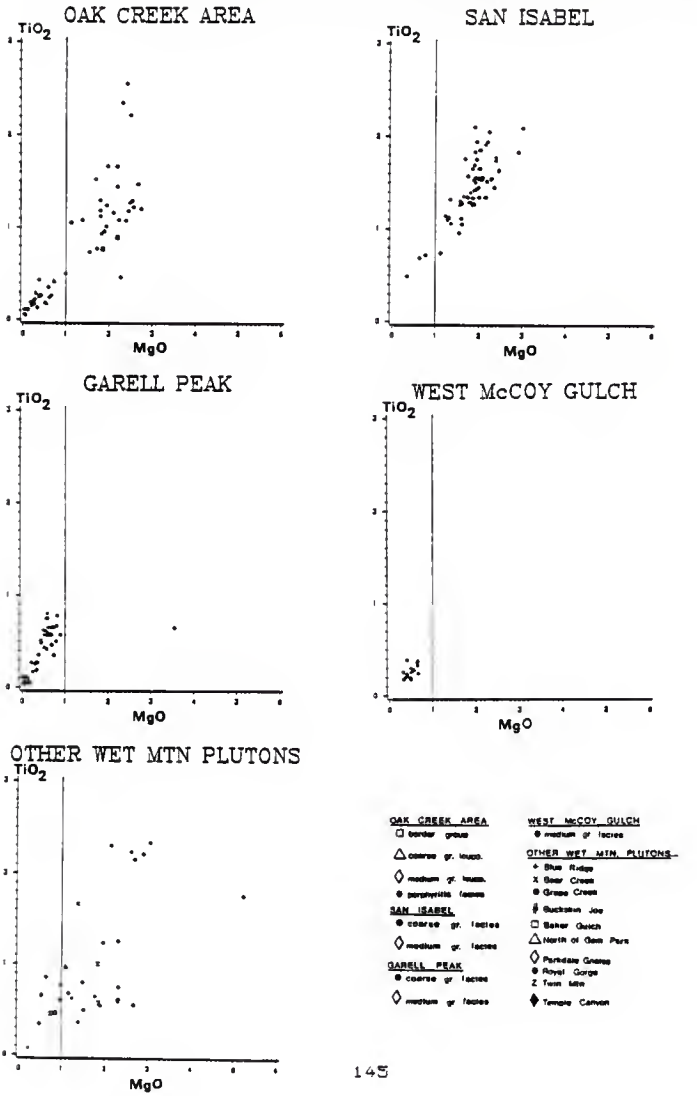

Figure 37: Comparison of CaO vs. FeO variation diagrams of selected Wet Mountain granitoids.

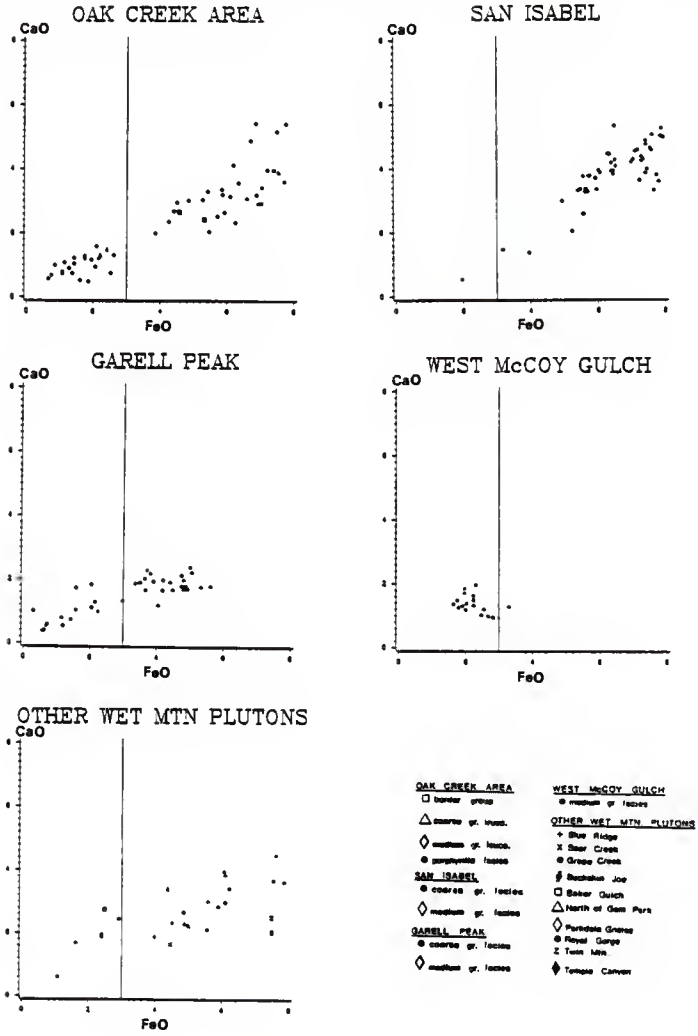

Figure 38: Comparison of K_2O vs. SiO_2 variation diagrams of selected Wet Mountain granitoids.

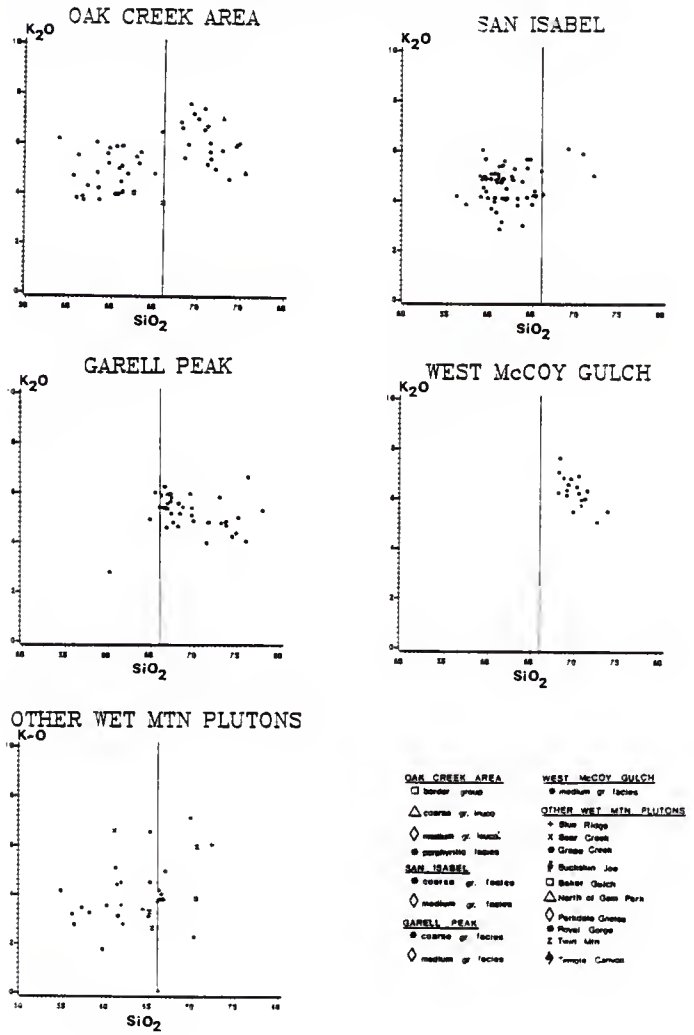

Figure 39: Comparison of Ba vs. Th variation diagrams of selected Wet Mountain granitoids.

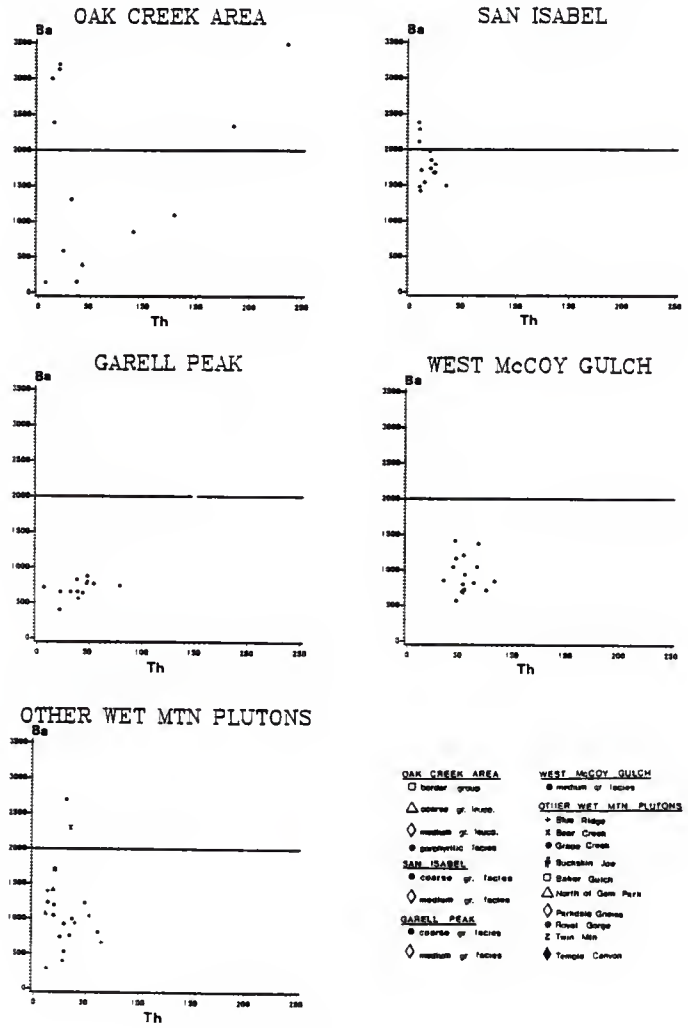

APPENDIX F: Elemental variation diagrams
(elements versus DI)

Figure 40: Variation diagrams of CaO, MgO, TiO_2, Fe_2O_3, and MnO versus differentiation index for the San Isabel batholith.

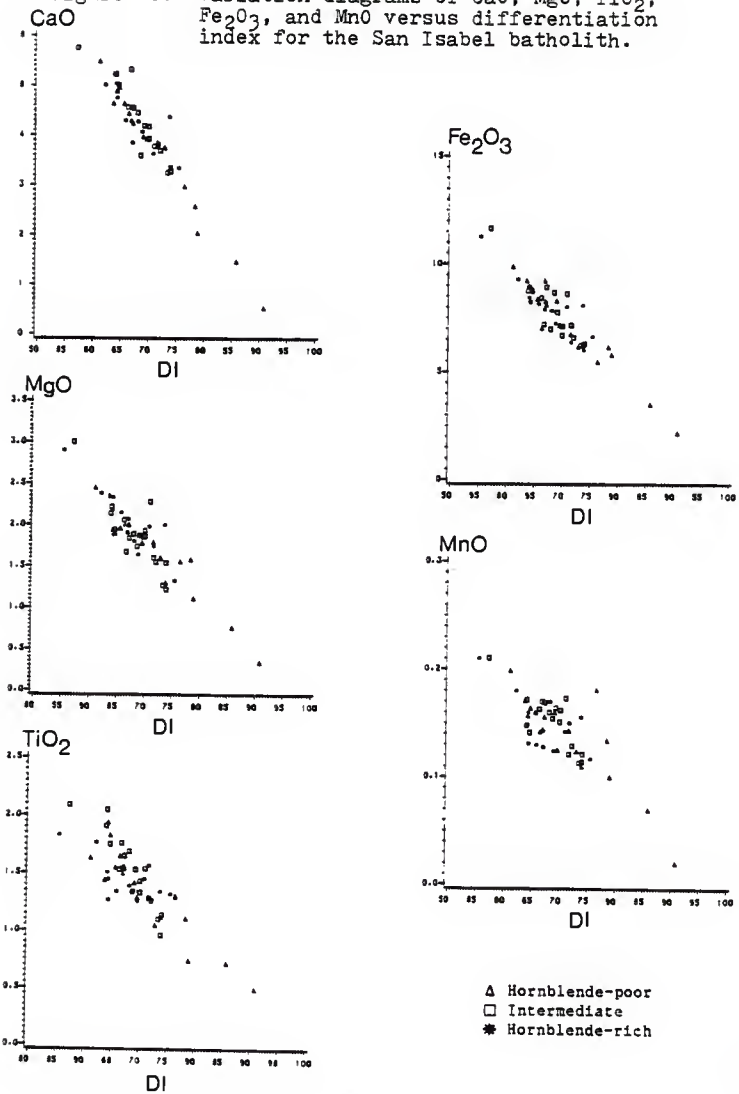

Figure 41: Variation diagrams of SiO_2, Al_2O_3, K_2O, Na_2O, and Rb/Sr versus differentiation index for the San Isabel batholith.

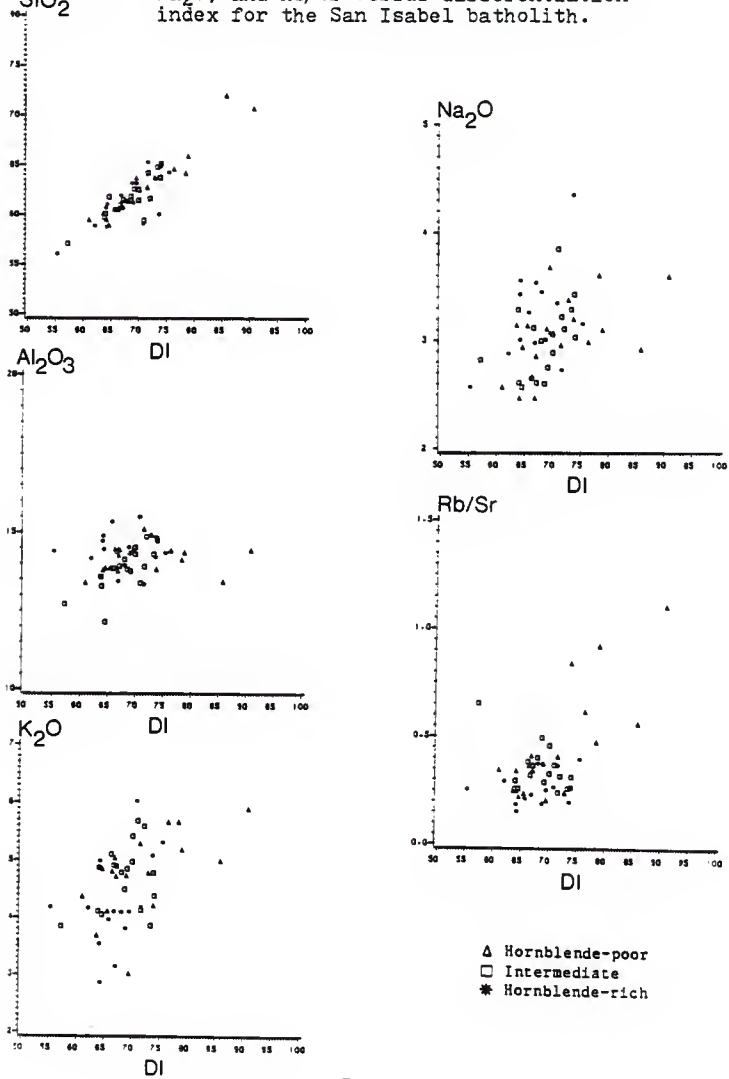

Figure 42: Variation diagrams of FER, SHAND, NKC, and NK versus differentiation index for the San Isabel batholith, (FER=FeO/FeO+MgO, SHAND=mol. Al_2O_3/K_2O+Na_2O+CaO, NKC=Na_2O+K_2O/CaO, and NK=Na_2O+K_2O).

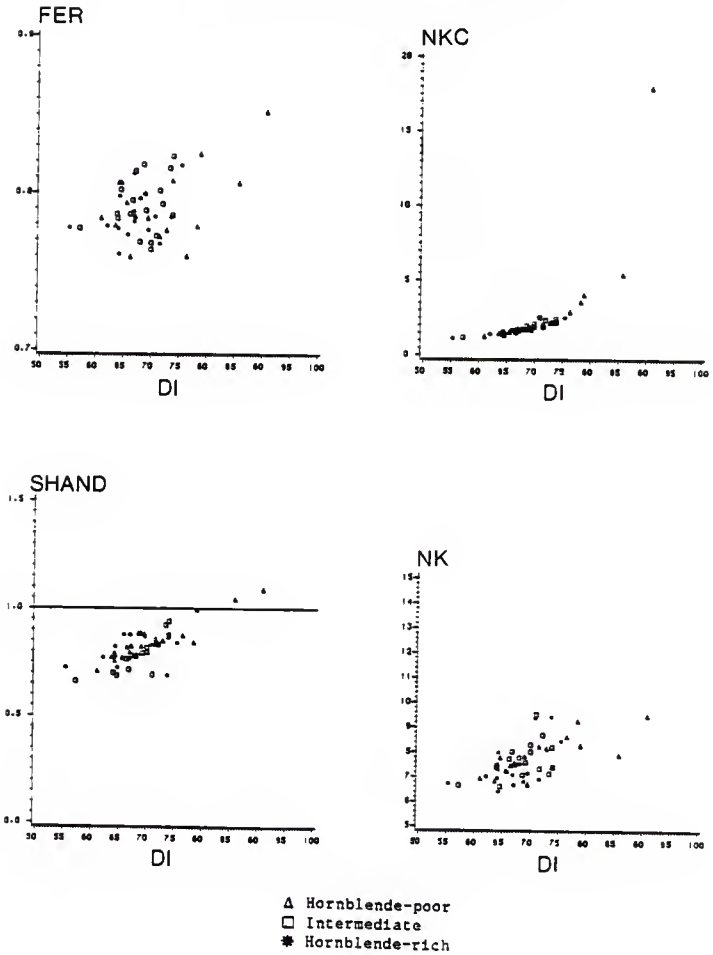

APPENDIX G: Petrographic descriptions

Rock descriptions of typical coarse-grained porphyritic, medium-grained, and quartz medium-grained samples are presented below.

TG-136: Coarse-grained porphyritic facies

This monzogranite porphyry consists of 25 percent subhedral to euhedral microcline phenocrysts, 0.8 to 3.5 cm long; and 5 percent subhedral to euhedral plagioclase laths, 0.5 to 0.8 cm long set in an inequigranular, phaneritic groundmass containing 25 percent anhedral to subhedral plagioclase, 1.5 to 6.0 mm long; 20 percent anhedral quartz, 1.0 to 6.0 mm across; 9 percent anhedral to euhedral biotite, 0.3 to 3.5 mm long; 7 percent anhedral to subhedral microcline, 1.0 to 7.0 mm long; 4 percent anhedral to subhedral hornblende, 0.5 to 3.0 mm long; 3 percent anhedral to euhedral sphene, 0.3 to 1.9 mm across; 2 percent anhedral to subhedral opaque minerals, 0.2 to 1.0 mm across; and 2 percent accessory minerals including anhedral to euhedral epidote, subhedral to euhedral apatite prisms, euhedral zircon inclusions in biotite, and anhedral hematite. Microcline is perthitic, tartan twinned, and contains inclusions of plagioclase, quartz, and biotite. Plagioclase (An_{25}-An_{30}) shows faint albite twinning, is extremely altered and sericitized, and contains poikilitic inclusions of opaques, hornblende, biotite, and sphene. Quartz is always interstitial to feldspars and exhibits strong undulatory extinction. Biotite occurs in early-formed

glomerocrysts with sphene, hornblende, and opaque minerals and as late-forming interstitial material with quartz. Inclusions of sphene, zircon, epidote, apatite, opaques, and quartz are present in the biotite. Hornblende is poikilitic and usually deeply embayed and resorbed. Embayments are usually filled with biotite, sphene, and opaque minerals. Sphene is usually fractured, sometimes twinned, and occurs in early-formed glomerocrysts with hornblende, biotite, and opaque minerals. Large glomeroporphyritic clusters are up to 5 cm across and contain predominantly mafic phases.

TG-56: Medium-grained facies

This hypidiomorphic monzogranite is composed of 33 percent anhedral to subhedral microcline, 0.8 to 4.0 mm long; 24 percent anhedral to subhedral plagioclase, 0.7 to 2.3 mm long; 25 percent anhedral quartz, 0.5 to 1.5 mm across; 7 percent anhedral to euhedral biotite, 0.5 to 1.7 mm across; 5 percent anhedral to subhedral hornblende, 0.5 to 1.0 mm long; 3 percent anhedral to euhedral sphene, 0.3 to 1.0 mm long; 2 percent anhedral to subhedral opaque minerals, 0.5 to 0.8 mm across; and 1 percent accessory minerals including anhedral to euhedral epidote, subhedral to euhedral apatite prisms, euhedral zircon inclusions in biotite, and anhedral hematite. Microcline is perthitic, tartan twinned, and contains inclusions of quartz, biotite, and highly altered plagioclase. Plagioclase (An_{25}-An_{35})

exhibits faint albite twinning and contains inclusions of biotite, hornblende, and apatite. Plagioclase grains are invariably altered and sericitized. Quartz is late-stage and interstitial and exhibits strong undulatory extinction. Biotite occurs in early-formed glomerocrysts with sphene, hornblende, and opaque minerals and as late-stage interstitial material with quartz. Inclusions of sphene, zircon, epidote, and quartz are present in the biotite. Hornblende is poikilitic and contains inclusions of sphene and opaque minerals. Alteration of hornblende to epidote is apparent along cleavage planes and within the embayments. Sphene is highly fractured and contains inclusions of apatite, altered opaques, and zircon. Fractures are usually filled with opaque minerals. Early-formed mafic glomerocrysts up to 7 mm across occur throughout the rock and are composed of biotite, hornblende, sphene, and opaque minerals.

Quartz medium-grained facies

The following rock description of a typical medium-grained sample is based on average modal analyses from Murray (1970). The average mode for the quartz medium-grained facies is 36.9 percent microcline, 29.0 percent quartz, 21.9 percent plagioclase, and 12.1 percent mafic minerals. Compared to the other textural facies, the quartz medium-grained facies has higher quartz and microcline and lower plagioclase and mafic minerals. Minor and accessory

mineral content is similar for all textural facies except for sphene which is absent in the quartz medium-grained facies. Textures grade from medium-grained equigranular to fine-grained.

APPENDIX H: Range of element contents in granitic rocks of the Wet Mountains, Colorado

Table 19: Range of element contents in granitic rocks of the Wet Mountains, Colorado (from Cullers and Wobus, 1986). Number of analyses are in parentheses.

	San Isabel Granite 1.36 b.y. (57)	Granite at Bear Basin 1.36 b.y. (4)	Small Granites near Bear Basin 1.36 b.y.?. (2)	Oak Creek Granite 1.44 b.y. (47)	West McCoy Gulch Granite 1.46-1.47 b.y. (18)	Beer Creek, Williams Creek, Cliff Creek Granites (7)	Gerell Peak Granite 1.66 b.y. (39)	Small folleted Stocks 1.7 b.y.1. (10)	Crempton Mt.-Twin Mt. 1.7 b.y. (22)
SiO_2	56.1-72.0	64.1-70.0	66.2-69.0	53.7-74.7	68.1-73.0	72.3-79	64.8-77	56.0-70.4	54.6-72.2
Al_2O_3	12.1-15.5	14.3-15.6	15.0-16.6	13.4-19.4	14.4-16.3	11.2-15.3	12.5-17.0	13.4-17.4	14.3-16.4
TiO_2	0.49-2.10	0.76-1.16	0.48-0.67	0.05-2.55	0.17-0.41	0.04-0.07	0.04-0.80	0.46-1.75	0.07-2.33
Fe_2O_3	2.17-11.6	3.26-5.53	3.64-4.01	0.73-8.57	1.89-3.70	0.36-0.94	0.62-6.24	2.75-11.9	1.18-11.6
MgO	0.34-3.0	0.62-1.22	0.72-0.94	0.04-2.74	0.31-0.69	0.01-0.12	0.02-0.88	0.51-5.20	0.21-3.03
CaO	0.53-6.1	0.83-2.32	1.05-1.06	0.49-5.44	0.94-1.72	0.86-1.22	0.38-2.39	1.64-3.82	0.60-6.06
Na_2O	2.47-4.35	2.72-3.11	2.98-3.30	2.62-4.75	2.73-3.89	2.16-2.76	2.79-6.17	2.50-5.04	1.81-3.84
K_2O	2.86-6.1	5.88-7.01	5.57-6.16	3.72-7.59	5.52-7.26	5.00-6.98	3.95-6.61	0.12-6.60	1.78-7.12
MnO	0.020-0.21	0.06-0.11	0.03-0.05	0.02-0.17	0.040-0.093	0.01-0.04	0.01-0.15	0.04-2.8	0.04-0.19
FeO/FeO+MgO	0.75-0.86	0.80-0.83	0.79-0.82	0.70-0.96	0.79-0.88	0.88-0.97	0.81-0.95	0.67-0.90	0.75-0.83
$\frac{Al_2O_3}{CaO+Na_2O+CaO}$	0.66-1.09	0.97-1.10	1.17-1.18	0.85-1.19	0.97-1.19	1.07	0.92-1.15	0.92-1.12	0.84-1.29
Rb	89-228	210-235	241-258	115-286	180-351	119-166	110-358	120-216	108-417
Sr	121-580	184-330	215-226	25-817	93-307	41-94	27-200	94-981	66-339
Ba	1420-2384	992-1480	1115-1280	139-3,500	570-1380	116-1456	401-875	690-2700	287-2300
La	86-236	125-347	225	11-841	58.5-180	2.7-138	0.05-153	39-446	24.1-570
Lu	0.8-2.2	1.37-2.38	0.18-0.34	0.20-2.0	0.38-1.40	0.045-1.0	n.d.-3.12	0.19-2.4	0.40-1.63
Σ REE	434-1,090	688-1,500	883-960	38-2484	285-749	35-480	26-802	227-1710	154-1,485
Eu/Sm	0.15-0.22	0.11-0.13	0.097-0.11	0.040-0.34	0.055-0.139	0.052-0.49	0.022-0.14	0.083-0.28	0.060-0.27
$(La/Lu)_{cn}$	6.0-17.3	9.0-19.3	66-126	1.2-255	7.2-38.5	0.26-35.6	2.1-12.0	4-39.5	2.2-60.8
Th	7.8-34	18.8-48.7	122-130	3.5-236	43-82	4.7-50.2	6-79	10.6-79.3	11.7-101
Hf	11.5-36	20-34	20-28	1.8-34.7	9.3-19	1.2-15.7	5.3-23	6.4-36.4	2.7-21.6
Sc	14-34	5.8-10.9	4.1-5.4	2.1-25.5	2.9-8.6	0.16-2.4	0.09-14	2.5-29.3	4.5-35.5
Cr	13-36	16-24	16-18	9.6-59	10-19	<5-15.8	8-29.8	13.9-176	19-51

APPENDIX I: Compilation of confidence intervals (C.I.) for major- and trace-element concentrations for textural and mineralogical facies of the San Isabel monzogranite.

Table 20: Compilation of confidence intervals (C.I.) for major- and trace-element concentrations for textural and mineralogical facies of the San Isabel monzogranite.

	Coarse-grained	Medium-grained	Hornblende-rich	Intermediate	Hornblende-poor
SiO_2	61.84 ± 1.40	62.09 ± 0.81	61.02 ± 1.31	61.67 ± 0.99	63.03 ± 1.83
Al_2O_3	14.25 ± 0.24	14.00 ± 0.27	14.39 ± 0.32	13.91 ± 0.36	14.14 ± 0.24
TiO_2	1.39 ± 0.14	1.47 ± 0.12	1.46 ± 0.09	1.52 ± 0.16	1.31 ± 0.19
Fe_2O_3	7.69 ± 0.78	7.57 ± 0.49	8.08 ± 0.64	7.84 ± 0.69	7.07 ± 1.02
MgO	1.86 ± 0.22	1.83 ± 0.13	2.01 ± 0.20	1.87 ± 0.20	1.68 ± 0.26
CaO	4.06 ± 0.47	4.13 ± 0.33	4.39 ± 0.39	4.28 ± 0.38	3.67 ± 0.65
Na_2O	3.25 ± 0.14	2.89 ± 0.13	3.22 ± 0.24	2.99 ± 0.17	3.05 ± 0.18
K_2O	4.47 ± 0.34	4.73 ± 0.23	4.24 ± 0.46	4.71 ± 0.28	4.77 ± 0.35
MnO	0.14 ± 0.02	0.15 ± 0.01	0.15 ± 0.01	0.15 ± 0.01	0.14 ± 0.02
Rb	127 ± 8	153 ± 9	122 ± 11	144 ± 9	149 ± 14
Sr	436 ± 52	435 ± 37	485 ± 49	434 ± 43	396 ± 69
Ba	1932 ± 404	1691 ± 148	1866 ± 361	1730 ± 287	1713 ± 480
La	140 ± 43	153 ± 32	116 ± 27	153 ± 14	197 ± 62
Ce	283 ± 69	277 ± 53	232 ± 42	283 ± 24	359 ± 118
Sm	25.3 ± 4.3	24.9 ± 4.3	23.1 ± 4.6	24.7 ± 3.0	28.9 ± 11.5
Eu	4.7 ± 0.9	4.2 ± 0.7	4.1 ± 1.0	4.4 ± 0.7	4.8 ± 1.5
Yb	9.7 ± 1.7	9.4 ± 2.1	8.3 ± 1.4	9.8 ± 2.9	11.4 ± 5.1
Lu	1.5 ± 0.6	1.4 ± 0.4	1.3 ± 0.4	1.4 ± 0.7	1.8 ± 0.8
Th	11.6 ± 6.4	20.4 ± 5.2	10.6 ± 4.6	19.1 ± 4.7	25.9 ± 9.8
Sc	20.8 ± 8.3	21.9 ± 3.2	21.8 ± 6.3	21.7 ± 7.4	20.8 ± 7.8
SHANO	0.82 ± 0.04	0.81 ± 0.04	0.81 ± 0.03	0.79 ± 0.04	0.85 ± 0.05
PER	0.79 ± 0.01	0.79 ± 0.01	0.78 ± 0.01	0.79 ± 0.01	0.79 ± 0.01
Rb/Sr	0.35 ± 0.09	0.38 ± 0.06	0.26 ± 0.04	0.35 ± 0.05	0.46 ± 0.13

ORIGIN AND CHEMICAL EVOLUTION OF THE SAN ISABEL BATHOLITH, WET MOUNTAINS, COLORADO

by

Thomas J. Griffin

B.S. Kansas State University, 1982

AN ABSTRACT OF A MASTER'S THESIS

submitted in partial fulfillment of the

requirements for the degree

MASTER OF SCIENCE

Department of Geology

KANSAS STATE UNIVERSITY
Manhattan, Kansas

1987

ABSTRACT

The 1.36 b.y. old San Isabel batholith is a weakly foliated granitic intrusion that is coeval with the 1.35-1.4 b.y. old granite/rhyolite terrane occurring in parts of Missouri, Oklahoma, Kansas, and Texas. The San Isabel batholith is mostly monzogranite and contains up to 35% total mafics (including interstitial biotite, deeply embayed hornblende, sphene, and magnetite). Mafic minerals frequently occur as glomerocrysts and clots and attest to the cumulate nature of the batholith. The intrusion is characterized by low SiO_2 (56.1-72.0 wgt. %), moderate Sr (121-580 ppm), high FeO (1.95-10.43 wgt. %), TiO_2 (0.49-2.10 wgt. %), K_2O (2.86-6.1 wgt. %), MnO (0.02-0.21 wgt. %), Ba (1420-2384 ppm), Sc (14-34 ppm), REE (total REE = 434-1090 ppm), FeO/FeO+MgO (0.75-0.86), and Na_2O+K_2O (6.4-9.6 wgt. %), and small, negative Eu anomalies (Eu/Sm = 0.146-0.218).

Partial melting of the following source rocks to form the San Isabel magma were tested: 1) metamorphic rocks similar in composition to the 1.8 b.y. old hornblende-biotite gneiss and granite gneiss country rocks, 2) quartz-normative tholeiitic gabbro, 3) granitic rocks similar in composition to the 1.7 b.y. old foliated plutons at Garell Peak, Royal Gorge, and Twin Mountain, and 4) tonalites and granodiorites similar in composition to other 1.7 b.y. old

granitoids in the mid-continent and having negligable Eu anomalies. The best-fit model involves partial melting of a previously melted tonalite/granodiorite residuum to form the San Isabel magma.

For example, twenty to thirty percent partial melting of a previously melted tonalite/granodiorite residuum with positive Eu anomalies, high Sr and Sc, and low Rb contents combined with limited separation of minor residual sphene could produce melts chemically similar to the least differentiated, hornblende-rich portions of the San Isabel batholith. Limited mixing of partially assimilated hornblende-biotite gneiss and granite gneiss xenoliths with the San Isabel magma may have also occurred.

The principal factors affecting the range of composition in the San Isabel monzogranite are: (1) the presence or absence of hornblende and (2) the relative abundance of cumulate mafic material. Mixing of cumulate mafic material with slightly fractionated liquid can produce the range of trace-element contents in the San Isabel monzogranite. The hornblende-rich facies of the batholith represents the more primitive liquid in which 10-20% cumulate mafic minerals are mixed with slightly fractionated liquid. One to five percent mafic cumulate plus 10-25% fractional crystallization of plagioclase/K-spar/quartz/biotite from the remaining liquid can produce the hornblende-poor facies of the San Isabel batholith. Temperature during

emplacement was approximately 725° C and pressure 5-7 Kb. H_2O content of the San Isabel magma, deduced from crystallization sequences, was 1.2-1.5 percent.

Formation of the San Isabel magma under anorogenic conditions is suggested by high Na_2O+K_2O contents, high $FeO/(FeO+MgO)$ ratios, presence of late, interstitial biotite and occasional fluorite, lack of foliation, abundance of perthitic K-spar, and contemporaneity with other recognized A-type granites in North America. I-type features of the San Isabel batholith may be the result of partial melting of mantle-derived tonalites and granodiorites in this anorogenic setting.